

The Togavirus RNA Replication Complex

Pekka Kujala

Institute of Biotechnology
Department of Biosciences, Division of Biochemistry
and
Viikki Graduate School in Biosciences
University of Helsinki, Finland

ACADEMIC DISSERTATION

To be presented, with the permission of the Faculty of Science of the University of Helsinki, for public criticism in the auditorium 1041 at Viikki Biocenter (Viikinkaari 5, Helsinki) on June 21st, 2000, at 12 o'clock noon.

Helsinki 2000

Supervised by:

Professor **Leevi Kääriäinen**
Institute of Biotechnology
University of Helsinki

Reviewed by:

Professor **Carl-Henrik von Bonsdorff**
Department of Virology, Haartman Institute
University of Helsinki

and

Docent **Vesa Olkkonen**
Department of Biochemistry
National Public Health Institute
Helsinki

Opponent:

Docent **Anu Jalanko**
Department of Human Molecular Genetics
National Public Health Institute
Helsinki

ISBN 951-45-9443-6
Helsinki 2000

To the memory of my father

THE TOGAVIRUS RNA REPLICATION COMPLEX

ABBREVIATIONS

ORIGINAL PUBLICATIONS

ABSTRACT	1
INTRODUCTION	2
1. Togaviruses	2
1.1 Alphaviruses	2
1.1.1. Semliki Forest virus	3
1.1.2. SFV virion structure	4
1.2. Rubiviruses	4
1.2.1. Rubella virus	4
1.2.2. RUB virion structure	5
2. Replication cycle of togaviruses	5
2.1. The alphavirus replication cycle	7
2.1.1. Alphavirus entry	7
2.1.2. Alphavirus replication and translation of the nonstructural polyprotein	7
2.1.3. Translation of alphavirus structural proteins and virus maturation	8
2.1.4. SFV in cell culture	9
2.2. The rubella virus replication cycle	11
2.2.1. RUB entry and translation of the nonstructural polyprotein	11
2.2.2. Translation of RUB structural proteins and virus maturation	11
2.2.3. RUB in cell cultures	12
3. The togavirus RNA replicase proteins	13
3.1. SFV RNA replicase proteins	13
3.1.1. Nsp1	13
3.1.2. Nsp2	14
3.1.3. Nsp3	14
3.1.4. Nsp4	15
3.2. RUB RNA replicase proteins	15
3.2.1. P150	16
3.2.2. P90	16
4. The togavirus RNA replication complex	16

AIMS OF THE STUDY	18
MATERIALS AND METHODS	19
RESULTS	23
1. Localization of individual SFV nonstructural proteins	23
1.1. Isolation and detection of Nsp2 by monoclonal antibodies	23
1.2. Nsp1 and actin cytoskeleton	23
1.3. Localization of SFV Nsp1, Nsp3 and Nsp4	24
2. Morphological identification of togavirus RNA replication complexes	28
2.1. SFV-infected cells	28
2.2. RUB-infected cells	28
3. Endosomal origin and biogenesis of SFV CPV -associated RNA replication complex	37
4. Biogenesis of SFV CPV structures	37
DISCUSSION	40
1. Viruses and the cytoskeleton	40
2. Membrane association of the RNA replication complex	43
3. CPV biogenesis	47
4. A model for CPV biogenesis and spherule circulation	47
5. Future aspects	49
ACKNOWLEDGEMENTS	50
REFERENCES	51

ABBREVIATIONS

aa	amino acid(s)
BHK	baby hamster kidney
CEF	chicken embryo fibroblast
CPE	cytopathic effect
CPV, CPV-I	cytoplasmic vacuoles type 1
CRS	congenital rubella syndrome
EE	early endosome
ELISA	enzyme linked immuno sorbent assay
ER	endoplasmic reticulum
FITC	fluorescein isothiocyanate
GA	glutaraldehyde
IEM	immuno electron microscopy
IPTG	isopropyl- β -D-thiogalactopyranoside
kDa	kilodalton(s)
LE	late endosome
NC	nucleocapsid
Nsp	nonstructural protein
nt	nucleotide
NTP	nucleoside triphosphate
m.o.i.	multiplicity of infection
ORF	open reading frame
PAGE	polyacrylamide gel electrophoresis
PFA	para-formaldehyde
PFU	plaque forming unit
p.i.	post infection
PM	plasma membrane
PNS	postnuclear supernatant
RER	rough endoplasmic reticulum
RUB	rubella virus
SEM	scanning electron microscopy
SDS	sodium dodecyl sulphate
SFV	Semliki Forest virus
SIN	Sindbis virus
TEM	transmission electron microscopy
TRITC	tetramethyl rhodamine isothiocyanate
TX-100	Triton X-100
wt	wild type

ORIGINAL PUBLICATIONS:

This thesis is based on the following articles, referred to in the text by their Roman numerals, and on unpublished results.

I. Kujala P., Rikkinen M., Ahola T., Kelve M., Saarma M., and Kääriäinen L. (1997). Monoclonal antibodies specific for Semliki Forest virus replicase protein Nsp2. **J. Gen.Virol.** **78**: 343-351.

II. Laakkonen P., Auvinen P., **Kujala P.**, and Kääriäinen L (1998). Alphavirus replicase protein Nsp1 induces filopodia and rearrangement of actin filaments. **J. Virol.** **72**: 10265-10269.

III. Kujala P., Ahola T., Ehsani N., Auvinen P., Vihinen H., and Kääriäinen L. (1999). Intracellular distribution of rubella virus nonstructural protein P150. **J. Virol.** **73**: 7805-7811.

IV. Kujala P., Ikäheimonen A., Ehsani N., Vihinen H., Auvinen P., and Kääriäinen L. (2000). The biogenesis of Semliki Forest virus replication complex utilizes endosomal apparatus. **Submitted.**

ABSTRACT

In general, viral RNA polymerases are multisubunit assemblies consisting of a catalytic subunit and accessory viral gene products. Togaviruses are small enveloped RNA viruses replicating in the cytoplasm of their host cells. Semliki Forest virus (SFV; an alphavirus) and rubella virus (RUB; a rubivirus) represent two different members of the family *Togaviridae*. Their RNA genome is replicated by virus-specific nonstructural (replicase) proteins, which are proteolytically processed from a single polyprotein and which form a membrane associated RNA replication complex. The SFV nonstructural polyprotein (2432 aa) is processed to yield Nsp1, 2, 3 and 4, whereas RUB polyprotein (2215 aa) gives rise to replicase proteins P150 and P90. The SFV and RUB nonstructural proteins share several homologous domains predicted to have similar functions in RNA replication.

In the present study specific antibodies were raised against SFV Nsp1-4 and RUB P150. The antigens used for immunization were produced by recombinant DNA techniques, and were expressed in *Escherichia coli*. The mono-specific antibodies produced in mouse, rabbit or guinea-pig were used to characterize structures associated with RNA replicase proteins in SFV- and RUB-infected cells using immunofluorescence and immuno electron microscopy techniques.

In SFV- and RUB-infected cells all nonstructural proteins were localized to the limiting membranes of cytopathic vacuoles (CPVs), which were covered by small invaginations, spherules, unique for togavirus infection. Newly incorporated bromouridine was associated within CPVs, and specifically with the spherules, suggesting that these structures are the actual sites of the active togavirus RNA replication complexes. Cellular markers identified CPVs as fusion derivatives of late endosomes. Based on studies of the biogenesis of CPVs in SFV-infected cells a model is proposed that the spherules are originally formed at the plasma membrane and then circulated between the plasma membrane and the perinuclear region by endosomal apparatus.

Alphavirus capping enzyme Nsp1 was found to provoke changes in actin cytoskeleton inducing filopodia-like structures and disrupting stress fibers in infected and transfected cells. In contrast to alphavirus nonstructural proteins, RUB P150 was also localized into large, convoluted, tubular membrane structures, which were associated with microtubular filaments. These P150-containing membrane tubules extended from CPVs late in infection and colocalized with capsid protein as well as with newly incorporated bromouridine indicating that the rubivirus assembly greatly differs from that of alphaviruses.

INTRODUCTION

1. TOGAVIRUSES

Togaviruses are small, enveloped non-segmented single positive-stranded RNA viruses. The family *Togaviridae* consists of two genera alphaviruses and rubiviruses (Schlesinger and Schlesinger, 1996). Despite the similarity of their genomic organization, phylogenetic analyses have suggested that alphaviruses and rubiviruses are only distantly related (Koonin and Dolja, 1993). In this literature review I will focus on the molecular biology of two representative members of togaviruses: Semliki Forest virus (SFV), an alphavirus, and rubella virus (RUB), the only rubivirus. The intention is to briefly describe the similarities and differences in the biology of alpha- and rubiviruses.

1.1. Alphaviruses

Historically alphaviruses are classified as group A arboviruses (arthropod-borne virus), since they are usually transmitted by arthropod vectors, mainly by mosquitoes of *Aedes* and *Culex* –families (Chamberlain, 1980; Johnston and Peters, 1996). Female mosquitoes acquire the virus by taking blood from viremic vertebrate hosts (Fig. 1). The virus elicits a persistent infection and replicates to high titers especially in the salivary glands of the insects (Chamberlain, 1980). By biting a vertebrate host the mosquito inoculates virus-containing saliva into the bloodstream of a new victim. The initial viremia causes a primary infection of endothelial cells followed by systemic symptoms such as fever, chills, backaches

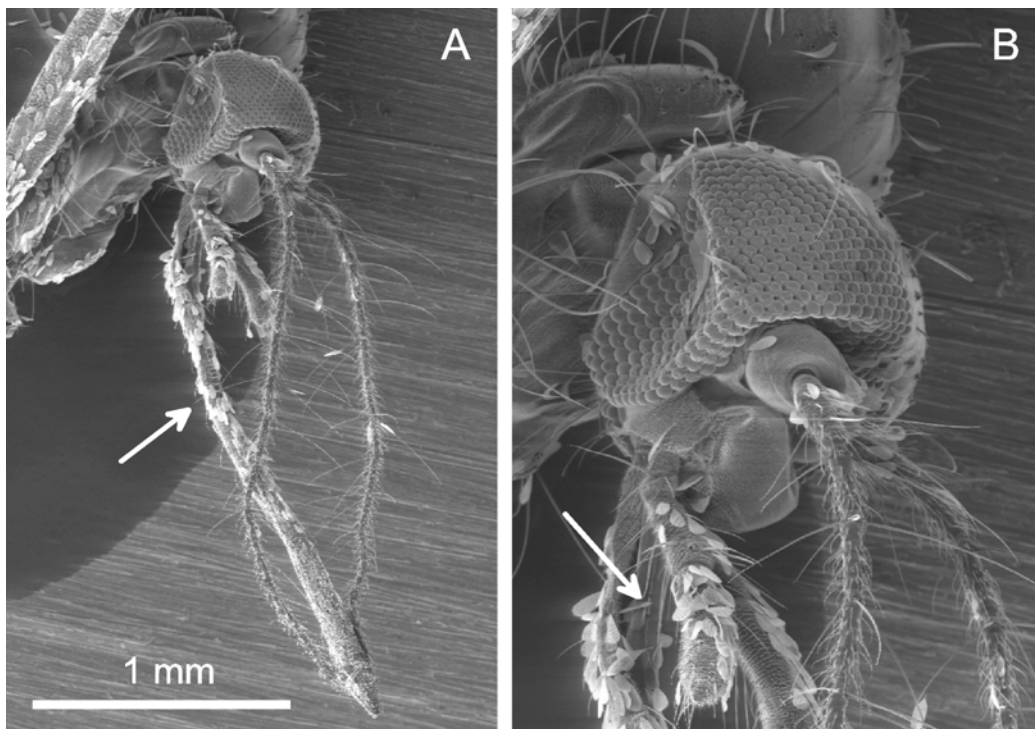


Figure 1. Alphaviruses are usually transmitted by mosquitoes. The head with labium of a female *Aedes communis* is presented by SEM (A). The labium (arrow) forms a protective gutter with length of 2 mm for the hypopharynx, through which the insect sucks blood from a vertebrate host. In (B) a close up of the insect head shows a short stretch of the hypopharynx (arrow) sheltered by the labium.

and flu-like symptoms within 3 to 7 days of infection. Depending on the virulence of alphavirus, a secondary viremia occurs affecting the brain, articulars, skin and vasculature (Johnston and Peters, 1996). Alphaviruses replicate in a broad range of vertebrate hosts including mammals, birds, amphibians and reptiles (Strauss and Strauss, 1994). Especially small mammals and birds serve as natural reservoir hosts of alphaviruses. A large population of viremic animals can develop in these species to continue the infection cycle of the virus (Johnston and Peters, 1996).

The alphaviruses as a group have a worldwide distribution, although no single virus is found throughout the world. They are divided into at least 27 serologically different members, some of which are significant human pathogens causing encephalitis [Eastern (EEE), Venezuelan (VEE) and Western (WEE) equine encephalitis viruses] or fever, rash and polyarthritis [Chikungunya, O'Nyong-Nyong (ONN), Ross River and Sindbis (SIN viruses)] (Strauss and Strauss, 1994). Large alphavirus epidemics have been rare, but occasionally millions of people have been affected by serious illness, such as in the outbreak of ONN infections in Africa in the mid-sixties (Rennels, 1984) and more recently febrile illness caused by Semliki Forest virus (SFV) among French soldiers in the Central African Republic (Mathiot et al., 1990). Man is usually a dead-end host that cannot spread the virus. Endemic regions are determined by the life cycle of the transmitting vector and thus infections occur most commonly in the summertime. For example, in Finland SIN causes a late summer disease known as Pogosta disease or Karelian fever, which is transmitted to humans by *Culex* mosquitoes from a reservoir of migrating birds (Francy et al., 1989; Turunen et al., 1998). The symptoms of Pogosta disease consist of fever, rash and joint ache, which may be severe and prolonged (Turunen et al., 1998). A

characteristic feature of an alphavirus epidemic is that more humans are infected than those showing significant symptoms (Johnston and Peters, 1996).

The laboratory strains of both Sindbis and Semliki Forest (SFV) viruses are considered avirulent to humans (Strauss and Strauss, 1994; Winkler and Blendin, 1995). SFV and SIN have been studied intensively over more than 30 years. Their laboratory safety combined with the relative ease and quick cultivation to produce high titer virus passages in various cell cultures, have made SFV and SIN important model viruses in the research of the closely related pathogenic alphaviruses and the entire alphavirus-like superfamily of viruses. These consist of rubivirus, hepatitis E virus, the insect viruses of *Tetraviridae* and several families of plant viruses, such as bromo-, cucumo-, tobamo-, tobra-, potex- and tymoviruses (Koonin and Dolja, 1993). Alphavirus studies have contributed to models used in the investigation of cellular transport of glycoproteins (Green et al., 1981; Griffiths et al. 1983; 1989; Saraste and Kuismanen, 1984; Simons and Warren, 1983). Furthermore, SFV and SIN genome based transient expression vectors are used for the production of commercially important proteins (Liljeström and Garoff, 1991; Lundström, 1999; Lundström et al., 1995; Ulmanen et al., 1997) as well as for the development of vaccines (Zhou et al., 1994; Atkins et al., 1996; Tubulekas et al., 1997).

1.1.1. Semliki Forest virus

SFV was first isolated in 1944 from mosquitoes in Uganda (Smithburn and Haddow, 1944). Later natural isolates have been obtained from several parts of sub-Saharan Africa, Russia and India, indicating a wide geographical distribution of this virus (Bradish et al., 1971; Strauss and Strauss, 1994). The original isolate of SFV was designated L10. Although apathogenic to humans, this isolate is neurovirulent in

mice, causing lethal encephalitis by infection of the central nervous system (reviewed in Atkins et al., 1999). The SFV strain used in laboratories is derived from the infectious L10 strain, but has lost some of its virulence during its passages through cell cultures (Glasgow et al., 1991). The nucleotide sequence of the structural protein coding region of SFV was published in 1980 (Garoff et al., 1980a; Garoff et al., 1980b) and the whole 11445 nt genome was sequenced six years later (Takkinen, 1986).

Interestingly, a natural avirulent strain of SFV designated A7 was isolated from mosquitoes in Mosambique (McIntosh et al., 1961). Although avirulent to adult mice, the A7 strain is lethal for the developing fetus. Similar to RUB, as discussed later in this chapter, an attenuated temperature sensitive mutant of A7 is nonlethal, but teratogenic for the developing fetus. The teratogenic effects induced by SFV include skeletal, skin and neural tube defects (Atkins et al., 1999).

1.1.2. SFV virion structure

Semliki Forest virion (diameter 65 nm) is composed of a nucleocapsid (NC, diameter 38-40 nm) core surrounded by a lipid bilayer (thickness 5 nm). The NC of SFV consists of 240 copies of capsid protein (C) and one molecule of single stranded RNA. The lipoprotein envelope consists of viral glycoproteins and lipids derived from the PM of the infected host cell. The glycoproteins form 80 spikes (length 7-8 nm) on the surface of the particle, where each spike consists of three copies of an E3-E2-E1 trimer (Fig. 2). The spike proteins in the virus particle, the integral membrane proteins E2 (422 aa, 52 kDa) and E1 (438 aa, 49 kDa) and the peripheral protein E3 (66 aa, 10 kDa) are organized as a T=4 icosahedral surface lattice (Vogel et al., 1986; Fuller, 1987; Fuller et al., 1995; Cheng et al., 1995).

1.2. Rubiviruses

1.2.1. Rubella virus

Rubella virus (RUB) is the only member of the genus rubiviruses (Schlesinger and Schlesinger, 1996). In contrast to alphaviruses, RUB is a non-arbo togavirus, which is transmitted by the respiratory route. Humans are the only natural host and known reservoir for RUB. Usually RUB infection causes a mild exanthematous childhood disease known as German measles, or in Latin rubella, meaning "little red". The relatively mild symptoms of German measles include maculopapular rash, lymphadenopathy, low-grade fever, conjunctivitis, sore throat and arthralgia, which can be accompanied by arthropathy and thrombocytopenia (reviewed by Wolinsky, 1996). The most serious consequences of RUB infection can occur during the first trimester of pregnancy. Placental transmission of the virus to the fetus may result in severe malformations

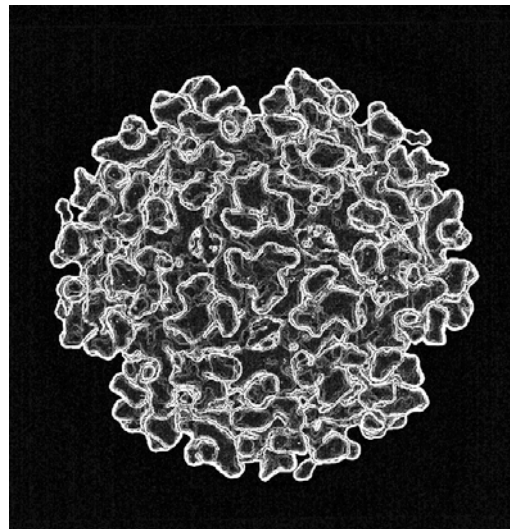


Figure 2. SFV virion surface with the glycoprotein spikes. Each spike consists of three copies of E3-E2-E1 trimer. The schematic presentation is based on cryoelectron micrographs of Dr. Stephen Fuller, EMBL, Germany.

affecting the ears, eyes and heart, known as congenital rubella syndrome (CRS). Resorption of the fetus, premature delivery and stillbirths are the potential outcomes of CRS. Most of patients with CRS show a variety of neuronal pathologies. Despite the wealth of clinical and epidemiological information regarding RUB, the molecular biology of the virus and the precise mechanisms of RUB teratogenesis have remained poorly understood (Wolinsky, 1996).

Although rubella was described already in 1866 by the German physician de Bergan, the virus was not isolated until 1962 (reviewed by Frey, 1994). This was due to difficulties in growing RUB in cell cultures. The introduction of vaccine against RUB in 1969 has successfully reduced the incidence of natural rubella (Wolinsky, 1996). In Finland, a two-dose vaccination program against measles, mumps and rubella (MMR) was started in 1982. This program has eliminated these diseases in Finland (Davidkin and Valle, 1998). However, vaccine failures and missed vaccination opportunities have produced epidemics of rubella in other parts of the world. The continued problem of rubella and CRS is associated with RUB's ability to persist in humans for many years in the absence of new detectable signs or symptoms, and its potential to cause immune-mediated human disease (Wolinsky, 1996).

The nucleotide sequence of the region coding the RUB structural proteins was published in 1988 (Vidgren et al., 1987; Takkinen et al. 1988), and the entire 9759 nt genome of the Therien strain of RUB was sequenced by 1990 (Frey et al., 1986; Frey and Marr, 1988; Dominquez et al., 1990). The RUB genome has the highest determined G+C content (RUB 68.5%; vs. SFV 53%) of all togaviruses sequenced so far, which has led to difficulties in the sequence determination. Sequencing errors have been reported in the originally published sequences, most of which have

been corrected in the literature (Frey and Marr, 1988; Clarke et al., 1988). At the molecular level, the characterization of RUB has lagged behind the related alphaviruses. In fact alphaviruses, especially SFV and SIN, have been served as comparative models in the molecular biology of RUB (Frey, 1994).

1.2.2. RUB virion structure

The RUB virion (diameter 60 nm) differs from SFV. The nucleocapsid is smaller (30-35nm) and more polymorphic in shape with often elongated, multi- or aberrant cores. The NC consists of a single positive-strand 40S RNA molecule surrounded by 32 capsomers arranged most probably in T=3 icosahedral symmetry (reviewed in Frey, 1994). A lipoprotein envelope with two membrane-spanning glycoproteins E1 and E2 surrounds the NC. A further characteristic of the RUB particle is a clear electron lucent zone between the glycoprotein fringe and the virion core (Fig. 4A), which is wider than in alphavirions (Wolinsky, 1996).

2. REPLICATION CYCLE OF TOGAVIRUSES

The togavirus replication occurs in the cytoplasm and can be divided into early genomic nonstructural and late subgenomic structural translation phases. Both translation products are polyproteins, which are processed further by viral and cellular proteases (Strauss and Strauss, 1994; ten Dam et al., 1999; Fig 3). The genomic and subgenomic RNAs have 5' methylated cap and 3' poly(A) sequences. The minus-strand intermediate RNA is not capped (Wengler et al., 1982). The synthesis of a separate subgenomic mRNA coding for structural proteins provides togaviruses with an efficient mechanism to regulate the biogenesis of encapsidation and replication proteins in both a temporal and qualitative manner.

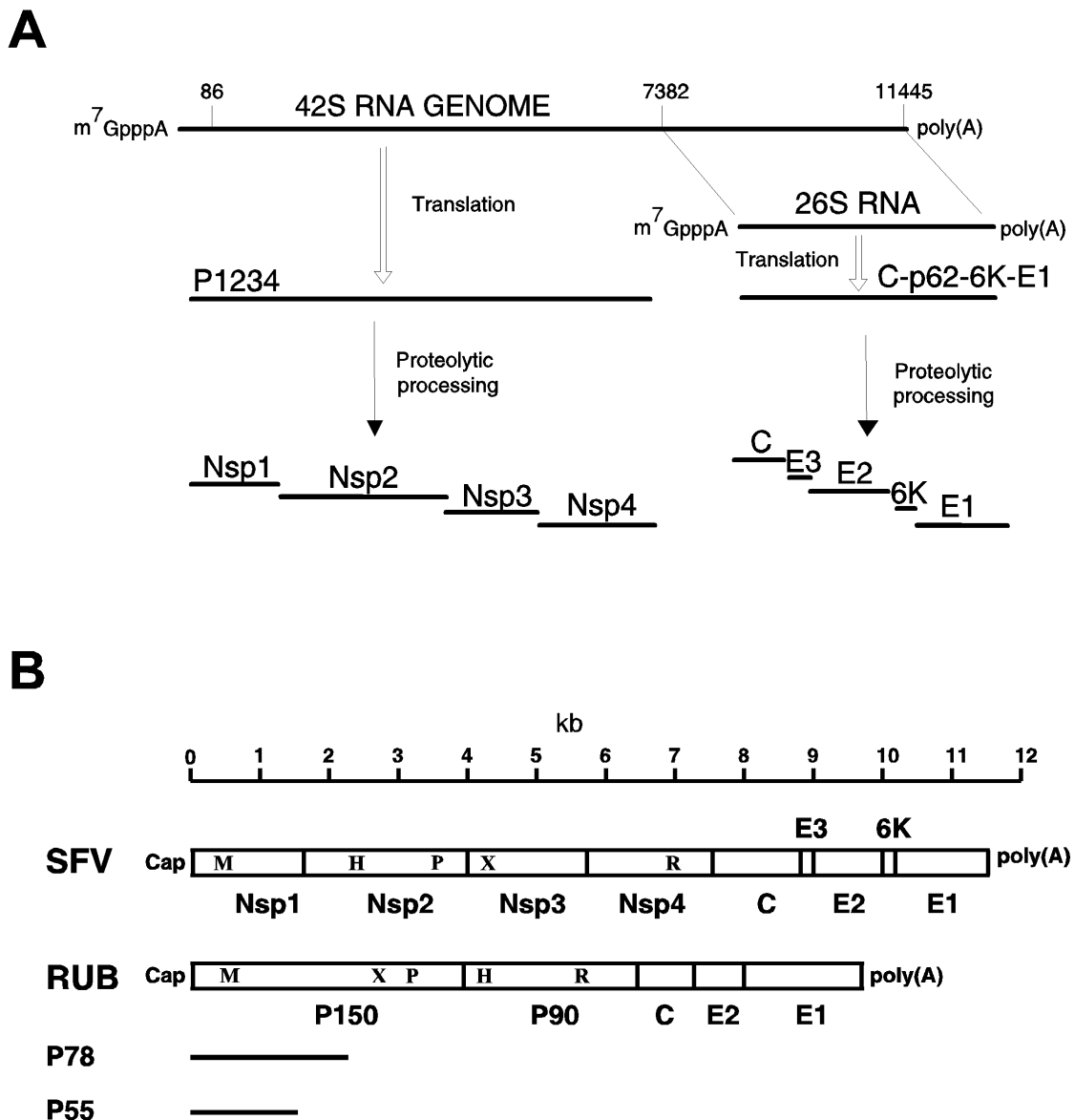


Figure 3. Protein synthesis directed by togavirus RNA molecules. (A) In SFV and other alphaviruses two polyproteins are translated: The N-terminal nonstructural polyprotein (P1234) codes for the replicase proteins Nsp1-4 and the C-terminal structural polyprotein (C-p62-6K-E1) codes for the structural capsid (C) and envelope proteins (E1-3 and 6K). (B) Schematic comparison of the genome organizations of SFV and RUB. Above is the scale in kilobases. RUB genome shows the nonstructural proteins P150 and P90 translated from the N-terminal polyprotein (P220) are followed by the structural capsid (C) and envelope proteins (E1 and E2) translated from a sub-genomic 24S mRNA as a polyprotein similarly to the alphaviruses. H denotes the helicase domain, P the protease domain and R the replicase domain. X is a domain of unknown function, and M the methyltransferase domain. p78 and p55 represent the localization and approximate size of the fragments of RUB genome that were cloned and expressed in III for antibody production. For further details refer to the text.

2.1. Alphavirus replication cycle

2.1.1. Alphavirus entry

The alphaviruses enter the cell by receptor-mediated endocytosis (Helenius et al., 1980; Kielian and Helenius, 1986). Receptor-mediated SFV intake from plasma membrane is shown to be very rapid and efficient as from 1500 up to 3000 virus particles can be internalized per min per cell at high multiplicity of infection (Marsh and Helenius, 1980). Many types of protein receptors can be involved in alphavirus intake at the host plasma membrane. This may explain the wide host range of alphaviruses and the capability to cause infection in various tissues. Most receptors are poorly characterized, but the high-affinity laminin receptor has been identified as a major receptor for SIN in mammalian cells (Wang et al., 1992).

The viral envelope fuses with the membrane of the endosome to deliver the nucleocapsid (NC) into the cytoplasm. The fusion process requires cholesterol on the target membrane (Kielian and Helenius, 1984). The fusion is initiated by a low pH - induced dissociation of the E1-E2 heterodimer leading to formation of E1 homotrimers (Wahlberg and Garoff, 1992; Wahlberg et al., 1992). In the cytoplasm the disassembly of the NC is facilitated by ribosomes, which actively remove the C-proteins, thus releasing the genomic RNA for translation (Singh and Helenius, 1992; Wengler et al. 1992).

2.1.2. Alphavirus replication and translation of the nonstructural polyprotein

Generally, the togavirus genome is translated in early nonstructural and late structural phases. However, the synthesis of structural proteins begins immediately as the subgenomic template for structural proteins is available. The 5' two thirds of the 42S alphavirus genome is translated into a single polyprotein P1234 (2342 aa), which is autocatalytically cleaved to produce

nonstructural proteins Nsp1, Nsp2, Nsp3 and Nsp4 (Keränen and Ruohonen, 1983; Strauss and Strauss, 1994; tem Dam et al., 1999; Fig 3A). These proteins form an RNA-dependent RNA polymerase complex that transcribes the genome into a full-length 42S minus-strand RNA-template, which in turn is replicated to produce more 42S plus-strand RNA. The RNA replication has been suggested to occur via a partly double-stranded RNA replicative intermediate (reviewed by Kääriäinen et al, 1987).

The minus-strand RNA synthesis in alphavirus infection is highly regulated and requires simultaneous viral protein synthesis (Sawicki and Sawicki, 1980). Early in the infection both plus- and minus-strand RNAs are synthesized, but after 3 h pi synthesis of minus-strand ceases and the number of RNA replication complexes becomes constant. Once started the synthesis of plus-strand 42S and 26S RNA continues throughout the infection, even if the viral protein synthesis is inhibited (Sawicki and Sawicki, 1980; Sawicki et al., 1981). The regulation of minus-strand synthesis has been shown to occur through a temporal proteolytic processing of the nonstructural polyprotein (Lemm et al., 1994). Autoproteolytic cleavage of P1234 occurs primarily in *cis* producing P123 and Nsp4. The short-lived intermediate P123 and Nsp4 are predominant forms of nonstructural proteins in the early infection, when the minus-strand RNA synthesis takes place. Later in the infection, when the concentration of P123 is high enough for efficient *trans* cleavage reaction, further processing of P123 continues. First Nsp1 and P23 are separated by cleavage, and finally all the individual nonstructural proteins Nsp1, Nsp2, Nsp3 and Nsp4 are cleaved. It has been hypothesized that proteolytic processing of the nonstructural polyprotein alters irreversibly the affinity of the RNA replicase from the plus-strand to the minus-strand template (Lemm et al., 1994). The number of minus-strands present in an SFV-infected cell has been estimated to be

between 4000 and 7000 molecules (Tuomi et al., 1975; Wang et al., 1991) and the time required to translate a full-length nonstructural polyprotein is estimated to be 8-10 minutes (Keränen and Ruohonen, 1983). The functions of individual nonstructural proteins will be discussed in detail later in this chapter.

2.1.3. Translation of alphavirus structural proteins and virus maturation

The structural proteins; the soluble capsid protein (C) and the membrane proteins p62, 6K and E1 are synthesized as a polyprotein from the 26S subgenomic RNA (Fig. 3A). The polyprotein C-p62-6K-E1 is cleaved cotranslationally (ten Dam et al., 1999). The C-protein possesses a serine protease activity that acts in *cis* to release itself from the nascent polypeptide. In the cytoplasm the C-protein rapidly associates with genomic 42S RNA to form icosahedral NC structures (Söderlund et al., 1973; Söderlund and Kääriäinen, 1974; Ulmanen et al., 1976; Söderlund and Ulmanen, 1977; Weiss et al., 1989; Choi et al., 1991; Forsell et al., 1996; Nicola et al., 1999). With the aid of a signal sequence at the N-terminus of p62, the remaining nascent p62-6K-E1 polypeptide is translocated through the ER membrane (Garoff et al., 1978; 1990). After signal peptidase cleavage, the membrane proteins p62, 6K and E1 are synthesized and translocated to the luminal side of ER, and undergo transport and processing through the cellular secretory pathway. The 6K polypeptide has its own signal sequence, which is essential for the proper ER translocation of the p62-6K-E1 polypeptide. Furthermore, 6K is found to be important for transport and virus assembly. Although it incorporates in small amounts into the final virion (7-30 copies/virion), it cannot be considered as a major structural component like the spike glycoproteins E1, E2 and E3 or the C-protein (Liljeström et al., 1991; Lusa et al., 1991).

The p62 and the E1 proteins form strong heterodimeric complexes in the ER.

Dimerization is essential for their transport through the ER and Golgi apparatus, and finally for particle formation (Wahlberg et al., 1989). Spike proteins are glycosylated by attachment of N-linked oligosaccharide chains, which are further modified during intracellular transport by cellular enzymes (Garoff et al., 1974). In mature SFV virion E1 carries one and E2 two oligosaccharide chains (Pesonen and Kääriäinen, 1982). The precise composition of the oligosaccharides of the virus is dependent on the host cell. Glycoproteins are palmitoylated at several cysteines oriented towards the cytoplasmic face of the lipid bilayer (Bonatti et al., 1989). In SIN the total number of the palmitoylation sites in the glycoproteins is probably between nine and eleven (p62 has four to six, 6K four and E1 one palmitoylation site). The role of the palmitoylation is not clear, but it probably affects the interactions and the orientation of these proteins within the lipid bilayer and takes place after exit from the ER (Bonatti et al., 1989). Mutation analysis has revealed that palmitoylated cysteine residues together with a tyrosine repeat motif in the cytoplasmic domain of SFV E2 glycoprotein are essential for virus budding (Zhao et al., 1994).

The spike complexes are transported to the plasma membrane. Before reaching the cell surface the precursor p62 is cleaved in the trans-Golgi network (TGN) by a furin-type protease into E2 and E3, while E2E1 heterodimeric association is preserved, although it is more labile than before cleavage (Wahlberg et al., 1989; Sariola et al., 1995). In SFV the E3 protein remains noncovalently attached to the spike complex, but in SIN it is released to the medium during virus budding (Wahlberg et al., 1989). Cytoplasmic NCs associate with membranes expressing the viral glycoproteins (Suomalainen et al., 1992; Zhao et al., 1992). A critical density of viral spike proteins is required for the interaction. The NC has binding sites for the C-terminus of the E2 in the glycoprotein spike, which

pulls the envelope tightly around itself. The budding event involves a very accurate sorting process, since only viral proteins are included in the bud and host proteins are excluded (reviewed by Garoff et al., 1998). Alphaviruses are released by budding from the plasma membrane, but later in infection, as the mature glycoproteins accumulate, to a smaller extent also through intracellular membranes. Late in the replication cycle, viral 26S RNA can account approximately for as much as half of the mRNA in the infected cell (Tuomi et al., 1975). It has been estimated that a SFV-infected BHK cell synthesizes about 10^5 molecules of each structural protein per minute (Quinn et al., 1984). The abundance of late 26S RNAs allows production of a large amount of structural proteins required for the assembly of the virus. It has been reported that only 5-10% of the full-length plus-strand 42S RNA is encapsidated during an 8 hour infection, resulting in a maximum yield of 20 000 virus particles per cell (Tuomi et al., 1975).

2.1.4. SFV in cell culture

The alphavirus infection of mammalian cell cultures results in a drastic inhibition of host macromolecular synthesis, allowing the efficient intracellular replication of viral progeny. In SFV-infected cells the synthesis of nonstructural proteins is shut off already at 4 to 5 hours p.i. The rate of virus production remains constant from 5 up to 9 hours p.i. (Acheson and Tamm, 1967), being approximately 2000 pfu/cell/hour (Tuomi et al., 1975). Viral production is associated with the cytopathic effect (CPE) that ultimately leads to cell lysis within 10-12 hours p.i.. The initial events of CPE include rounding of cells and loss of cell to cell contacts, which is followed by classical features of programmed cell death or apoptosis such as nuclear condensation, membrane blistering, cytoplasmic vacuolization, cell fragmentation, and finally cell death (Levine et al., 1993).

The death of most SFV-infected cells results from induction of apoptosis

(Glasgow et al., 1997; Scallan et al., 1997). In general, virus-induced apoptosis is a cellular response to limit viral spread by restricting the level of viral replication (reviewed by O'Brien, 1998). In SIN infection the transmembrane domains of envelope glycoproteins E1 and E2 were shown to be essential for the induction of apoptosis (Joe et al., 1998), whereas in SFV infection the C-terminal region of Nsp2 is reported to contribute to the induction of cell death (Glasgow et al., 1998). Already in the mid 90s Frolov and Schlesinger (1994) had shown some evidence for the critical role of the structural proteins in SIN-induced CPE. Using SIN replicons in BHK cells they found that expression of the SIN nonstructural genes alone was sufficient for host shutoff but that the expression of a replicon encoding the structural genes was required for rapid cytopathic effects similar to wildtype infection (Frolov and Schlesinger, 1994). Contrary to the data of Joe et al. (1998) Grandgirard et al. (1998) suggested that the capsid protein triggers the activation of the cell death machinery in alphavirus (i.e. SIN and SFV) infected cells. According to them capsid protein has three biological activities that could contribute to apoptosis. Firstly, it is able to shut down protein synthesis at high expression levels by provoking the phosphorylation and activation of the interferon-induced double-stranded RNA-activated serine/threonine protein kinase (PKR) as shown by Favre et al. (1996). In SIN the apoptotic pathway has been shown to be triggered by the activation of the nuclear transcription factor NF- κ B (Lin et al., 1995). Activated PKR can phosphorylate the NF- κ B inhibitor I- κ B leading to the release and activation of NF- κ B and thus trigger apoptosis (Grandgirard et al., 1998). Secondly, the capsid protein rapidly translocates into the nucleus where it associates with nucleolar structures (Michel et al., 1990; Favre et al., 1994). Thirdly, capsid protein has a chymotrypsin-like protease activity that acts

in *cis* to release itself from the structural polyprotein as already earlier described (reviewed in ten Dam et al., 1999). The capsid protease could act in *trans* to cleave and activate caspases and thus provoke apoptosis (Grandgirard et al., 1998).

The host defense system can be circumvented by overproduction of endogenous anti-apoptotic proteins, such as bcl-2. Overproduction of bcl-2 by transfection inhibits SIN-induced cell death, with an accompanying shift of the infectious cycle from a lytic into a persistent phase (Levine et al., 1991; 1993). Bcl-2 is a cellular oncogene that acts as a key negative regulator of caspase-mediated cell death. Through its hydrophobic C-terminus bcl-2 is anchored to the outer membranes of mitochondria, the ER and the nuclear envelope, where it forms a cation selective ion channel similar to some bacterial toxins. Bcl-2 is proposed to block the release of cytochrome c from mitochondria into cytosol and attract cytosolic adapter molecules, which probably serve to prevent the activation of caspases in response to apoptotic stimuli (reviewed by Kroener, 1997). In addition to bcl-2 several other gene products that can block the SIN-induced apoptotic pathway have been identified including another member of the bcl-2 oncogene family, namely bcl-XL (Cheng et al., 1996). Neuronal apoptosis has been shown to be a central mechanism in SIN-induced encephalitis in susceptible mice (Levine et al., 1996; Lewis et al., 1996). The death of SFV-infected neurons is reported to occur by necrosis rather than apoptosis (Atkins et al., 1990; Glasgow et al., 1997).

Taken together, the results obtained for apoptosis induction by alphaviruses are conflicting. It is not likely that SFV and SIN would have different mechanisms in apoptotic induction, and the fundamental viral function leading to apoptosis through the caspase-mediated cleavage of bcl-2 is not completely resolved (Atkins et al., 1999). Interestingly, two of the proposed

candidates for provoking apoptosis in alphavirus infected cells, i.e. Nsp2 and capsid protein, have some common features. They are both serine proteases, which can act in *trans* and thus may activate caspases as suggested by Grandgirard et al., (1998). Furthermore, both of them have karyophilic properties and are targeted to the nucleus (Rikonen et al., 1992; Michel et al., 1990).

During alphavirus infection two main types of morphologically distinct, virus-induced cytopathic vacuoles can be observed. Cytopathic vacuoles of type I (CPV-I) form in the early phase in infection (Acheson and Tamm, 1967, Grimley et al., 1968). They represent the sites of viral RNA replication and CPV-I structures will be discussed in detail later in the chapter on the togavirus RNA replication complex. Type II (CPV-II) vacuolar structures form in the late phase in alphavirus infection and consist of numerous nucleocapsids attached to the cytoplasmic face of membranes (Grimley et al., 1968). This is due to spike proteins, which tend to accumulate in the Golgi complex late in infection and start to bind nucleocapsids. A third type of cytopathic structures are dense membrane tubular formations with nucleocapsids lined up against the periphery of internal membranes, sometimes termed CPV-III (Zhao et al., 1994). They are presumably a variation of CPV-II structures. Griffiths et al. (1983) have used the term intracellular capsid-binding membranes (ICBM) collectively for CPV-II and CPV-III structures.

Alphavirus infected cells are affected by a phenomenon known as homologous interference or superinfection exclusion. This is a virus-established state, where the infected cell rapidly becomes resistant to superinfection by a virus of the same or related species. Several mechanisms leading to superinfection exclusion have been suggested (reviewed in Strauss and Strauss, 1994). Firstly, a host protein or other cell component required for viral replication may be a limiting factor for the initiation of

a new replication cycle. Secondly, temporal regulation of minus-strand synthesis of the superinfecting virus by P123 and Nsp4 may be prohibited, since cleaved functional nonstructural proteins produced by the first infecting virus already exists in the cell. Or thirdly, the first virus has reached a kinetic advantage in the exponential increase of its minus-strand synthesis, which the second virus is unable to overcome. Thus the first infecting virus could sequester limited cellular components in a specific membrane bound replication compartment unavailable for further superinfecting viruses (Strauss and Strauss, 1994).

2.2. The rubella virus replication cycle

2.2.1. RUB entry and translation of the nonstructural polyprotein

The initial stages of RUB replication cycle resemble that described for SFV. The virus attaches to an undefined receptor on the plasma membrane and is internalized by a clathrin-dependent endocytic pathway. The viral envelope fuses with the membrane of the endosome following acidification of the endosomal lumen and the single stranded 40S RNA genome is released into the cytoplasm (Petruzzello et al., 1996). Virus-specific RNA replicase is synthesized as a large P200 polyprotein (Fig. 3B), which is processed into two nonstructural proteins P150 and P90 (Marr et al., 1994; Fornig and Frey, 1995, Chen et al., 1996, ten Dam et al., 1999). The RUB RNA replicase proteins will be discussed in more detail in the chapter the togavirus RNA replicase proteins.

2.2.2. Translation of RUB structural proteins and virus maturation

Structural proteins of RUB are produced from a subgenomic 24S RNA (Fig 3B). It encodes three structural proteins, which are produced from a single polyprotein precursor C-E2-E1 (3327 nt) (Oker-Blom et

al., 1983; Oker-Blom, 1984; Frey et al., 1989; Dominguez et al., 1990). A signal sequence mediates translocation of E2 and E1 to the ER lumen, where a luminal signalase catalyzes the cleavage of C-E2 and E2-E1. RUB C-protein lacks the autoprotease activity found in alphaviruses (Oker-Blom et al., 1984, Clarke et al., 1988). Thus the C-protein remains associated with the E2 signal sequence and the ER membrane (Suomalainen et al., 1990). The maintenance of E2 signal sequence as part of the C-protein is unique for RUB (Frey, 1994). The phosphorylated C-protein forms a noncovalently bonded dimer (Baron and Forsell, 1991) before the mature molecule can interact with genomic 40S RNA. Similarly to alphavirus spike proteins, a number of cotranslational and posttranslational modifications of RUB glycoproteins take place during their transport (Hobman et al., 1990). These include glycosylation by predominantly high mannose glycans and palmitoylation, which is believed to occur in the ER. RUB NC assembly occurs with association of virus modified membranes and is synchronized with virus budding (Hobman et al., 1990; Frey, 1994). Accumulation of membranes containing viral glycoproteins and virus budding are generally observed in the Golgi region (Fig. 4A). In addition to Golgi, budding occurs to some extent through ER membranes and into intracellular vacuoles, but at later times also at the PM (von Bonsdorff and Vaheri, 1969; Bowden and Westaway, 1989; Lee et al., 1992). The capacity of RUB to mature within the cell hidden from the host immune system may be an important feature for the establishment of persistent infections in humans. Taken together, although it appears that RUB and SFV share similar strategies with regard to entry and RNA replication (Petruzzello et al., 1996, Magliano et al., 1998), it has become clear that the assembly pathways of RUB and the alphaviruses are quite different.

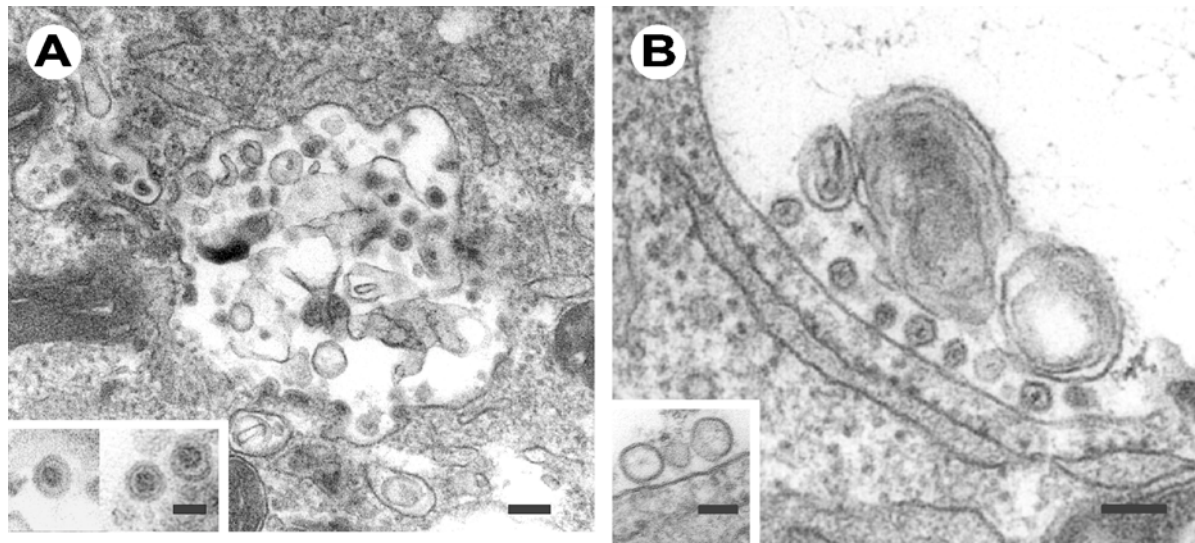


Figure 4. RUB virions and membrane associated RNA replication complexes form morphologically distinct entities. RUB buds mainly into intracellular vesicles derived from the Golgi region, whereas the RNA replication takes place on the limiting membrane of endolysosomal vacuoles. TEM micrographs of budding virions with large dense cores and characteristic halo between core and envelope (A) and RUB replication complexes (i.e. spherules) at the limiting membrane of a large endolysosomal vacuole (B), which is closely surrounded by ER-derived membranes. In contrast to virions, spherules have a thread-like appearance and a tiny electron dense core with thin hairy spokes radiating towards the clearly bilayered limiting membrane of the spherule. Bars 200 nm, in enlarged inserts 50 nm.

2.2.3. RUB in cell cultures

RUB replicates slowly and to relatively low titers in a number of primary cell cultures and continuous cell lines of vertebrates. RUB is most productive in BHK and Vero cell lines, where virus titers up to 10^7 pfu/ml can be obtained (Frey, 1994). The RUB infection is not synchronous, even at high multiplicities of infection, and only a fraction of the cells are infected. An absence of uniform infection is apparent in immunofluorescence studies, especially with RUB-infected BHK cells, whereas Vero cells are more confirmly infected (Hemphill et al., 1988). Superinfection exclusion described for alphaviruses has not been reported to occur in RUB-infected cells. In contrast, interference with other viruses has been reported and for example the original isolation of RUB was carried out from cells coinfecting with poliovirus (reviewed in Frey, 1994).

In RUB-infected Vero cells a gradual increase of virus titer starts after about a 12 h lag phase and levels off at 36-48 h p.i. (Lee et al., 1992; Frey 1994; Pugachev et al., 1997). The synthesis rate of the viral genomic 40S RNA and the subgenomic 24S RNA peaks at about 24 h p.i. (Hemphill et al., 1988). The number of virions produced in RUB-infected cells is at least 100-fold lower compared to the yield of alphavirus infection (Frey, 1994).

The molecular basis of the inefficiency of RUB replication is not known. However, it has been suggested that the high G+C-content of RUB genome leads to a pattern of codon usage that is different from that found in human genes. Thus the rate of translation of the RUB RNAs could be limited by the availability of the required tRNA species in infected cell. Secondly, and maybe more likely, the high G+C content imparts greater stability to the

secondary structures of RUB single-stranded RNAs and the double-stranded RNA replicative complexes (Frey, 1994).

Generally, RUB produces little or no cytopathic effect (CPE) in infected cells. CPE observed in RUB-infected Vero cell cultures consists of cell rounding and detachment, cell vacuolation and the presence of cell debris or secreted cellular material adhering to the cell monolayer (Frey, 1994). RUB infection causes stimulation of membrane biosynthesis and proliferation of smooth membranes. Especially alternations in the membrane systems of the ER, the Golgi complex and mitochondria have been reported (von Bonsdorff and Vaehri, 1969; Lee et al., 1994). Cytoskeletal effects include depolymerization of actin filaments and disturbance of microtubular organization (Bowden et al., 1987). In no RUB-infected cell line is cell destruction complete, and a persistent infection with minimal cytopathology is established within 12 weeks (Pugachev and Frey, 1998a). RUB-infection does not have a major effect on host macromolecular synthesis early in infection (Hemphill et al., 1988). However, varying effects on macromolecular synthesis are observable late in infection. RUB causes genetic alterations, such as chromosomal breaks, and perturbs the physiological cell cycle regulation. Thus, RUB-infected cells grow and divide more slowly than uninfected cells (Vaehri et al., 1965; Plotkin and Vaehri, 1967).

RUB-mediated apoptosis is reported to occur through p53 and bcl-2 independent pathways in R13 and Vero cells (Pugachev and Frey, 1998b; Duncan et al., 1999; Hofman et al., 1999; Megyeri et al., 1999). However, in RUB-infected BHK cells increased expression of Bcl-X_L (a member of bcl-2 family) by transfection protected cells from apoptosis (Duncan et al., 1999) indicating a variety of apoptotic responses to RUB in different cell lines. RUB has similar E1, E2 and capsid structural proteins, which have been suggested to

induce apoptosis in alphavirus infected cells (Joe et al., 1998; Grandgirard et al., 1998). However, expression of RUB structural proteins does not induce apoptosis, implicating that replicating virus is necessary to provoke apoptosis (Hofman et al., 1999). RUB strain differences in cytopathogenicity map to the nonstructural proteins further suggesting a role of RNA replicase proteins in apoptosis induction (Pugachev et al., 1997).

3. THE TOGAVIRUS RNA REPLICASE PROTEINS

3.1. SFV RNA replicase proteins

The functions of the SFV Nsps in virus RNA replication have been studied using genetic and biochemical approaches, as well as sequence comparisons (Kääriäinen et al., 1987; Strauss and Strauss, 1994). Individual Nsps have been expressed in different host cells including bacteria, insect and mammalian cells (Ahola and Kääriäinen, 1995; Laakkonen et al., 1994; Peränen, 1991; Peränen and Kääriäinen, 1991; Peränen et al., 1988, 1990, 1991, 1995; Rikkinen, 1996; Rikkinen et al., 1992, 1994; Takkinen et al., 1990, 1991, Vasiljeva et al., 2000).

3.1.1. Nsp1

Nsp1 (537 aa, 64 kDa) is the viral mRNA capping enzyme, which catalyzes two virus-specific reactions: firstly it functions as a guanine-7-methyltransferase methylating GTP into m⁷GTP, and secondly acts as a guanylyltransferase Nsp1 forming a covalent complex with m⁷GMP (Ahola and Kääriäinen, 1995; Laakkonen et al., 1994; Ahola et al., 1997). Identification of the virus-specific capping reaction has formed the basis for designing compounds which can inhibit virus replication without affecting the host cell. Nsp1 is needed for the initiation of the minus-strand RNA-synthesis (Sawicki et al., 1981; Hahn et al., 1989a; Wang et al., 1991). It is

palmitoylated on cysteine residues 418-420 (Peränen et al., 1995; Laakkonen et al., 1996). Palmitoylation is not required for the enzymatic activities involved in capping, but affects the membrane association of Nsp1 as palmitate inserts into the lipid bilayers. When the protein is expressed alone in mammalian cells, the palmitoylated Nsp1 binds very tightly to the membrane, whereas a nonpalmitoylated mutant is more loosely membrane-attached (Laakkonen et al., 1996). The palmitoylation-independent mechanism of Nsp1 membrane association appears to involve a direct interaction of the protein with anionic phospholipid headgroups. This interaction is mediated by a conserved polybasic Nsp1 segment (aa 245-264), which is distant from the palmitoylation site in the primary sequence (Ahola et al., 1999). Interaction of Nsp1 with negatively charged lipids is required to activate the methyl- and guanylyltransferase activities needed in the capping of the viral RNAs (Ahola and Kääriäinen, 1995; Ahola et al., 1999).

3.1.2. Nsp2

Nsp2 (799 aa, 86 kDa) is a multifunctional enzyme that plays a role in the regulation of the synthesis of the subgenomic 26S RNA (Sawicki and Sawicki, 1985; deGroot et al., 1990; Suopanki et al., 1998). Nsp2 is required for the shutoff of minus-strand synthesis (Hahn et al., 1989a; De et al., 1996). The carboxy-terminal papain-like thiol proteinase domain of Nsp2 is responsible for the processing of the nonstructural polyprotein P1234 (Ding and Schlesinger, 1989; Hardy and Strauss, 1989; Hardy et al., 1990). Nsp2 is shown to be an NTPase (Rikkonen, 1996; Rikkonen et al., 1994), an RNA helicase (Gomez de Cedron et al., 1998) and an RNA triphosphatase (Vasiljieva et al., 2000). These activities essential for viral RNA replication were partly predicted by sequence comparisons, since the N-terminal region of Nsp2 contains at least six amino acid motifs of the NTPase/helicase

superfamily (Gorbalenya and Koonin, 1989; 1993; Koonin, 1991). During infection half of the Nsp2 is transported to the nucleus and nucleoli (Peränen et al., 1990). Expression of Nsp2 alone allowed the identification of a nuclear targeting signal (NLS) with a core sequence P⁶⁴⁸RRRV (Rikkonen et al., 1992). A mutation in NLS, which prevented the nuclear transport, did not affect virus replication in cell cultures, but abolished the neuropathogenicity of the virus for mice (Rikkonen, 1996). In the cytoplasm about 50% of Nsp2 is associated with membranes, whereas 50% remains soluble (Peränen et al., 1988). Soluble Nsp2 may be associated with ribosomes (Ranki et al., 1979). Nsp2 has been suggested to participate in the induction of apoptosis. Deletion of a C-terminal part (Δ 2572-3914) of the SFV Nsp2 gene has abolished both induction of apoptosis and viral RNA synthesis (Glasgow et al., 1998).

3.1.3. Nsp3

Nsp3 (482 aa, 61 kDa) is a component essential for viral RNA replication, but its specific functions are not known (Hahn et al., 1989a). Studies of temperature-sensitive and linker-insertion mutants of SIN Nsp3 have implicated the necessity of the protein in minus-strand RNA synthesis, and presumably also in the synthesis of the subgenomic 26S RNA (Wang et al., 1994; LaStarza et al., 1994). The N-terminal third of Nsp3 shares a small domain without known function conserved in alphaviruses, RUB, hepatitis E virus and coronaviruses, termed the X-domain (Koonin and Dolja, 1993). Recently it has been shown that a homologous domain is more widely distributed in bacteria, archaeobacteria and eukaryotes, and a more divergent domain is found in unusual histone variants, the macrohistones (Pehrson and Fuji, 1998). The middle third of Nsp3 is conserved among alphaviruses, whereas the C-terminal third represents a hypervariable region with varied length among alphaviruses. Alphavirus Nsp3 is posttranslationally

modified by phosphorylation (Peränen et al., 1988; Li et al., 1990). Phosphoamino acid analysis of SFV Nsp3 showed that serine and threonine residues are phosphorylated, whereas no phosphotyrosine could be found (Peränen et al., 1988). Deletion analysis of the nonconserved region of SIN Nsp3 considerably reduced Nsp3 phosphorylation, suggesting that the C-terminal tail is the major site of the phosphorylated amino acid residues (LaStarza et al., 1994). In SFV Nsp3 the major phosphorylation sites have been localized to the region of aa 320-367, where up to 16 serine and threonine residues can be phosphorylated depending on the infected or transfected host cell line (Vihinen and Saarinen, 2000; Vihinen et al., 2000).

3.1.4. Nsp4

Nsp4 (614 aa, 68kDa) is thought to be the actual RNA polymerase unit of the RNA replication complex. It displays the conserved GDD motif found in RNA polymerases of other animal and plant viruses (Kamer and Argos, 1984; Argos, 1988). Although direct biochemical proof is still lacking, there is genetic evidence supporting this hypothesis (Keränen and Kääriäinen, 1974; Hahn et al., 1989b; Sawicki et al., 1981). Nsp4 is suggested to interact with host protein components which modulate the viral RNA replication (Lemm et al., 1990). In alphavirus infected cells Nsp4 is unstable and rapidly degraded by the N-end rule pathway of ubiquitin mediated degradation (deGroot et al., 1991). SIN Nsp4 is produced in extremely low quantities partly due to low frequency of translation through an amber stop-codon located upstream of the coding region in the RNA plus-strand (Strauss et al., 1983).

3.2. RUB RNA replicase proteins

Compared to the alphaviruses our current knowledge of RUB nonstructural proteins is limited and based mainly on sequence homology analyses (Frey, 1994).

The biochemical characterization of RUB nonstructural proteins has been hampered by a lack of specific antibodies of sufficient quality. The G+C rich open reading frame (ORF) encoding for nonstructural proteins has been extremely difficult to clone for antibody production (Frey 1994; Auvinen, P. and Merits, A., personal communication). However, Marr et al. (1994) succeeded in expressing three RUB Nsp-ORF-specific products (200, 150 and 97 kDa, respectively) in a vaccinia virus transient-expression system. Mutagenesis of a cysteine predicted by computer alignment to be a critical residue of a protease active site resulted in disappearance of both the P150 and P90 species, demonstrating that a RUB nonstructural protease is responsible for the proteolytic processing of the precursor P200 to P150 and P90 nonstructural proteins (Marr et al., 1994). Further immunoprecipitation studies with antibodies against bacterial fusion proteins containing regions of the RUB nonstructural polyprotein confirmed that two nonstructural proteins P150 and P90 are produced and can be found in RUB-infected cells (Froning and Frey, 1995). P150 corresponds to the N-terminal and P90 to the C-terminal part of the nonstructural polyprotein (Froning and Frey, 1995). These two proteins share common methyltransferase, protease, helicase and polymerase domains with sequence similarity to alphavirus RNA replicase proteins (Nsp1-4), but arranged in a different order (Koonin and Dolja, 1993; Fig 3B).

Phylogenetic analyses of the nonstructural region have suggested that RUB is more closely related to hepatitis E virus than to alphaviruses. In a similar analysis alpha-viruses turned out to be more related to the plant virus members (tobacco mosaic, brome mosaic and alfalfa mosaic viruses) of the alphavirus-like superfamily than to RUB (Koonin and Dolja, 1993). This indicates that togavirus evolution is complicated and further suggests that alphaviruses may have arisen by

recombination between a rubella-like virus and another alphavirus-like superfamily member of plant viruses, such as tobacco mosaic virus (Frey 1994; Chen et al., 1996).

3.2.1. P150

P150 (1301 aa, 140 kDa) contains a papain-like protease, which mediates the proteolytic processing of nonstructural P200 polyprotein by a single *cis* cleavage (Gorbalenya et al., 1991; Marr et al., 1994; Forng and Frey, 1995; Chen et al., 1996). A more recent *in vitro* study has shown that in the presence of divalent cations RUB protease can also function in *trans* (Liu et al., 1998). By deletion mutagenesis the proteinase domain has been localized between aa 1006 and 1508 of the nonstructural polyprotein, Cys 1151 being the catalytic residue of the RUB protease (Marr et al., 1994). P150 shares the X-motif of unknown function with alphavirus Nsp3 discussed already in the context of SFV Nsp3. Interestingly, the X-domain is present only in the genome of animal virus families within the alphavirus-like superfamily. The weakly homologous common methyl-transferase domain localizes at the N-terminal part of P150, which corresponds to alphavirus Nsp1 (Gorbalenya et al., 1991; Koonin and Dolja, 1993).

3.2.2. P90

P90 (904 aa, 100 kDa) has the conserved GK(S/T) motif indicative for RNA helicase, and the GDD motif indicative of RNA polymerase activity (Argos, 1988; Koonin and Dolja, 1993; Frey 1994). Evidence consistent with an RNA helicase activity was obtained when the RUB RNA helicase domain (aa 1225 to aa 1664 in the nonstructural polyprotein) was expressed as a bacterial fusion protein. This expression construct possessed NTPase activity, which was stimulated in the presence of poly(U), poly(C) and poly(T), but inhibited in the presence of poly(G) (Gros and Wengler, 1996).

4. THE TOGAVIRUS RNA REPLICATION COMPLEX

The RNA replication of alphaviruses takes place in the cytoplasm in association with cellular membranes. The parental RNA of the infecting SIN was shown to be bound to intracellular membranes if the protein synthesis was not inhibited (Sreevalsan, 1970). Early electron microscopic studies identified morphologically distinct membrane-bound vacuoles in SFV infected cells (Acheson and Tamm, 1967; Friedman and Berezsky, 1967), which were designated as cytopathic vacuoles type I or CPV-I (Grimley et al., 1968). CPV-I were described as complex vacuolar structures with a diameter of 0.6-2 μ m. They contained small 50 nm membrane invaginations or spherules, which lined the limiting membrane at regular intervals and pointed towards the vacuolar lumen. Each spherule had a dark electron dense central spot in an otherwise lightly staining interior, and was connected through a narrow membranous neck to the limiting membrane of the CPV-I (Acheson and Tamm, 1967; Grimley et al., 1968; 1972).

CPV-I formed early in infection and were observed first at 3 hours p.i. with high m.o.i. Batches of spherules were also observed on the surface of the plasma membrane. Inhibition of host RNA synthesis by actinomycin D had no effect on neither virus replication nor CPV-I formation. In contrast, inhibition of protein synthesis by cycloheximide early in infection (2 h p.i.) prevented CPV-I formation, but not any more at 4 h p.i. This indicated that host translation machinery was required for the initial formation of the viral RNA replication sites. Acid phosphatase activity was also shown to be associated with many CPV-Is (Grimley et al., 1972). Electron microscopic autoradiography, carried out with cells pulse-labeled with tritiated uridine, suggested that the limiting membrane of

CPV-I and the plasma membrane represented significant elements of the alphavirus RNA replication complex (Grimley et al., 1968; 1972). Friedman et al. (1972) isolated by isopycnic sucrose gradient centrifugation a membranous fraction from SFV-infected cells with a density of 1.16 g/cm^3 , which was enriched in CPV-Is, had RNA polymerase activity *in vitro* and was enriched in pulse-labeled viral RNA.

The cytoplasmic membranes exhibiting alphavirus RNA replicase activity can be pelleted by centrifugation at $15,000 \times g$ (Ranki and Kääriäinen, 1979). The resulting membrane fraction P15, contains various cellular organelles, such as mitochondria, peroxisomes, ER-membranes and endolysosomal vesicles, but also the viral RNA replication complexes consisting of the viral RNAs and nonstructural proteins (Ranki and Kääriäinen, 1979; Barton et al., 1991). Biochemical studies have shown that the major pool of each Nsp is found associated with P15 membranes. However, the amino acid sequences of the alphavirus Nsps are hydrophilic (Strauss et al., 1984; Takkinen, 1986), and thus the mechanism of membrane attachment of the RNA replication complex cannot be predicted from the sequence. Expression of individual Nsps in animal cells has indicated that Nsp2 and Nsp4 do not associate with membranes, whereas Nsp3 and especially Nsp1 show an affinity for membranes (Peränen and Kääriäinen, 1991; Peränen et al., 1993; Peränen et al., 1995).

The synthesis of Nsps initially from a polyprotein would favor their interaction to form a RNA replication complex. A majority of RNA replication complexes are formed before 4 h p.i. and are stable once formed (Gomatos et al., 1980; Sawicki and Sawicki, 1986a; Sawicki and Sawicki, 1986b; Wang et al., 1991; Barton et al., 1991). Purification of SFV RNA replication complexes after solubilization of the P15 fraction with detergents released smooth membranes and increased the density of the

RNA replication complex fraction to 1.25 g/ml (Barton et al., 1991). The biochemical characterization revealed that the Tx-100-deoxycholate-solubilized RNA replication complex retained some RNA polymerase activity *in vitro* and was associated with a cytoskeletal framework including actin, tubulin and myosin. Immunoprecipitation of the solubilized RNA polymerase fraction indicated that all nonstructural proteins were complexed together with an undefined host component of 120 kDa (Barton et al., 1991).

An important contribution to the studies of the origin of CPV-I was supplied by Froshauer et al. (1988). They demonstrated the endosomal origin of CPV-Is with cationic ferritin as a tracer. By immunoperoxidase cytochemistry they showed that the majority of CPV-Is stained positively with late endosomal/lysosomal markers lamp-1 and lamp-2 but also with lysosomal hydrolase cathepsin L. However, the normal isolation procedure of lysosomes from SFV and SIN infected CHO cells by free-flow electrophoresis revealed that CPV-Is enriched into a different fraction than the soluble lysosomal marker β -hexosaminidase. CPV-Is were found in a more protein-rich fraction together with nascent viral RNA molecules labeled in the presence of actinomycin D with [^3H]-uridine indicating that the RNA polymerase did not locate in the β -hexosaminidase-positive lysosomal fraction. Further analysis confirmed that immunoprecipitation of [^{35}S]-methionine-labeled SIN nonstructural proteins could be detected only in the nonlysosomal fractions containing the CPV-Is.

Pre-embedding immuno-EM localization of SIN Nsp3 and Nsp4 in semi-permeabilized and saponin-treated CHO cells labeled fibrous, granular material, which seemed to be attached to CPV-Is at the base of the spherules. This material extended into the cytoplasm as a complex, fibrillar and granular network and it often contained granules which corresponded in size and morphology to ribosomes and to

nucleocapsids. A close connection of CPVIs and RER membranes was suggested as a mechanism of transfer of newly made mRNAs directly to the site of structural protein synthesis and assembly of nucleocapsids. It was concluded that alphavirus RNA replication occurs in complex ribonucleoprotein structures on the surface of CPV-Is, which are derived from endosomes and lysosomes. Modification of endosomes and lysosomes into viral RNA replication factories was suggested to be a direct consequence of viral entry by adsorptive endocytosis and subsequent fusion of the virus envelope with the endolysosomal membranes (Marsh and Helenius, 1980; Marsh et al., 1983; Kielian and Helenius, 1986). The increasing number of CPV-Is during infection was found to be directly proportional to the amount of incoming virions (Froshauer et al., 1988).

Some of the conclusions drawn by Froshauer et al. (1988) were challenged by Peränen and Kääriäinen (1991). By using a temperature-sensitive ts1 mutant of SFV they showed that the time of appearance, but not the number of CPV-Is, was dependent on the multiplicity of infection. SFV ts1 mutant does not produce virus particles at restrictive temperature and is thus unable to superinfect the cells (Keränen and Kääriäinen, 1974). The CPV-Is were observed also when BHK cells were transfected with purified infectious RNA derived from either wild type SFV or ts1 (Peränen and Kääriäinen, 1991).

Structures similar to alphavirus CPV-Is have been described also in RUB-infected cells (Lee et al., 1992; 1994) suggesting that the spherules are structures characteristic of the RNA replication process of togaviruses in general. Despite their similar dimensions, spherules and virions are morphologically clearly separate entities (Fig 4). The round or ovoid electron dense cores of RUB virions are distinct from the irregular fibrous or thread-like inclusions observed in RUB spherules (Lee et al., 1992). The RUB CPV-Is double-stain with antisera against double-stranded RNA and lysosomal marker such as lamp-1 which as seen by immunoelectron microscopy localize not only in the immediate vicinity of the limiting membrane of CPV-I but also to spherules (Magliano et al., 1998). For convenience, the abbreviation CPV for CPV-Is, and the collective term ICBM for nucleocapsid associated membranes and vacuoles of the CPV-II and the CPV-III types will be used from here on.

AIMS OF THE STUDY

The aim of this study was to characterize viral structures associated with the togavirus RNA replicase components in infected and transfected cells. For this purpose specific antibodies were raised against the individual SFV (Nsp1-4) and RUB (P150) non-structural proteins, to be used in immunofluorescence and immunoelectron microscopic studies.

MATERIALS AND METHODS

Cells and viruses

Baby hamster kidney cells (BHK-21) were maintained in Dulbecco's modified minimal essential medium supplemented with 10% fetal or newborn calf serum (PAA Laboratories, Austria), and 100 U/ml of penicillin and 100 µg/ml streptomycin (Life Technologies Inc., USA). The cultivation of Green monkey kidney cells (Vero cells) has been described (Oker-Blom et al., 1983). For antibody production the propagation of plasmids was carried out in *Escherichia coli* DH5α (Bethesda Research Laboratories) and the antigens were expressed in *E. coli* BL21(DE3) (Novagen) or JM109 (Promega). For production of mAbs Pa1 myeloma cells (Sinijärvi et al., 1988) and BALB/c female mice were used to produce hybridoma cell lines. The propagation of SFV prototype has been documented by Keränen and Kääriäinen (1974). The full-length Sindbis virus infectious cDNA clone was kindly supplied by Dr. Charles M. Rice (Washington University, St. Louis, USA). The origin, cloning and cultivation of rubella virus, Therian strain, has been described previously (Oker-Blom et al., 1983). The vTF7-3 recombinant vaccinia virus stock was prepared in HeLa cells as described by Fuerst et al., (1986). Recombinant vaccinia virus Ankara (MVA) was grown and expressed as described by Wyatt et al., (1995). Both recombinant vaccinia strains were kindly provided by Dr. Bernard Moss (National Institutes of Health, Bethesda, MD, USA).

Antisera

Semliki Forest virus anti-Nsp1 and anti-Nsp3 are polyclonal antisera prepared in rabbits (Hyvönen et al., unpublished). The SFV structural proteins were localized with antisera against purified envelope glycoproteins E1 and E2 (Väänänen, 1982) and with anti-capsid antisera (Väänänen and Kääriäinen, 1980) all prepared in rabbits.

For visualizing the rubella structural proteins monoclonal mouse antibodies, clones C2 and C7, against RUB capsid protein (Wolinsky et al., 1991) and rabbit polyclonal rubella E2 envelope antibody (Oker-Blom, 1984) were used. A rat mAb (BU1/75 [ICR1]; Harlan Sera-Lab Ltd., Loughborough, UK) raised against bromodeoxyuridine (BrdU) was used to detect viral RNA metabolically labeled with bromo-UTP (BrUTP; Sigma). Cytoskeletal elements were visualized with a mouse anti-β-tubulin mAb (B-5-1-2; Sigma) and Oregon green-conjugated phalloidin (Molecular Probes Europe BV, the Netherlands). Anti-vimentin (24BA6 and 65EE3) and anti-keratin (4B11 and 2A4) monoclonal antibodies were obtained from Dr. E. Lehtonen and Dr. I. Virtanen (University of Helsinki, Finland). Mouse monoclonal antibody against CD44 (Hermes 3) was obtained from Dr. Sirpa Jalkanen (National Public Health Institute, Turku, Finland). Anti-paxillin (Z035) was purchased from Zymed (USA). Anti-vinculin (hVIN-1), anti-talin (T-3287) and anti-phosphotyrosine (PT-66) were from Sigma (USA). Mouse monoclonal antibody against ezrin (3C12) was a kind gift of Dr. Antti Vaheri (Haartman Institute, University of Helsinki).

For characterization of the cellular origin of SFV CPVs the following cellular markers were used: human lysosome-associated membrane glycoproteins 1 and 2 (lamp-1 and lamp-2; Karlsson and Carlsson, 1988), cation-independent mannose 6-phosphate receptor (CI-MPR; Dr. Eeva-Liisa Eskelinen, Institute of Biotechnology, Helsinki), Rab7 (Dr. Marino Zerial, EMBL, Heidelberg, Germany), p58 (Sigma), Cab 45 (Dr. Vesa Olkkonen, National Public Health Institute, Helsinki), protein disulfide isomerase (PDI; Dr. Steven Fuller, EMBL, Germany), early endosome associated antigen 1 (EEA1; Dr. Harald Stenmark,

Radium Institute, Oslo, Norway), lysobisphosphatidyl acid (LBPA; Kobayashi et al., 1999) and human transferrin receptor (h-TfR; mAb B3-25, Boeringer Mannheim). Polyclonal anti-BiP directed against the C-terminus of rat grp78, was from StressGene (Victoria, Canada).

Methods

The methods used in this study are listed in Table 1 and are described in the original manuscripts as indicated, or they have been used according to the manufacturers' instructions. DNA manipulation and cloning were performed by standard methods (Sambrook et al., 1989). Only morphological methods will be described in detail in this section.

Confocal immunofluorescence microscopy (III, IV)

Confocal immunofluorescence microscopy was carried out for infected or transfected cell monolayers on cover slips. After fixation with 3% paraformaldehyde in 10 mM MES, pH 6.1, 138 mM KCl, 3 mM MgCl₂, 2 mM EGTA and 0.32 M sucrose, the aldehyde groups were quenched with 50 mM NH₄Cl. The cells were permeabilized with 0.05% Triton X-100, treated with the primary antibody followed by either fluorescein isothiocyanate (FITC) or rhodamine (TRITC) conjugated secondary antibody. The samples were analyzed with a Bio-Rad MRC-1024 confocal microscope

Table 1. List of methods used in the present study.

<i>Method</i>	<i>Used in publication(s)</i>
Coimmunoprecipitation	I, IV
Cryo immunoelectron microscopy	III, IV
Dot blot analysis	I
ELISA	I
Immunoprecipitation	I, III, IV
Indirect immunofluorescence microscopy	I, II, III, IV
Metabolic labeling of proteins	III, IV
Metabolic labeling of RNA	III, IV
Metal-affinity chromatography	I, IV
PCR-amplification	III
Plasmid construction	I, III, IV
Pre-embedding immunoelectron microscopy	III, IV
RNA isolation	III
Scanning electron microscopy	II
SDS-PAGE	I, III, IV
Transfection	II, IV
Transmission electron microscopy	II, III, IV
Tunneling electron microscopy	II
Video microscopy	II
Virus infection	I, II, III, IV
Western analysis	I, II, III, IV
Whole-mount transmission electron microscopy	II

(Bio-Rad, Cambridge, Mass.), with an argon-krypton ion laser (American Laser Corporation, Salt Lake City, Utah). FITC-stained samples were imaged by excitation at 488 nm and with a 505- to 540-nm bandpass emission filter; TRITC-stained samples were imaged by excitation at 568 nm and with a 598 nm to 621 nm bandpass emission filter.

Video microscopy (II)

Cells were grown on coverslips and transfected as described by Peränen et al., (1995). The coverslips were washed 3 times after incubation with the virus and after the transfection. Transfected cells and control cells were transferred to a new Petri dish containing Optimem and 10 mM hydroxyurea. The Petri dishes were placed on a Linkman LO 102 thermoplate (USA) and observed at 37°C for 30 to 60 min as indicated. The images were collected using a Zeiss axiowert 100 microscope (Germany) equipped with a COHU High performance CCD camera (USA), and recorded with a Panasonic time lapse video AG-TL700 recorder (Japan).

Scanning electron microscopy (SEM) (II)

Cells grown on coverslips were stabilized at RT in the presence of unlabeled phalloidin (Molecular Probes) in a cytoskeleton stabilizing buffer (CS-buffer; 10 mM PIPES (pH 7.2), 0.3 M sucrose, 0.1 M NaCl, 3 mM MgCl₂, 10 mM leupeptin, 1 mM EGTA) according to Singer et al. (1989) as modified by Sormunen (1993). The cells were fixed in 4% glutaraldehyde in 0.2 M PIPES (pH 7.2) for 10 min and dehydrated in ethanol and hexamethyldisilatzane (Fluka, Switzerland) at RT. The coverslips were then coated thinly with platinum using Jeol Fine Coat JFC-11000 (Tokyo, Japan) sputtering device and examined with a Zeiss Digital Scanning Microscope 962. For tunneling microscopy ethanol and hexamethyldisilatzane-dehydrated cells on coverslips were left without platinum coating and examined

with Nanoscope Multimode Scanning Probe Microscope equipped with a Nanoscope IIIa System Controller (Digital Instruments, USA).

Transmission electron microscopy (TEM) (II, III, IV)

For conventional TEM processing (III, IV) infected cells grown on coverslips were fixed with 2.5% glutaraldehyde in 0.2 M cacodylate, pH 7.2, for 20 min at RT. Samples were postfixed in 1% OsO₄ in 0.2 M cacodylate for 30 min at RT and then left overnight in 1% uranylacetate in 0.3 M sucrose (in distilled water) at 4°C before ethanol dehydration and embedding in Epon resin. For whole-mount TEM (II) cells were grown on carbon and Formvar coated gold grids (300 mesh) on coverslips, and stabilized as for SEM. Cells were fixed in 4% paraformaldehyde in PBS for 10 min and permeabilized with 0.5% saponin in PBS for 30 min at RT. Immunolabeling was carried out as for the pre-embedding samples described next.

For pre-embedding antibody labeling (III, IV) cells grown on coverslips were fixed, permeabilized and treated with primary antibody as for the immunofluorescence samples. For single labeling 10 nm gold-conjugated protein A was used, and for double staining 5 nm gold particles conjugated with goat anti-rabbit IgG and 10 nm gold particles conjugated with goat anti-rat IgGs were used as secondary antibodies. The pre-embedded samples were post-fixed with 3% glutaraldehyde in 0.2 M PIPES, pH 7.2, before osmium-treatment, and treated otherwise as described above. Detection of antibody labeling by ultrasmall gold (Nanogold) enhanced by silver and gold toning was done as described in Punnonen et al. (1999). Briefly, PFA-fixed, NH₄Cl treated and saponin permeabilized cells on coverslips were treated with primary antibody as for immunofluorescence. Nanogold (diameter 1.4 nm) particles conjugated with Fab-fragments (Nanoprobes; New York, NY) were diluted 1:100

in TBS-saponin (0.1 M Tris, pH 7.4, 170 mM NaCl, 0.1% saponin) containing 1% BSA and incubated at RT for 1 h. Cells were washed 4 times for 5 min with TBS-saponin and were fixed with 3% GA in PIPES. Nanogold was silver-enhanced with the HQ Silver kit (Nanoprobes) for 5 min and then toned with gold chloride to make the signal more stable for osmium tetroxide and irradiation (Liposits et al., 1982; Trembleu et al., 1994). The cells were treated with 2% sodium acetate three times for 5 min, then with 0.05% gold chloride (Sigma) on ice in the dark for 10 min, and finally with a fresh solution of 0.3% sodium thiosulfate on ice in the dark twice for 10 min. The samples were rinsed in distilled water and PIPES and postfixed in osmium tetroxide and further processed as conventional Epon embedded TEM-samples. All conventional and pre-embedded TEM samples were examined at 60 kV by a Jeol 1200 EX transmission electron microscope (Tokyo, Japan).

Cryo-EM of ultrathin sections (III, IV)

Ultrathin frozen sections (thickness 60-80 nm) were prepared according to the Tokuyasu method (Tokuyasu, 1973; 1989; Griffiths et al., 1984). Briefly, cell pellets were fixed in a mixture of 4% PFA and 0.25% GA in 0.2 M PIPES, pH 7.2, for 30 min at RT. The pellets were infiltrated with 2.1 M sucrose in 20% polyvinylpyrrolidone for 15 min at RT and frozen in liquid

nitrogen, and sections (60-80 nm) were cut at -110°C . Retrieval of sections from the knife was achieved with a 1:1 mixture of 2% methylcellulose (Sigma) and 2.3 M sucrose according to Liou et al. (1996). Immunolabeling was carried out on grids and the primary antibody was detected with gold-conjugated protein A or gold-conjugated secondary antibody. Finally, sections were stained with a 9:1 mixture of 1.8% methylcellulose and 0.3% uranyl-acetate, and the grids were air-dried on loops in a thin support film of 1.8% methylcellulose. The samples were examined at 80 kV in a Jeol 1200 EX transmission electron microscope (Tokyo, Japan).

Other methods

Colloidal gold particles (5 nm diameter) were prepared according to the method of Slot and Geuze (1985) and coated with bovine serum albumin (BSA; Tjelle et al., 1996) (III, IV). The BSA-gold (250 $\mu\text{l/ml}$ growth medium) was either included in the virus inoculum or added at different time points to the culture media. The newly synthesized viral RNA in SFV-infected BHK cells was labeled at 4 h p.i for 5 min with 20 mM bromo-UTP (BrUTP; Sigma) introduced to the cells by lipofectin transfection. The host cell mRNA transcription was shut down by including 5 $\mu\text{g/ml}$ actinomycin D (Sigma) in the medium starting at 15 min before the BrUTP labeling.

RESULTS

1. LOCALIZATION OF INDIVIDUAL SFV NONSTRUCTURAL PROTEINS (I, II, IV)

1.1. Isolation and detection of Nsp2 by monoclonal antibodies (I)

A panel of monoclonal antibodies (mAbs) were raised against SFV Nsp2. Mice were immunized with Nsp2, which had been expressed as a histidine fusion protein in *Escherichia coli*, and then purified by metal affinity chromatography (Rikkonen et al., 1994). Supernatants of hybridoma cell cultures were prepared by standard techniques (Harlow and Lane, 1988) and tested by ELISA against purified recombinant Nsp2, which was bound to plastic microwells with rabbit polyclonal antibodies against Nsp2. In the ELISA altogether 108 positive clones were obtained. The supernatants of these were screened in an ECL-based dot-blot assay, using the 15,000 x g membrane fraction (P15) from SFV-infected and mock-infected cells as antigens. In the dot-blot assay 50 supernatants were regarded as positive. Further cloning resulted in 33 mAb producing cell lines. Aliquots of all mAbs obtained were tested by immunoblotting, indirect immunofluorescence microscopy and immunoprecipitation. Of these 30 mAbs recognized Nsp2 in Western blotting, and 25 were found to be positive in indirect immunofluorescence microscopy of SFV-infected cells (I: Table 1).

In indirect immunofluorescence microscopy the mAbs showed variations in detection of Nsp2 in different cellular compartments. This phenomenon most probably reflects compartment-specific exposure of Nsp2 epitopes in different subcellular compartments. 18 mAbs showed reactivity against the cytopathic vacuoles type 1 (CPV). Two of them (mAbs 2A11

and 3B5) recognized only CPVs, as shown by double immunofluorescence staining with polyclonal anti-Nsp3 antiserum, while most of the mAbs (20/33) recognized the nuclear form of Nsp2 (I: Table 1 and Fig. 6). Immunoprecipitation with mAbs in native conditions revealed that the SFV nonstructural proteins are associated with each other (I: Fig. 4 and 5). None of the mAbs recognized Sindbis virus Nsp2 in immunoblotting, indicating that they were directed to non-conserved sequences specific for SFV. These epitopes were located mostly within the N-terminal half of Nsp2 (I: Table 1, Fig. 2). Interestingly, one of the raised mAbs (1E9) cross-reacted strongly with a host protein of 78 kDa from uninfected human (HeLa), murine (BHK), avian (CEF) and insect (Sf9) cells (I: Fig. 3). This protein was identified as the immunoglobulin binding protein, BiP, by 2-D gel mapping and reaction with a commercial anti-BiP antiserum.

1.2. Nsp1 and actin cytoskeleton (II, unpublished)

Expression of the RNA replicase protein Nsp1 of Semliki Forest virus and Sindbis virus using the vaccinia virus expression vector vTF7-3 (Fuerst et al., 1986) resulted in massive induction of filopodia-like and thicker lamellipodia-like extensions in several cell lines (HeLa, BHK, PC12 and human fibrosarcoma cell line HT1080). The appearance of filopodia and lamellipodia is normally coupled to cell motility (Mitchison and Cramer, 1996). Time lapse video microscopy revealed increased membrane motility of Nsp1 expressing cells. Early after transfection (30 to 60 min) only thin filopodia were seen on the cell surface and in the leading edge of the cells, which later developed into lamellipodia-like extensions with numerous filopodia at their distal parts. Late after transfection (3 to 5 h) the body of

many cells retracted towards the proximal parts of lamellipodia-like structures leaving long retraction fibers behind the dying cell, finally followed by a rapid pyknotic collapse of the cell. Cells in these different stages were visualized with better resolution by scanning electron microscopy (Fig. 5A to C). Tunneling electron microscopy of uncoated cells showed that the filopodia were up to 50 μm long (Fig. 5D). The diameter of the filopodia was fairly uniform, about 50 nm, and many of them were branched. Whole-mount transmission electron microscopy of saponin permeabilized cells on Formvar coated grids revealed that Nsp1 was present along the entire length of the cytosolic side of filopodia (Fig. 5E and F).

With indirect immunofluorescence microscopy the Nsp1-induced filopodia were shown to be devoid of detectable F-actin (II: Fig. 3) and focal contact proteins (e.g. paxillin and vinculin), which are typical components of normal filopodia (Burrige et al., 1997). Cytochalasin D inhibited the formation of the thicker extensions but not the induction of filopodia (II: Fig. 4). No stress fibers were detected in cells expressing Nsp1, whereas vimentin, keratin and tubulin networks appeared intact (Fig. 6A-C).

Critical amino acid residues in SFV Nsp1, which are required for palmitoylation, methyltransferase and guanylyl-transferase activity have been previously identified by deletion and point mutation analysis (Laakkonen et al., 1996). To study the effects of Nsp1 on the distribution of actin filaments and induction of filopodia mutated Nsp1 derivatives were expressed with vaccinia virus vTF7-3 system (Fuerst et al., 1986). Table 1 in publication II shows that redistribution of actin filaments and induction of filopodia were not due to Nsp1 methyltransferase or guanylyltransferase activities. However, palmitoylation of Nsp1 was found to be essential for the induction activity (II: Tab.1). Disruption of stress fibers was not caused by the disappearance

of focal adhesions as paxillin and vinculin distribution remained unchanged at the cell periphery both in mock- and Nsp1-expressing cells. Neither intermediate filaments nor microtubules were seen in the induced filopodia (Fig. 6A to C), whereas ezrin, CD44 and G-actin colocalized with Nsp1 (II: Fig. 4.). Induction of filopodia was inhibited by latrunculin A suggesting that short actin stretches with high turnover rate might serve as a driving force in the extension of filopodia. The disappearance of stress fibers and induction of filopodia were also seen in SFV and SIN infected cells (Fig. 6D-G), indicating that these phenomena represent a normal cellular response to alphavirus infection.

1.3 Localization of SFV Nsps with polyclonal antibodies (IV)

Polyclonal antibodies against Nsp4 with aminoterminal deletion of 61 aa residues, and full-length SFV Nsp1 and Nsp3 were raised in guinea pig and rabbit. The His₆-tagged proteins used for immunization were expressed in *E.coli* and purified by metal-affinity chromatography (Rikkonen et al., 1994). The antibody specificity was controlled by immunoblotting and immunoprecipitation. Nsps were localized in SFV infected BHK cells by confocal microscopy using double-labeling with pairs of guinea pig and rabbit antisera against the different Nsps. All Nsps were present in large cytoplasmic vacuoles, which by EM were verified to be CPVs (Fig. 7 and 8). Otherwise each Nsp had a different intracellular distribution: Nsp1 was found at the cytosolic surface of plasma membrane and filopodia-like structures; Nsp2 was in the nucleus but also diffusely in the cytoplasm (detected here also by Nsp2 mAbs 2C7 and 2H3, publication I); Nsp3 was associated with intracellular membranes (Fig. 7A,B), and Nsp4 showed diffuse cytoplasmic distribution. When individual Nsps were expressed in vaccinia (MVA) transfected BHK cells, Nsp1 was localized to the plasma membrane, Nsp2 to

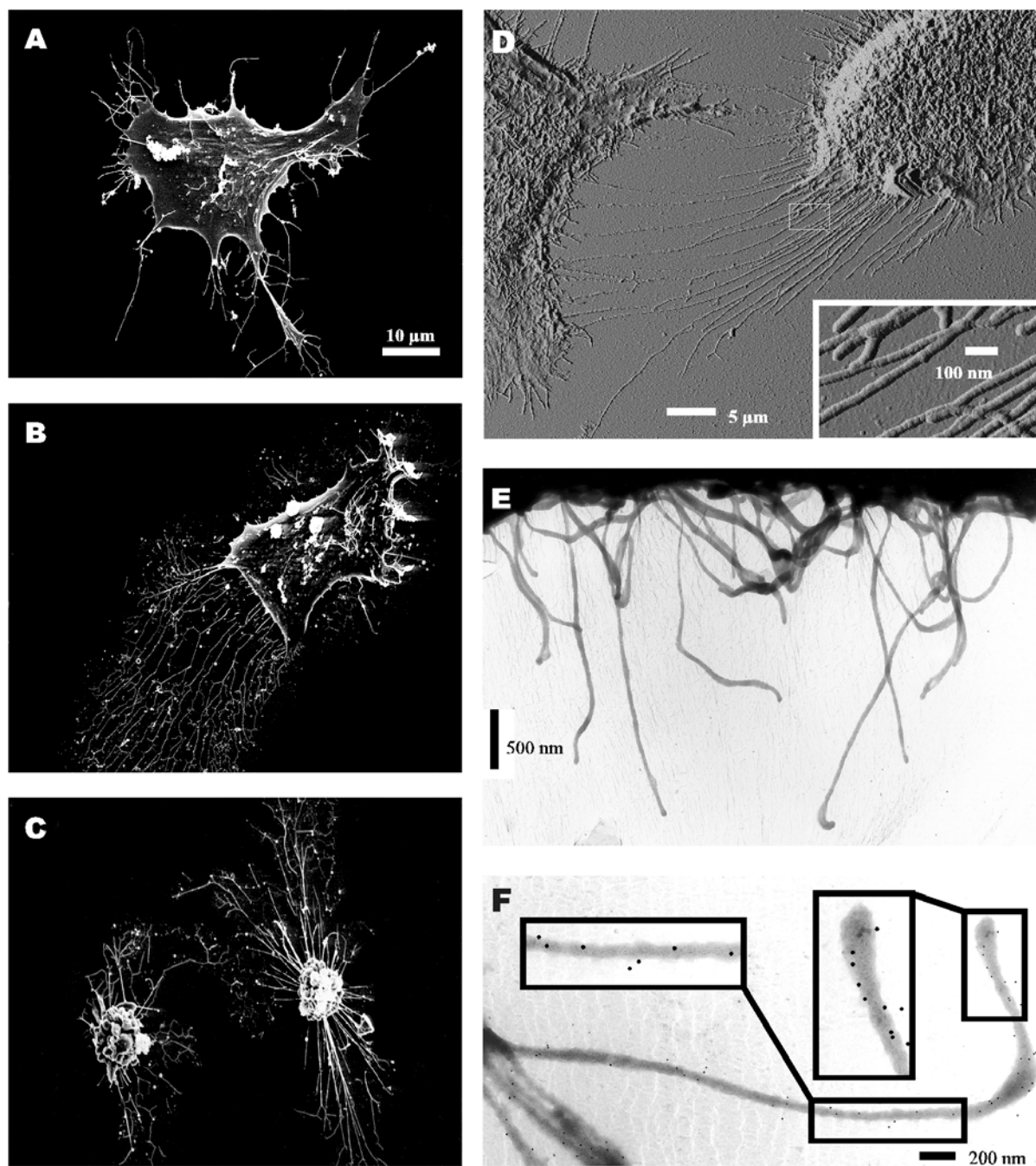


Figure 5. Nsp1-induced filopodia in transfected HeLa cells. Cells were infected with vTF7-3 for 45 min followed by transfection with pTSP1, prepared for SEM (A to C), tunneling EM (D) and whole-mount TEM (E and F) 3 h (D to F) or 5 h after transfection (A to C). SEM micrographs of a HeLa cell with filopodia and lamellipodia-like structures (A), a HeLa cell showing long parallel retraction fibers (B) and a collapsed HeLa cell surrounded by retraction fibers (C). Tunneling microscopy revealed that the filopodia had an uniform diameter of 50 nm and some of them were branched (D). Filopodia contain Nsp1 along their whole length which is located at the cytosolic side of the plasma membrane. Non-permeabilized (E) and saponin-permeabilized filopodia (F) on Formvar coated grids after treatment with anti-Nsp1 antibodies followed by addition of protein A-gold particles.

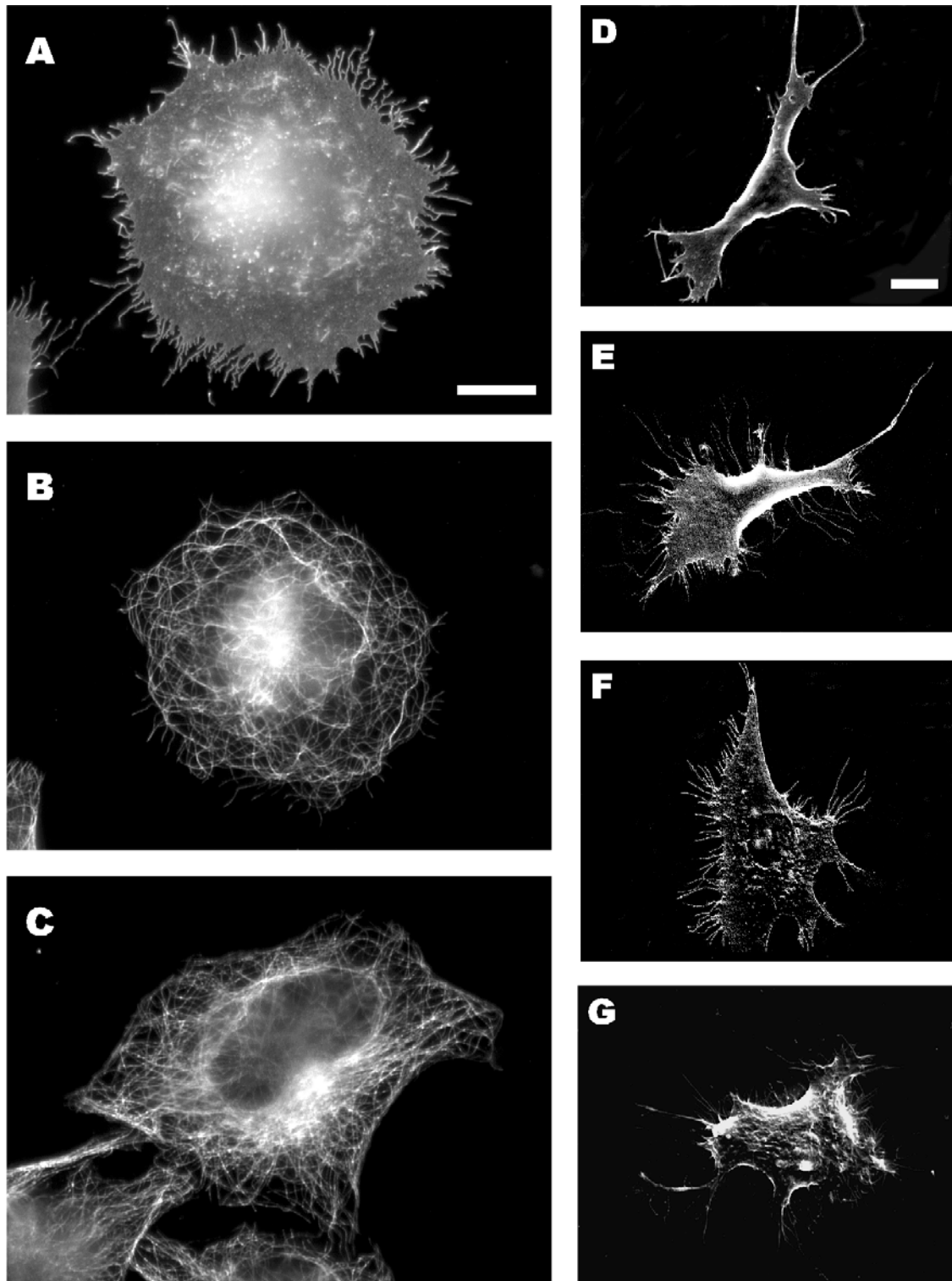


Figure 6. Nsp1-induced filopodia do not contain microtubules (A to C). HeLa cells expressing Nsp1 at 3 h post transfection, an anti-Nsp1 staining (A), the same cell double-stained with anti β -tubulin antibodies (B). Mock-transfected HeLa cell stained with anti-tubulin (C). SFV-infected BHK cells show progressive filopodia formation during infection as demonstrated by SEM (D to G). BHK cells were infected with SFV (200 PFU/cell) and prepared for SEM at 1 h (D), 3 h (E), 4 h (F) and 6 h (G) post infection. Bars, 10 μ m.

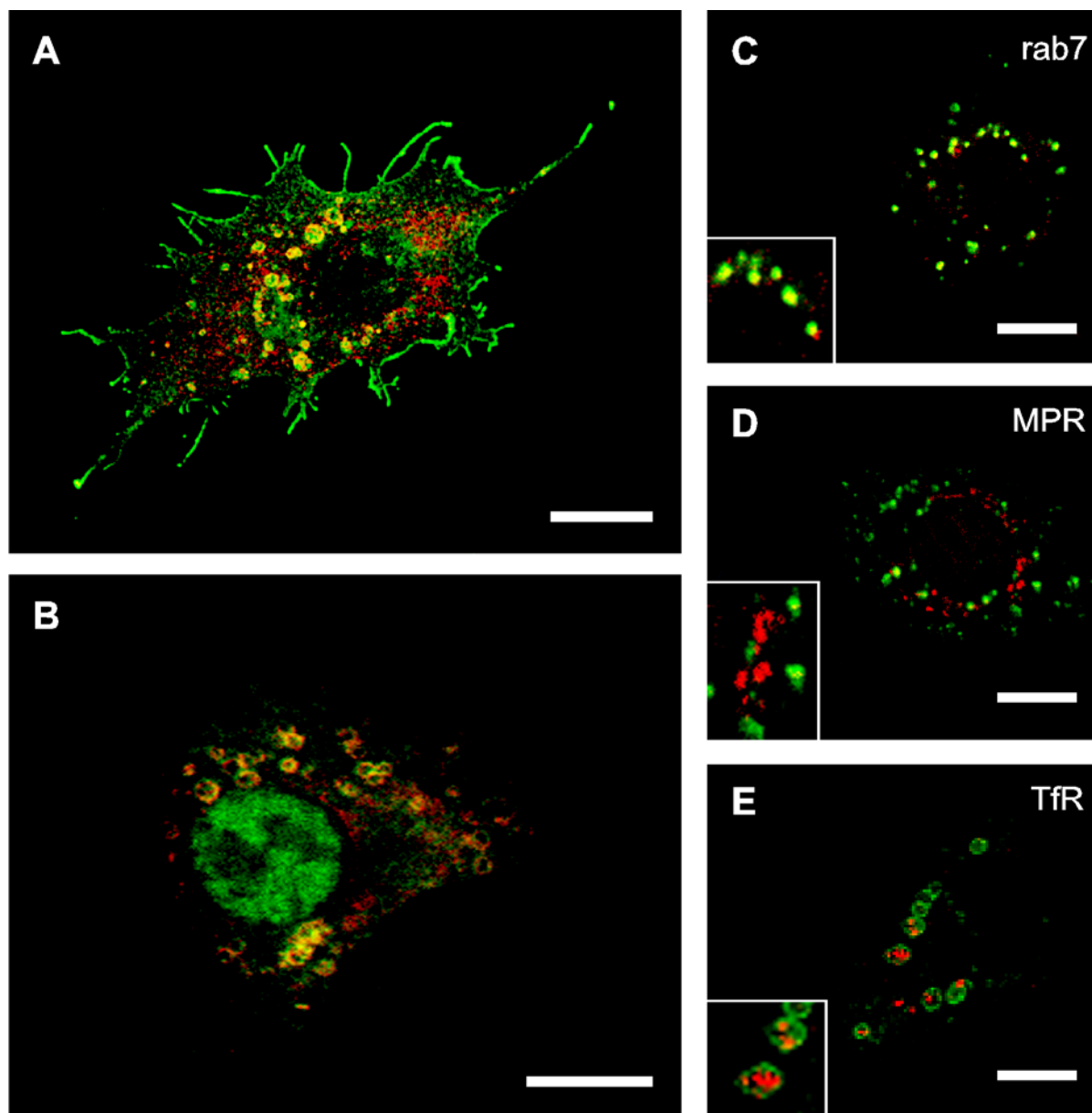


Figure 7. Confocal immunofluorescence images of SFV-infected BHK cells. Double-labeled cells at 4 h (A,C,D) and 6 h p.i. (B,E) are presented. Nsp3s are colocalized in intracellular vacuoles (CPVs, yellow); in (A) cell stained with Nsp1 (green) and Nsp3 (red); and in (B) a cell stained for Nsp2 (green) and Nsp3 (red). Nsp3s have also individual patterns: Nsp1 localizes to the plasma membrane and filopodia-like extensions (A), Nsp2 to the nucleus (green in B), and Nsp3 into intracellular vacuoles (red in A and B). Dual labeling with Nsp3 (green) and various cellular markers (red) reveals that Rab7 (C) colocalizes predominately with Nsp3-stained CPVs, whereas MPR (D) remains mainly in a different pool. TfR (E) is found inside CPVs indicating serious disturbance of membrane traffic in SFV-infected cells late in infection. Bars, 10 μ m.

the nucleus, Nsp3 in small intracellular vesicles, while Nsp4 appeared diffuse in the cytoplasm (IV: Fig 2). Coimmunoprecipitation of radio-labeled Nsps revealed that they all were close to each other, but only in the cytoplasmic membrane fraction (P15) (IV:Fig. 4). Colocalization and coimmunoprecipitation were observed only for Nsp1/Nsp3 and Nsp1/Nsp4 pairs in double-transfected cells.

2. MORPHOLOGICAL IDENTIFICATION OF TOGAVIRUS RNA REPLICATION COMPLEXES (III, IV)

2.1. SFV-infected cells (IV, unpublished)

Ultrastructural studies were performed with SFV-infected BHK-cells. Conventional transmission electron microscopy revealed typical CPV structures with spherules on the limiting membrane (Fig. 8). Inside each spherule a electron dense spot with hairy thin spokes radiating towards the clearly bilayered limiting membrane of the spherule was observed. Immunoelectron microscopy of ultrathin cryosections localized all Nsps to the limiting membrane of CPV - structures (Fig. 8). However, antisera against SFV structural proteins E1, E2 or capsid protein failed to label CPVs, whereas late in infection (6 h p.i.) in addition to budding profiles at the plasma membrane, numerous intracellular capsid binding membrane structures (ICBMs) of CPV-II and CPV-III types were heavily labeled (Fig. 9 and 10, unpublished). These virus-specific structures consisted of intracellular membranes and were often located in close vicinity to the CPVs. By pre-embedding immunoelectron microscopy Nsp3 was localized together with newly synthesized BrdU-RNA at the limiting membrane of CPVs with remnants of detergent-treated spherules (IV: Fig. 3B). Localization of all Nsps at the limiting membrane of CPVs was verified by pre-embedding labeling of saponin permeabilized cells with Nsp-antisera. The antigen detection in these

samples was accomplished by silver enhancement and gold toning of Nanogold particles conjugated to the secondary antibody (Fig. 11, unpublished).

2.2. RUB-infected cells (III, unpublished)

To characterize rubella virus (RUB) RNA replication complex in infected Vero cells, rabbit antisera against two amino-terminal fragments (p55) and (p78) of the RUB nonstructural polyprotein were prepared. RNA was isolated from purified RUB strain Therian virions and cDNA was prepared with reverse transcriptase and an oligo(dT) primer. This was used in PCR with P150 specific primers, the products were cloned, and the inserts were sequenced. For expression in *Escherichia coli* BL21(DE3) the inserts was transferred to the vector pHAT (Peränen et al., 1996) yielding pHATRUB1 (encoding aa 1-505, p55) and pHATRUB2 (encoding aa 1-712, p78). For use in the vaccinia virus expression system, the cDNAs were cloned under the T7 promoter to give pTRUB1 and pTRUB2, respectively. Plasmids pHATRUB1 and pHATRUB2 were transformed to *E. coli* BL21(DE3), and expression was induced with isopropyl- β -D-thiogalactopyranoside (IPTG). The cells were pelleted and broken with a French press.

Rabbits were immunized with purified inclusion bodies of p55 and p78. The sera detected RUB RNA replicase proteins P200 and P150 from infected cells in immunoprecipitation and immunoblotting (III: Fig.1). P150 was membrane-bound but was neither palmitoylated nor phosphorylated like its alphaviral homologues Nsp1 and Nsp3 (Fig. 12, unpublished). Confocal immunofluorescence microscopy of infected cells at 24 h p.i. revealed vesicular and vacuolar structures stained with anti-p55 antibodies (Fig 13A and C). At 48 h p.i large convoluted tubular structures costained with anti-p55 and anti-RUB capsid protein and co-oriented with microtubular filaments

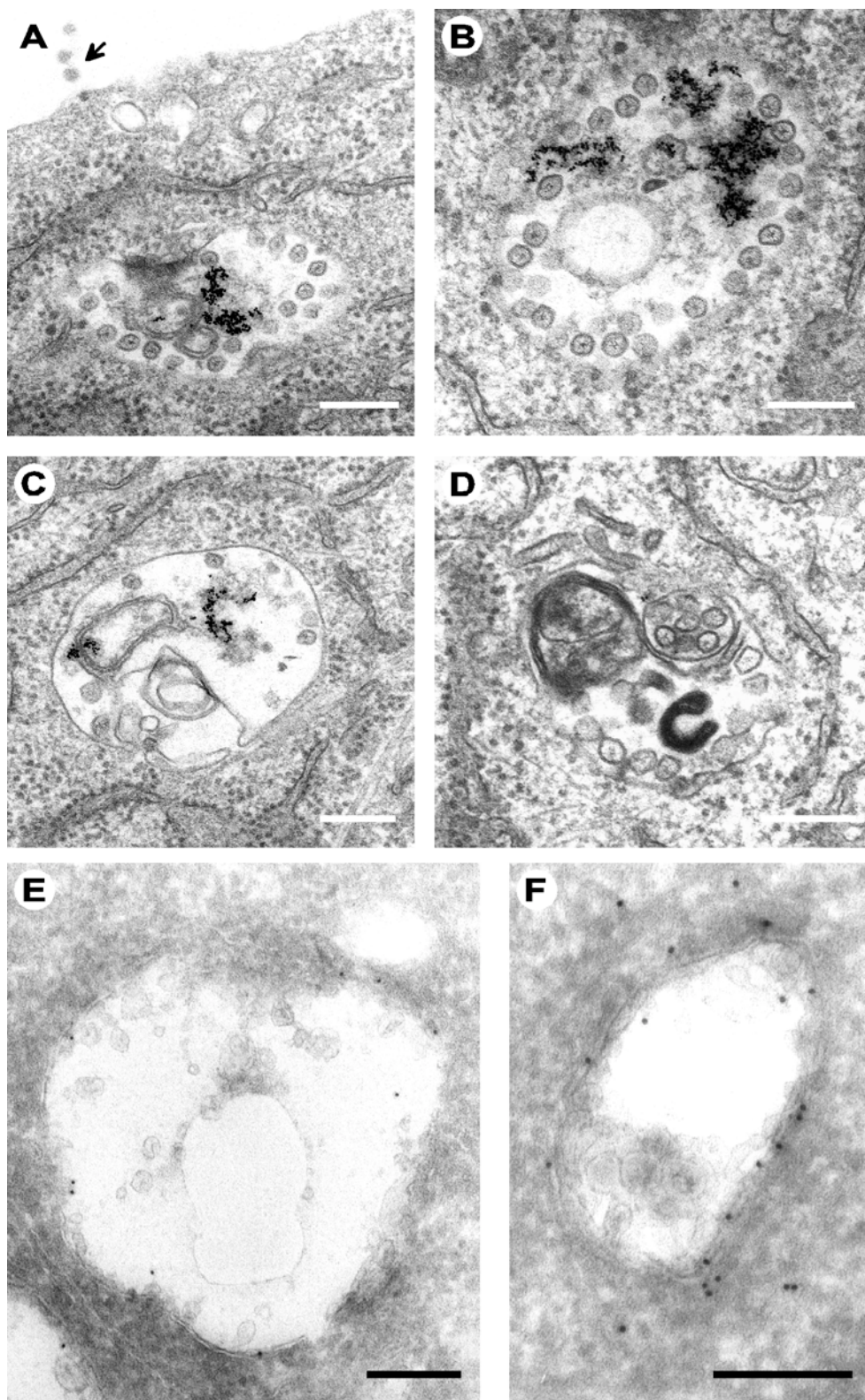


Figure 8. Ultrastructure of SFV CPVs. TEM images of Epon embedded sections of CPVs at 5 h p.i. in SFV-infected BHK cells labeled with BSA-gold (A to D). Several internal membranes and small vacuoles are observed, suggesting that fusion and selection events must have taken place. Endocytosed BSA-gold is present in the lumen of CPVs as dark precipitates (A to C). Spherules are lining the limiting membrane of the vacuole. Some dense virions at the plasma membrane are indicated with an arrow in A. Cryo-IEM images of Nsp1 (E) and Nsp3 (F) immunolabeled CPVs. Both nonstructural proteins, detected by 10 nm gold conjugated to protein A, localize predominately to the limiting membrane and the spherules. Bars, 200 nm.

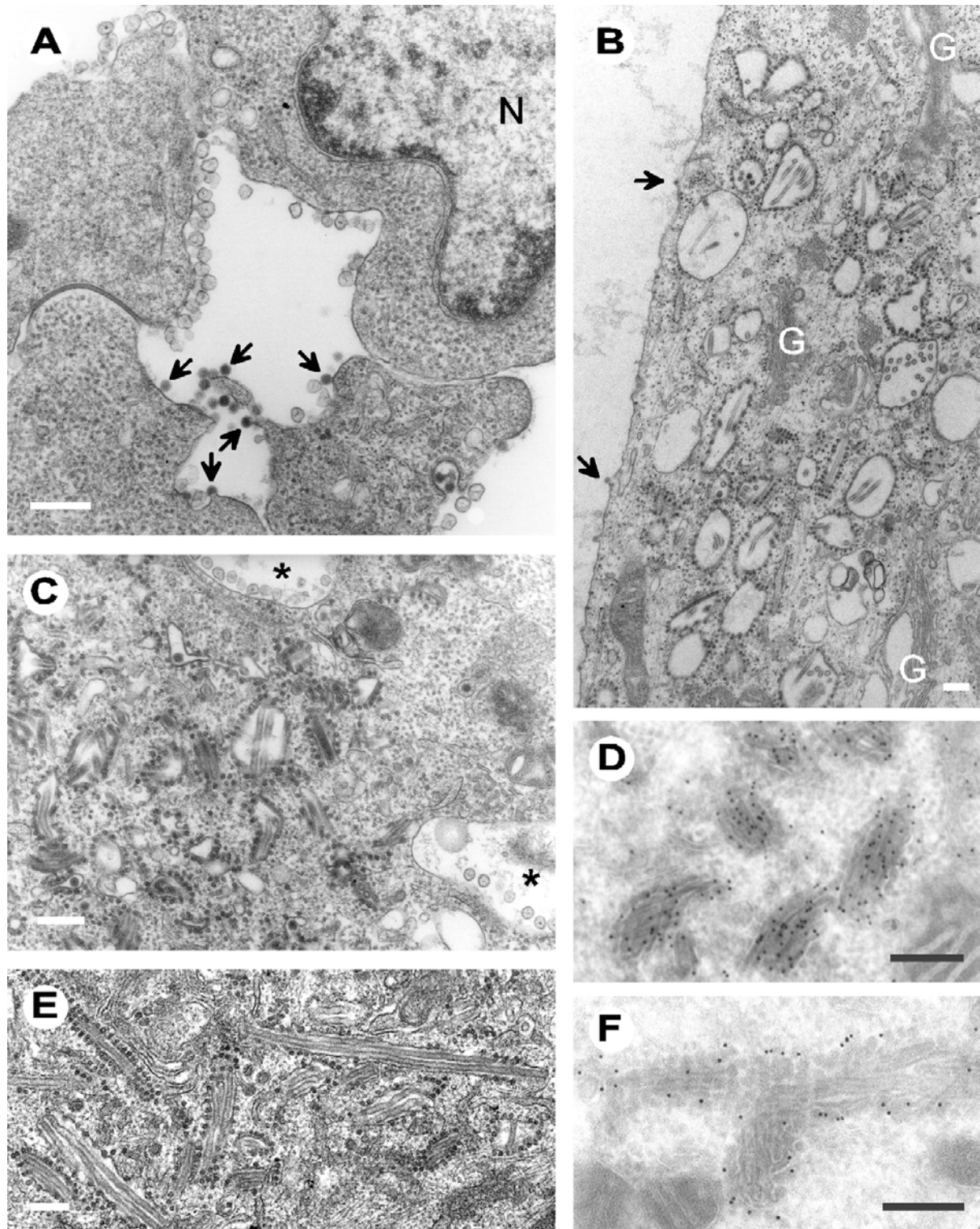


Figure 9. Intracellular capsid binding membranes (ICBM) in SFV-infected cells. Cytopathic structures associated with the synthesis of virus structural proteins in SFV-infected BHK cells at 6 h p.i. are presented. ICBM consist of numerous nucleocapsids attached to virus-induced membranes where the envelope glycoproteins are accumulated. In (A) budding of several virions on the cell surface is presented together with clusters of spherules. CPV-II vacuoles surrounded by nucleocapsids in the Golgi region (B) and CPV-III membrane tubules in the vicinity of two CPV-Is (asterisks) (C). Some CPV-III tubules can become more than 1 μm in length (E). Cryo-IEM confirmed that glycoprotein E1 (D) is localized to the internal membranes, while the capsid protein decorates the cytosolic face (E) of ICBMs. G indicates the Golgi stacks and N the nucleus, budding virions at the PM are pointed by arrowheads. Bars, 200 nm

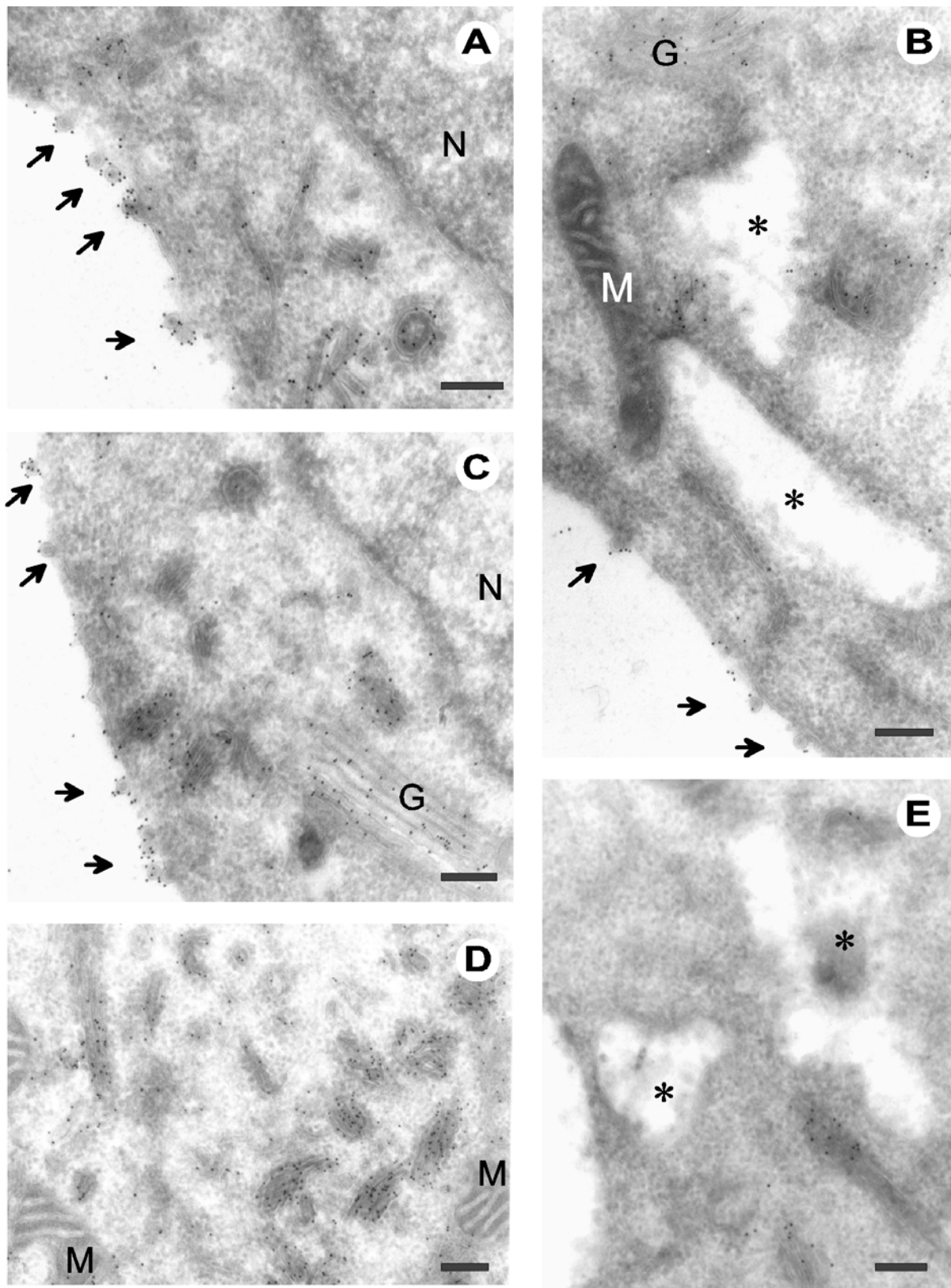


Figure 10. Cryo-IEM images of SFV-infected BHK cells late in infection. Cells fixed at 6 h p.i. were treated with polyclonal anti-E1-antibodies followed by 10 nm protein A gold. Intense E1-specific labeling is seen at various ICBM structures (A to E), at Golgi stacks (B and C), on budding virions at the PM (A to C; arrowheads), but not at CPV-Is (B and E; asterisks). N denotes nucleus, G Golgi stacks and M mitochondria. Bars, 200 nm.

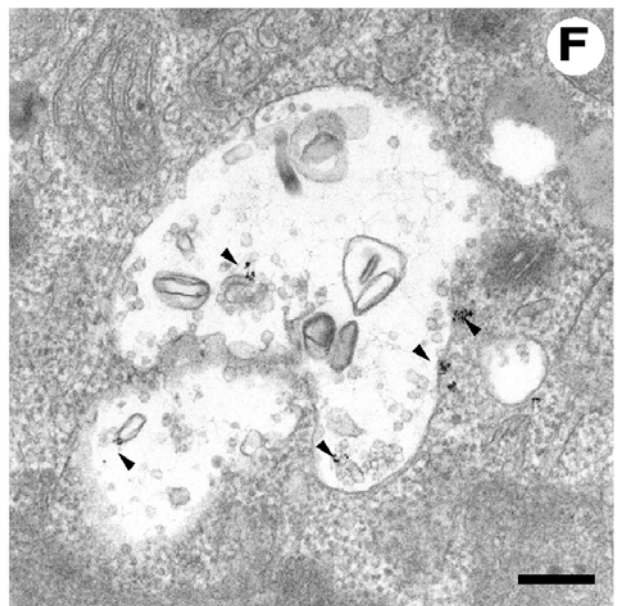
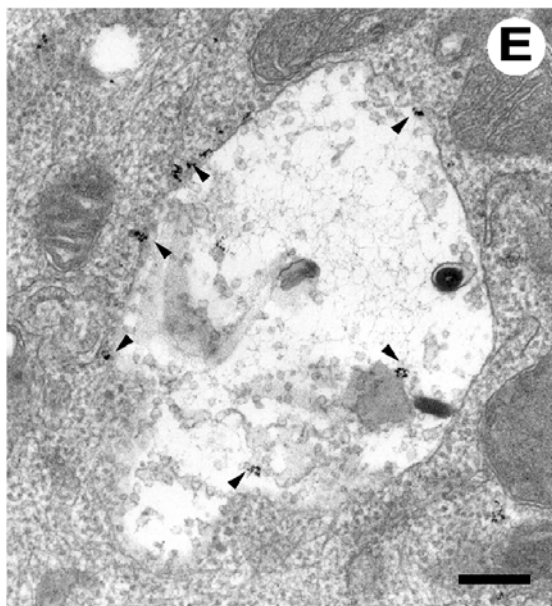
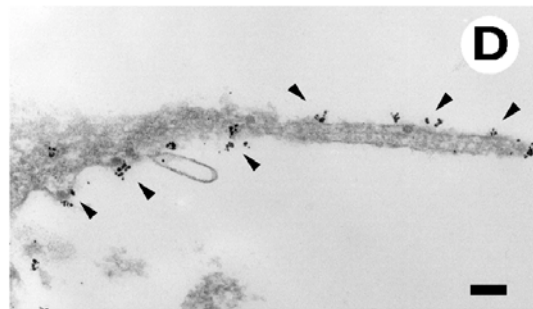
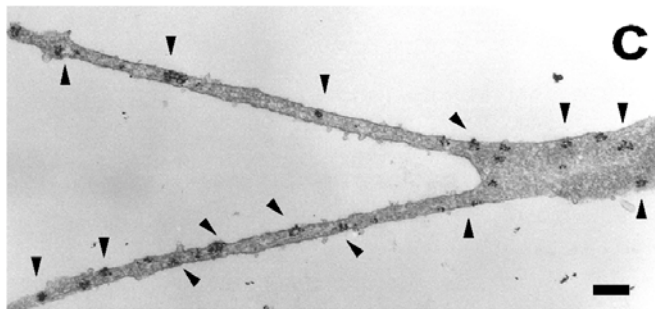
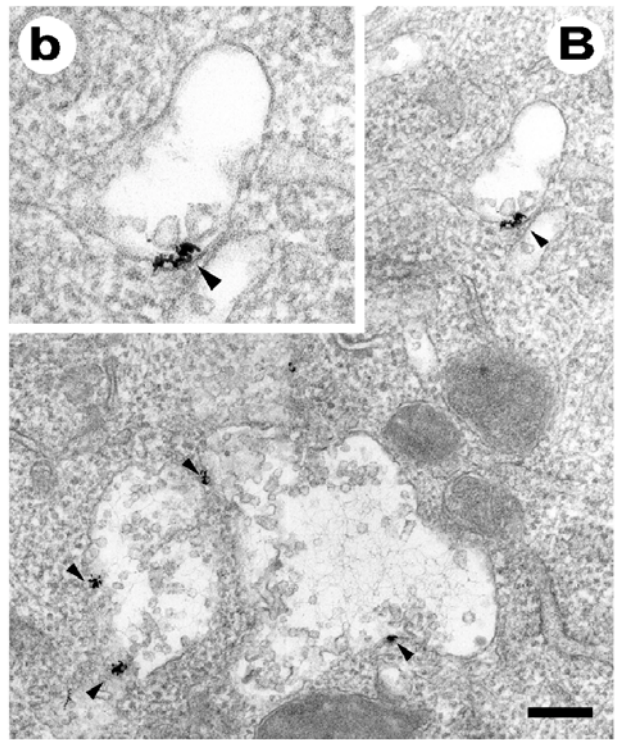
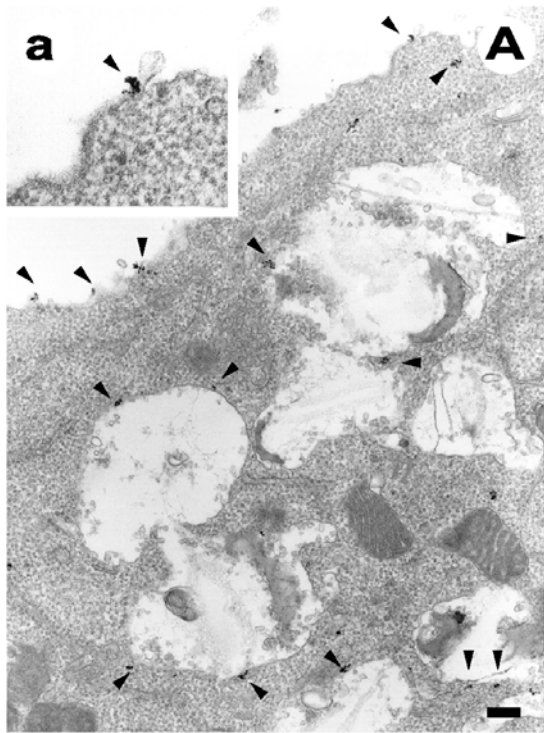
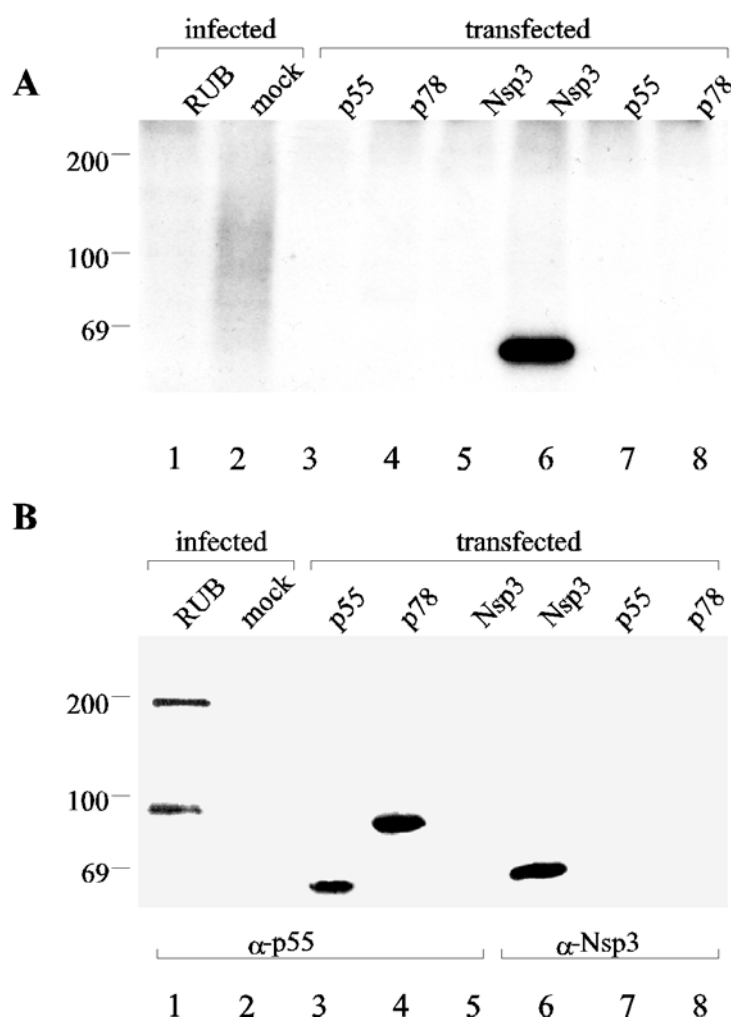


Figure 11. (The opposite page) Nanogold localization of Nsp1 and Nsp3. SFV-infected BHK cells were fixed and permeabilized with saponin at 5 h p.i. After labeling with primary antisera the antigens were detected by ultrasmall (1.4 nm) gold particles conjugated to Fab fragment as a secondary antibody and enhanced by silver and gold toning as described in Materials and Methods. After silver enhancement the label was observed as small (about 40 to 80 nm in diameter) precipitates (arrowheads), the diameter of which was dependent on the length of the enhancement period. Nsp1 was located mainly at the plasma membrane, the limiting membrane of CPVs and the cytosolic side of the filopodia-like extensions (A to C) and often to the mouth of spherules (enlarged inserts in A and B). In contrast to Nsp1, the E1 glycoprotein specific label in filopodia-like structures was located to the outer surface of the PM (D). Nsp3 was located to the limiting membrane of CPVs and the spherules (E and F), but seldom at the PM (not shown). Note that after saponin treatment the morphology of the spherules is altered and the characteristic small electron dense cores are often lost. Bars, 200 nm.

Figure 12. Analysis of the phosphorylation of RUB P150. (A) RUB-infected and mock-infected Vero cells were labeled with [32 P]orthophosphate for 3.5 hours from 43 h p.i. In parallel HeLa cells were infected with vaccinia virus vTF7-3 for 45 min followed by transfection with pTRUB1, pTRUB2 and pTSFV3. Two hours after transfection the cells were labeled with [32 P] ortho-phosphate for 2.5 hours. Immunoprecipitations were carried out from cell lysates. Molecular mass markers are shown on the left. Lane 1: RUB-infected Vero cells, lane 2: mock -infected Vero cells, lanes 3 and 7: pTRUB1 transfected HeLa cells; lanes 4 and 8 pTRUB2 transfected cells, lanes 5 and 6: pTSFV3 transfected cells. Samples in lanes 1-5 were precipitated with anti-p55 antibodies, and samples in lanes 6-8 with SFV anti-Nsp3 antibodies. Phosphorylated proteins were detected by autoradiography. (B) The presence of proteins in the cell lysates was verified by immunoblotting identical samples as used in panel A. Samples in lanes 1-5 were detected with anti-p55 antibodies and samples in lanes 6-8 with anti-Nsp3 antibodies.



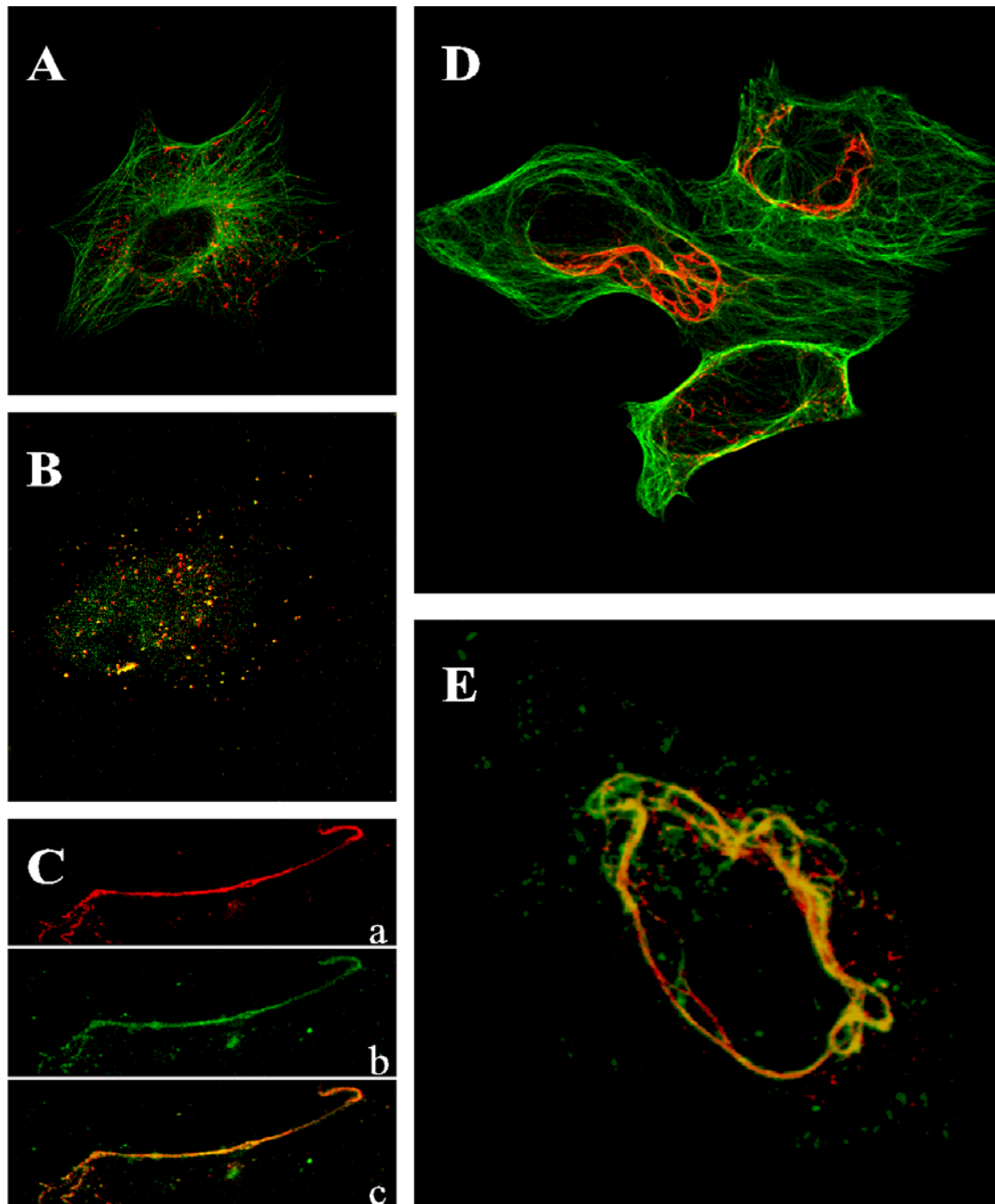


Figure 13. Confocal fluorescence images of RUB-infected Vero cells. Intracellular distribution of RUB RNA replicase component, P150 (red), shown together with the microtubular network (green) (A and D). At 24 h after infection (A) P150 appears in small vacuolar structures, which are at 48 h p.i. (D) extended from their endolysosomal origin into a large unique convoluted tubular network. Colocalization (yellow) of P150 (red) with metabolically incorporated bromo-uridine (green) is evident in confocal images at 24 h p.i. as bright dots (B) and later at 48 h p.i. also in tubular structures (C). Capsid protein colocalizes with P150 in membrane tubules at late infection. A confocal image of P150 (red) and capsid protein (green) shows both of these antigens (yellow) in the virus-induced convoluted tubular structures at 48 h p.i. (E).

(Fig. 13B, D and E). Association of the tubular structures with microtubules was verified by nocodazole treatment (Liao et al., 1995) of the RUB-infected cells at 48 h p.i. Addition of nocodazole resulted in disruption of the microtubular networks and the RUB-induced tubules, but after removal of nocodazole these structures were reformed within 2 hours along newly polymerized microtubular bundles (Fig. 14, unpublished). Electron microscopy showed vacuoles filled with membraneous material, which were related to endosomes and lysosomes, since they contained endo-

cytosed BSA-gold particles (Fig. 15). RUB P150 was localized in the close vicinity of the vacuolar membrane, which also contained invaginations, and spherules with a diameter of 50 nm (III: Fig. 3C). Morphologically the RUB spherules resembled those of alphavirus CPVs with a characteristic electron dense central spot. Newly incorporated BrUTP derived label was associated with the vacuoles and RUB-induced tubular structures, as well as with the spherules, indicating that they are the sites of viral RNA synthesis (III: Fig. 3D).

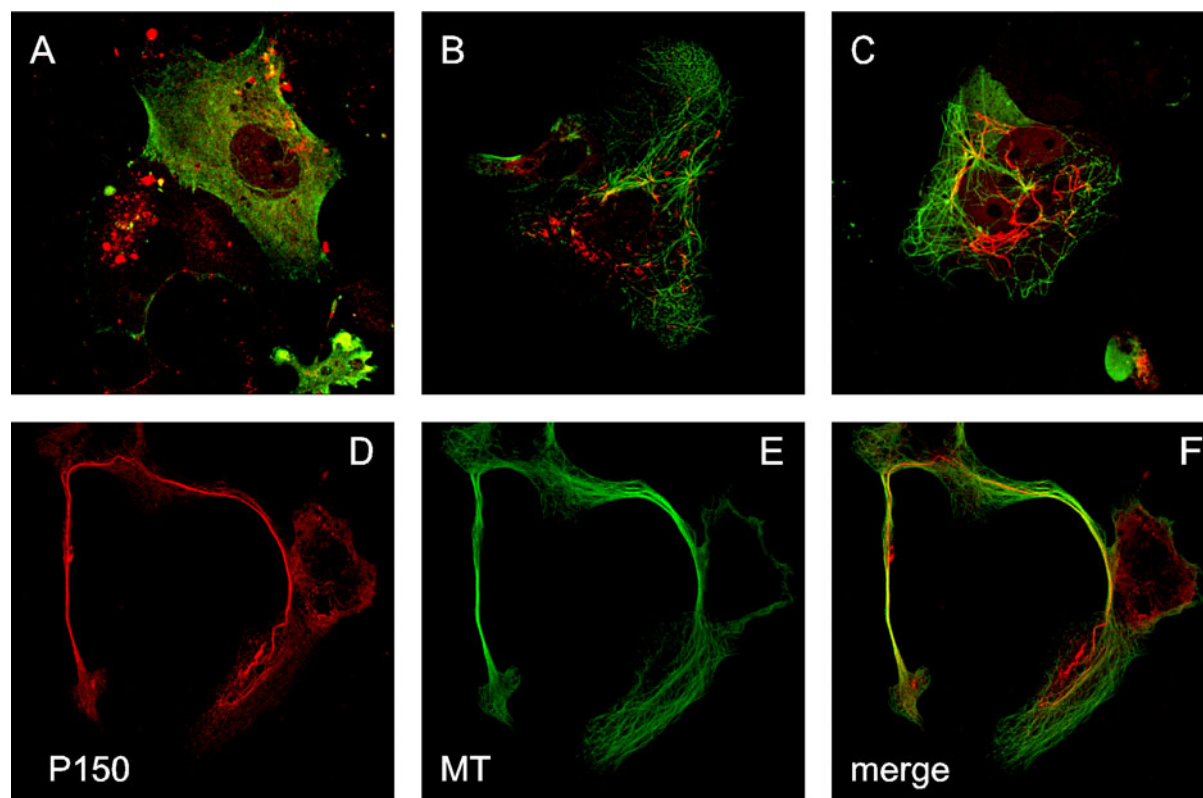


Figure 14. RUB P150 containing convoluted membrane tubules are associated with microtubules. Confocal images of RUB-infected Vero cells exposed to nocodazole-treatment at 48 h p.i. (A to C). The microtubular (green) organization and P150 containing convoluted tubules (red) are reversibly disrupted within 30 min after adding of nocodazole to the growth medium (A). When nocodazole is washed away microtubules and P150 tubules start to reform again as shown at 1 h (B) and 2 h (C) after removal of the microtubule disrupting agent. In untreated RUB-infected cell at 48 h p.i. (D to F) P150 containing membrane tubule (D; red) with a microtubular core (E; green) is able to fuse with a neighboring cell as seen merged in (F).

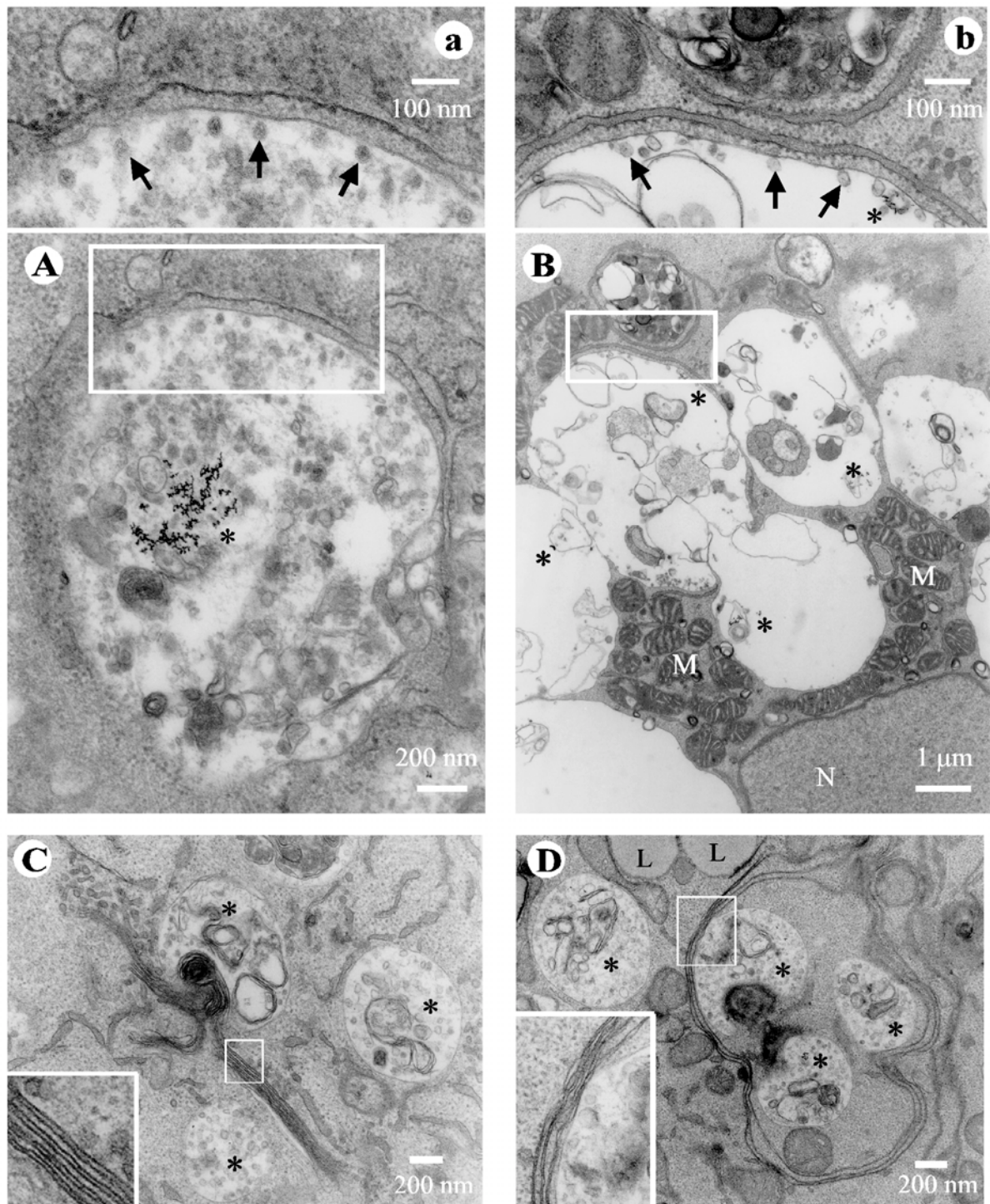


Figure 15. Ultrastructure of RUB cytopathic vacuoles. In (A) a CPV at 18 h after RUB-infection shows endocytosed BSA-gold in the lumen (asterisks) and, small spherules at the inner aspect of the vacuolar membrane [enlarged in (a)]. (B) is a general view of a large vacuolar structure at 24 h p.i. containing BSA-gold (asterisks) with numerous mitochondria (M) near the nucleus (N). The enlargement shown in (b) demonstrates spherules (arrows), BSA-gold (asterisks) and the close vicinity of ER membranes aligning with the vacuole membrane. Panels C and D show at 48 h p.i. long virus-induced tubular membrane structures connecting several endocytosed gold containing CPVs (asterisks). Often these large proliferated membrane structures consisted of several stacked lamina-like membranes close to CPVs (enlarged inserts).

3. ENDOSOMAL ORIGIN OF SFV CPV-ASSOCIATED RNA REPLICATION COMPLEX (IV)

CPVIs have earlier been defined as modified endosomes or lysosomes (Froshauer et al., 1988). However, what is known about the endosomal apparatus and especially of the late endosomal compartment has increased over the few past years (Gruenberg and Maxfield, 1995; Hunziker and Geuze, 1995; Clague, 1998; Soldati et al., 1995; Vitelli et al., 1995; Mullock et al., 1998; Gu and Gruenberg, 1999; Bucci et al., 2000). To update and characterize more precisely the origin of CPV membranes in SFV-infected BHK cells confocal immunofluorescence microscopy and dual-labeling of Nsp3 with several well-defined organelle-specific markers were used. Double-labeling experiments revealed that CPV colocalized only with markers of late endosomal compartments. The most evident colocalization was obtained with the small GTPase Rab7, a known regulator of the membrane trafficking in late endosomal compartment (Fig. 7C). Remarkable colocalization was observed also with integral lysosomal glycoproteins lamp-1 and lamp-2, both cellular markers for late endosomes and lysosomes. In addition, lysobisphosphatidyl acid (LBPA), which concentrates in late endosomal membranes, colocalized intensively in the perinuclear region with CPV. Instead, two other late endosomal markers, CI-MPR (Fig. 7D) and Rab9 failed to colocalize with CPV structures. However, late in infection (6 h p.i.) also some CI-MPR –specific labeling accumulated in CPV-membranes.

A clear spatial partnering between vesicles containing the early endosomal marker EEA1 and CPV was observed. The EEA1-positive elements colocalized to a limited extent in the cell periphery early in infection (3 h p.i.), presumably with premature CPV structures. Later in infection (5 h p.i.) colocalization with mature CPV

was not observed, but still both markers formed complexes of vesicles apparently in close vicinity to each other. A protein marker of the recycling compartment between early endosomes and plasma membrane, transferrin receptor (TfR), did not colocalize with CPV. However, it was found late in the infection (6 h p.i.) inside the large CPV structures as separate small vesicles (Fig. 7E). This suggests an abnormal autophagy-type fusion process and reorganization of the endocytic pathway in SFV-infected cells late in infection.

4. BIOGENESIS OF SFV CPV STRUCTURES (IV)

The time-dependent events leading to CPV biogenesis during SFV infection were studied by electron microscopy of BSA-gold labeled BHK cells. BSA-gold was used as a tracer for the endocytotic pathway. Two separate studies with samples collected at one hour intervals were performed at physiological temperature. The first series consisted of cells infected with low m.o.i. (20 pfu/cell); the BSA-gold was introduced into the cells together with the virus inoculum and was washed away after one hour adsorption. In the second series high m.o.i. (200 pfu/cell) was used and the BSA-gold was introduced to the cells at different times after infection for periods of ten minutes, after which the uninternalized tracer was washed away. The infection was allowed to continue for another 10 minutes before the cells were fixed.

In the first series (low m.o.i. and BSA-gold together with the virus inoculum) the endocytosed tracer was found immediately after the removal of free BSA-gold and virus inoculum in small tubule-like membrane compartments, presumably early endosomes. No signs of virus particles or their remnants were observed at the plasma membrane or in the intracellular space. At 2 h p.i. BSA-gold was found in larger vesicles with internal membranes, presumably

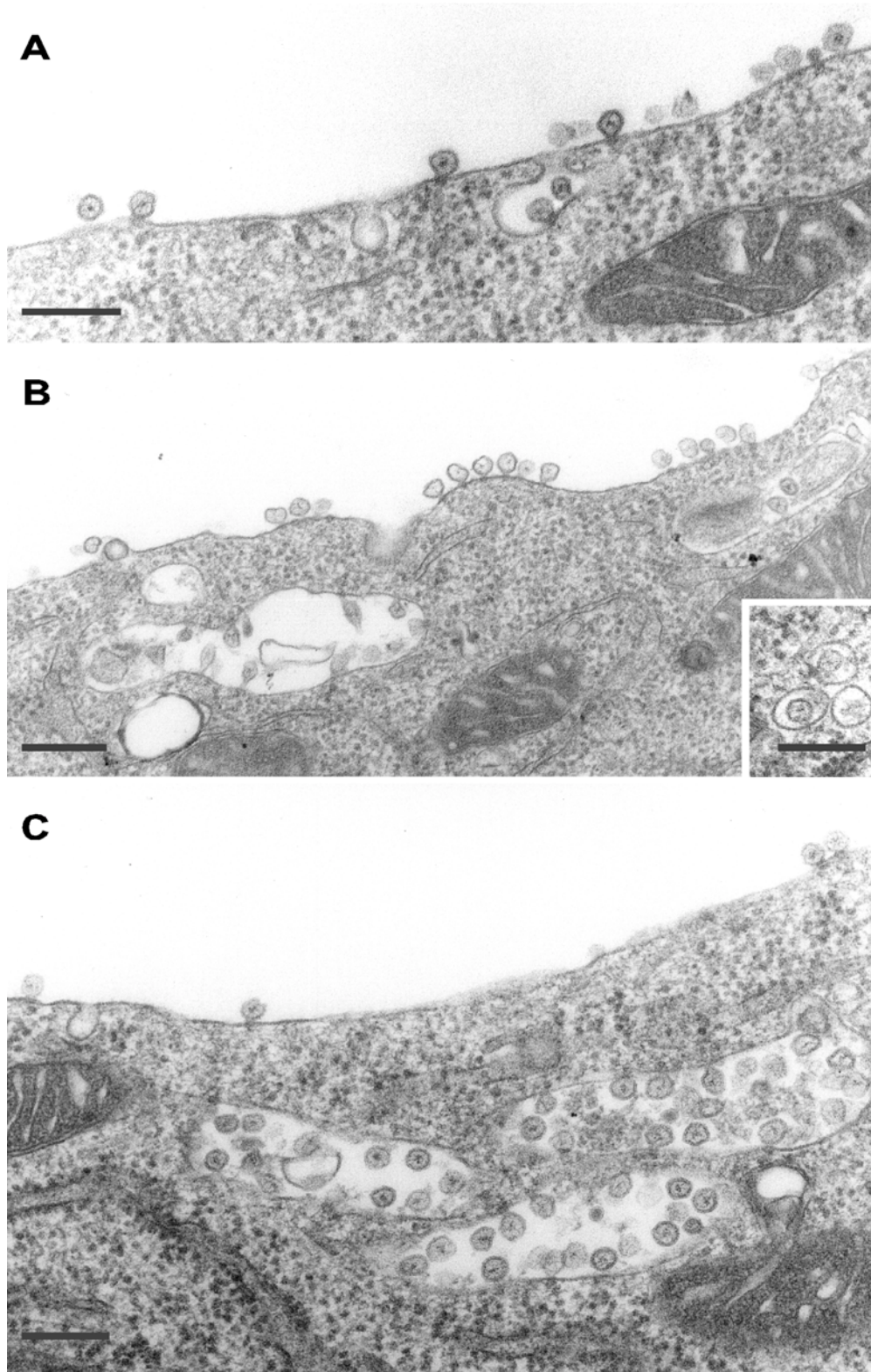


Figure 16. Biogenesis of CPV structures. EM images of fusion events of CPV structures with the PM of SFV-infected BHK cells at 4 to 5 h p.i. Spherules are observed at the PM individually (A) or as clusters (B). They become associated with internalization profiles and intracellular vacuoles with close connection to the PM (B). Simultaneously individual spherules can be seen in coated vesicles (insert in B). Clusters of flattened CPVs are often observed near the PM (C). The spherule-specific membrane traffic may occur bidirectionally resulting in recycling of CPVs between the PM and perinuclear region. Bars, 200 nm.

representing late endosomes, but without spherules (IV: Fig.6). The virus-induced spherules were first observed in intracellular vacuoles without BSA-gold 3 h p.i. At the same time some spherules were seen at the plasma membrane and in coated vesicles. At 4 h p.i. spherules were frequently seen at the plasma membrane accompanied with internalization profiles. At 5 h p.i. clusters of spherules were present at the plasma membrane, in evident contact with CPVs beneath the plasma membrane or flattened CPV clusters near the plasma membrane (Fig. 16). Not until this time were mature CPVs with spherules and internalized BSA-gold observed. Some BSA-gold labeled CPV fused with the plasma membrane releasing their spherules into the medium in a process resembling secretion described for exosomes (i.e., secreted endosomal vacuoles of lymphocytes (Escola et al., 1998).

In the other series (high m.o.i. and 10 min BSA-gold pulse) CPV structures were observed earlier, starting from 3 h p.i., and they could be labeled with short BSA-gold pulses at time points starting from their

appearance at 3 h p.i. to 6 h p.i., indicating a free flow of the tracer from the plasma membrane into CPVs. Exosome-type exocytosis of BSA-gold labeled CPVs was also occasionally observed in this second study (Fig. 17, unpublished).

The results presented above are consistent with confocal immunofluorescence studies of SFV-infected cells (50 pfu/cell) double-labeled with Nsp1 and Nsp3 antisera (IV: Fig 2). Recall that Nsp3 is able to form small intracellular vesicles when expressed alone (IV: Fig 2F). Positive double-labeling confirmed that the observed vesicles are most likely actual CPVs. In early infection (2 h p.i.) colocalization of Nsp1 and Nsp3 was first observed at or in small vesicles just beneath the plasma membrane. This was followed by intracellular accumulation of costained CPVs first in the close vicinity of the plasma membrane (3 to 4 h p.i.) and later (5 to 6 h p.i) they increased in size and accumulated in the perinuclear region, even though some still remained in obvious contact with the plasma membrane.

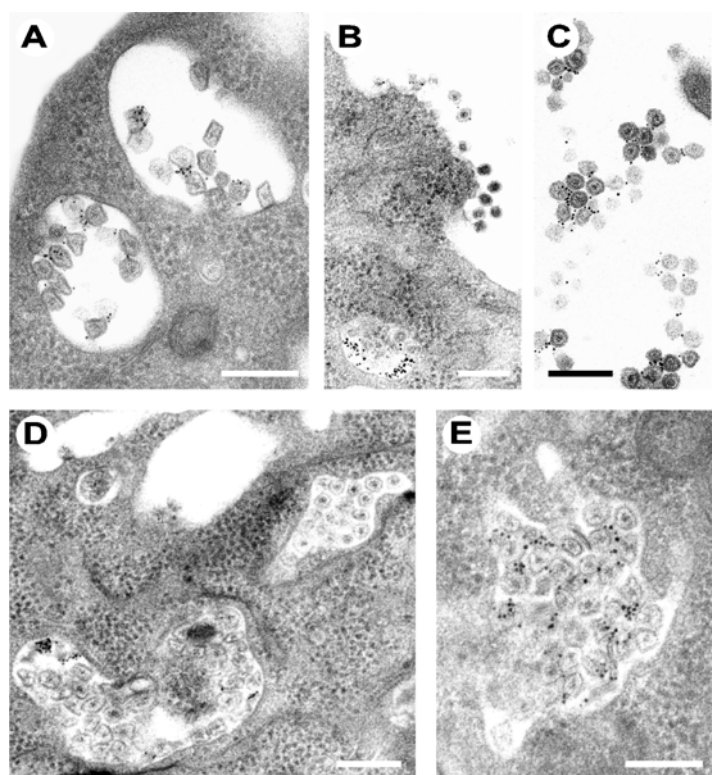


Figure 17. The CPVs are closely connected to the cell surface. SFV-infected BHK cells (moi 200/cell) were exposed to BSA-gold added to the medium 10 min before fixation. CPVs labeled with BSA-gold were observed at 3 h (A), 4 h (B) and 6 h (D and E) p.i. and BSA-gold was also associated with spherules secreted to the medium (B and C). Note dense budding virions in B. Bar, 200 nm.

DISCUSSION

Togavirus infection provides a versatile target for basic cell biological research. Due to their limited genetic capacity, togaviruses have to utilize the basic cellular mechanisms for entry, protein synthesis, post translational modifications (e.g. glycosylation and palmitoylation) and intracellular transport. The virus enters the cell by receptor mediated endocytosis and the virus replication occurs in the cytoplasm. Protein synthesis is mediated by the cellular ribosome and ER -based synthetic and translocation machinery. All nonstructural proteins are enriched to specific endocytotic organelles (CPVs), although the individual proteins appear to additionally localize to specific sites within the cell, such as SFV Nsp1 at the plasma membrane or SFV Nsp2 in the nucleus as confirmed in this study. The structural glycoproteins are translocated, processed and modified in the secretory pathway. The nucleocapsid assembly takes place either free in cytoplasm (SFV) or attached to the membranes (RUB). The budding of alphaviruses occur at the plasma membrane, whereas RUB buds mainly into intracellular vesicles. During infection virus proteins interact with the cytoskeleton. Thus, it can be concluded that togavirus infection has an influence on several compartments and the infrastructure of the host cell.

1. TOGAVIRUSES AND THE CYTOSKELETON

In this study we observed that alphavirus capping enzyme Nsp1 induced filopodia-like structures in infected and transfected cells. In addition, stress fibers were disrupted both in SFV and RUB-infected cells. Furthermore, RUB P150 containing convoluted membrane tubules co-oriented with microtubular filaments.

Actin filaments are involved in normal cellular processes such as adhesion, motility, cell division, endocytosis and intracellular transport of organelles (Pollard and Cooper, 1986; Sundell and Singer, 1991; Goode et al., 2000). Filopodia and lamellipodia are cellular extensions, whose appearance is often coupled to cell motility (Fig. 18). F-actin filament bundles serve as their supporting skeletons, connected at the tip of the filopodia by a complex array of proteins to the cytoplasmic side of the plasma membrane. Some of these proteins are in contact with transmembrane proteins, which in turn interact with extracellular matrix proteins at focal contacts or adhesion plaques (Craig and Johnson, 1996; Joskusch and Rüdiger, 1996; Burrige et al., 1997). Synthesis of F-actin takes place at the tip of the filopodia by continuous incorporation of G-actin to the barbed (+) end of the filament (Schafer and Cooper, 1995; Mitchison and Cramer, 1996). In lamellipodia and membrane ruffles, which are rapidly moving sheet-like processes, the actin filaments are organized into cross-weaves (Machesky and Hall, 1996; Mitchison and Cramer, 1996; Nobes and Hall, 1995).

Filopodia can be induced by microinjection of purified GTP-binding protein Cdc42 into cultured cells (Nobes and Hall, 1995), while injection of the closely related regulatory protein Rac induces lamellipodia and membrane ruffles (Ridley et al., 1992). Rac also stimulates Rho-regulated synthesis of stress fibers (Ridley and Hall, 1992; 1994; Hall, 1998). These Ras-related GTPases act hierarchially: Cdc42 activity is needed for activation of Rac, which is in turn needed to activate Rho (Nobes and Hall, 1995; Ridley, 1996). Thus formation of filopodia, lamellipodia and stress fibers results from the sequential activation of Cdc42, Rac and Rho, respectively (Fig. 18). The mechanism of this hierarchial control is poorly

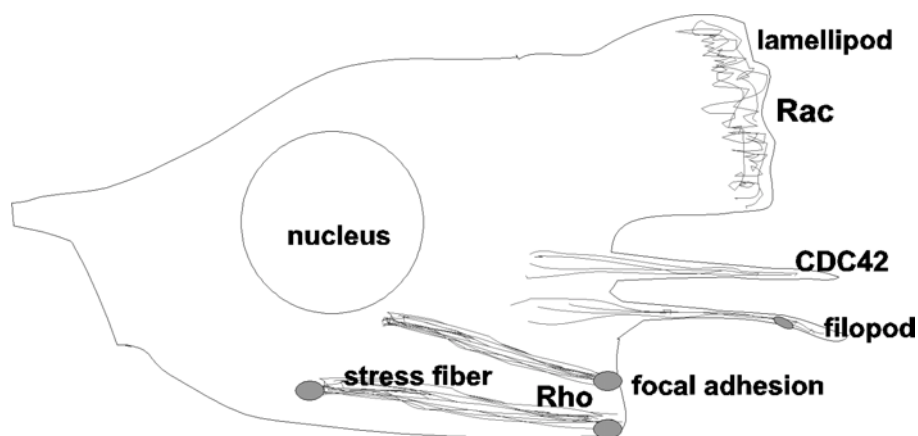


Figure 18. Actin cytoskeleton is composed of highly dynamic structures. Schematic representation of the dynamic actin cytoskeleton structures and their regulatory components, which are involved in cellular processes determining the cell shape and motility. Lamellipodia are large sheet-like structures of cross-weaved actin filaments at the cell edge. Filopodia are thin cell extensions with F-actin core, and stress fibers are intracellular F-actin bundles between focal adhesions. The formation of lamellipodia is regulated by Rac, filopodia by CDC42 and stress fibers by Rho. These Ras-related regulatory GTPases act hierarchially: CDC42 activates Rac, which in turn activates Rho. For details see the text.

understood. Normally, the members of the Rho family respond to many external stimuli via signaling pathways resulting in e.g. cell movements and cell division (Machesky and Hall, 1996; Nagata and Hall, 1996; Ridley, 1996; Zigmond, 1996; Hall, 1998).

In the present study, the overexpression of alphavirus-specific Nsp1 in several vertebrate cell lines caused fundamental changes in the actin filaments and induced massive amounts of filopodia-like structures containing Nsp1, but devoid of detectable F-actin. However, induction of filopodia was inhibited by latrunculin A suggesting that short actin stretches with high turnover rates might serve as a driving force in the extension of filopodia. Induction of filopodia and disruption of stress fibers were also observed, although less pronounced, in both SFV and SIN infected cells, indicating that these phenomena are natural responses to alphavirus infection. Expression vectors have been developed based on both SFV and SIN replicons lacking the genes for structural proteins (Liljeström and Garoff, 1991; Schlesinger,

1993). As these vectors express the RNA replicase proteins including Nsp1, they also induce changes in the host cytoskeleton, a fact which has to be taken account when analyzing the effects of expressed foreign proteins. Especially all processes involving polymerization of actin (e.g. endocytosis) should be properly controlled using other expression systems.

In RUB-infected cells no filopodial extensions were induced. However, the disappearance of stress fibers was observed indicating virus-induced changes in the actin cytoskeleton. Moreover, the P150 containing tubular extensions formed late in infection seemed to co-orient with microtubular filaments. The interaction was verified by nocodazole treatment (Liao et al., 1995), which resulted in the P150 containing tubular structures being first disrupted and then reformed in close association with newly organized microtubular bundles after removal of the drug. Close association of P150 and replicating RNA with microtubules may provide a mechanism for the virus to spread from cell to cell without exposure to the

host immune system. In fact, long virus-induced membrane-bound extensions containing P150, capsid protein and replicating RNA were observed in RUB-infected Vero cells. The extensions contained also a cytoskeletal core of a single microtubule filament or a bundle of microtubules, as well as envelope glycoproteins at the limiting membrane. The precise molecular mechanisms behind the interaction of microtubules and P150 containing membranes remain to be elucidated. Transport of the tubular membranes along microtubules may require microtubule associated proteins such as kinesin and dynein or other microtubule-dependent motors (for a review see Hirokawa, 1998).

Many other viruses have been shown to interact with the actin cytoskeleton (reviewed by Cudmore et al., 1997). Enveloped viruses utilize actin microfilaments during the process of budding and maturation of virus particles (Bohn et al., 1986; Damsky et al., 1977; Griffin and Compans, 1979). The maturation of retroviruses involves an interaction of the virus core with F-actin, and is inhibited by cytochalasin D (Maldarelli et al., 1987; Pearce-Pratt et al., 1994; Sasaki et al., 1995; Mortara and Koch, 1986; 1989). Some viruses have been reported to disrupt the stress fibers [adenovirus, herpes simplex virus, cytomegalo virus, murine leukemia virus (MLV) and vesicular stomatitis virus (VSV) (Cudmore et al., 1997). The responsible virus-coded protein has been identified in adenovirus as E1 (Jackson and Bellet, 1989), in MLV as protease, and in VSV as the L-protein, which is an RNA polymerase (Simon et al., 1990).

In Newcastle disease virus-infected cells the virus-specific ribonucleoprotein responsible for RNA replication is attached to the cytoskeletal framework consisting of actin, tubulin and vimentin, suggesting the involvement of the cytoskeletal components in viral RNA synthesis (Hamaguchi et al., 1985). A similar interaction with

cytoskeletal framework has been suggested also for the alphavirus RNA replication complex (Barton et al., 1991). The requirement of actin for *in vitro* transcription of genomic RNA has been documented for paramyxoviruses, such as HPIV3 and respiratory syncytial virus (De et al., 1991; Huang et al., 1993). In contrast, measles and Sendai virus transcription was shown to be activated by tubulin (Moyer et al., 1986; 1990). Altogether these findings strongly suggest that the cytoskeletal components play an important role in viral gene expression *in vivo*. Indirect involvement of cytoskeletal framework in the virus life cycle has been suggested at least for the measles virus (Bohn et al., 1986), VSV (Cervera et al., 1981) and RUB (Bowden et al., 1987). The most striking interaction between the virus and actin cytoskeleton is, however, reported for the vaccinia virus. Release of the extracellular form of the vaccinia virus is driven by polymerization of actin which pushes the virus particle through extensions resembling filopodia, to the extracellular space or to neighbouring cells and serves as a mechanism for viral spread (Cudmore et al., 1995; 1996; 1997). In addition, vaccinia-infected cells develop branched projections up to 160 μm in length which have growth cone-like structures. These projections, which resemble the extensions observed in RUB infected Vero cells in the present study, are formed by extension and condensation of lamellipodia from the cell body and are distinct from the polymerization of actin tails (Sanderson et al., 1998).

Summing up, interactions of virus proteins with cytoskeletal components have been suggested to be involved in various viral activities, such as genome replication, assembly and release of progeny viruses, and protein synthesis. However, the mechanisms of interaction of the viral gene products with the cytoskeletal components have not been solved. Analysis of interactions of viral proteins with host

proteins has expanded our knowledge of many central cellular processes, such as DNA replication, transcriptional control, regulation of translation, nuclear transport, signal transduction, and apoptotic cell death, as well as folding, modification, transport and targeting of exocytic membrane proteins (reviewed by Knipe, 1995). The results obtained in this study with alphavirus Nsp1 and RUB P150 provide another two examples of the deep involvement of viral proteins in basic cell functions: Either as intervention in the delicately controlled and complex regulation of actin cytoskeleton by alphavirus Nsp1, or as a potential mechanism which enables viruses to spread from cell to cell. Understanding the molecular mechanisms behind these alternations of the cytoskeleton should reveal new aspects in the regulation cascades that control the shape and movement of cells.

2. MEMBRANE ASSOCIATION OF THE RNA REPLICATION COMPLEX

In this study all SFV Nsps could be localized to the limiting membrane of CPVs. This is consistent with previous studies, where alphavirus RNA replicase components were shown to be tightly membrane-associated and present in the mitochondrial pellet fraction P15 of SFV-infected cells. During the recent emergence of virus replication research, it has become clear that positive strand RNA viruses are adapted to replicate in the cytoplasm associated with different organelle-specific membranes. These viruses include, in addition to togaviruses, at least picornaviruses (Bienz et al., 1987; 1992; Schlegel et al., 1996), coronaviruses (van der Meer et al., 1999), arteriviruses (Pedersen et al., 1999; van der Meer et al., 1998), flaviviruses (Westaway et al., 1997; Mackenzie et al., 1999), tobamoviruses (Mas et al., 1999), bromoviruses (Restrepo-Hartwig and Ahlquist, 1996) and

potyviruses (Schaad et al., 1997). The membrane association may offer a suitable microenvironment to concentrate the RNA replicase components and facilitate the recruitment of membrane-associated host factors required for the viral replication and transcription (Pedersen et al., 1999). Different families of positive strand RNA viruses appear to carry out RNA replication at different membrane sites or compartments of the cellular secretory and endocytosis pathways. Interestingly, with the exception of arteriviruses, those animal viruses with positive strand RNA genome whose genomic structure allows the translation of nonstructural proteins before structural ones (e.g. toga- and coronaviruses) have been reported to replicate at the membranes of the endocytic pathway. In contrast, picorna- and flaviviruses, whose structural proteins are translated before nonstructural ones, replicate in ER- or intermediate compartment (IR)-derived membranes of the secretory pathway. Since formation of cytoplasmic membrane complexes consisting of viral RNA, replicase proteins, and host-derived membranes is one of the earliest steps in the virus growth cycle, the membranes in the close vicinity of the virus entry site are the locations where RNA replication is likely to occur. Membrane association may play a structural role in the assembly and function of the RNA replication complex and allow exploitation of specific enzymatic functions associated with various types of cytoplasmic membranes (Restrepo-Hartwig and Ahlquist, 1996).

The replication of poliovirus occurs in vesicular structures with double-membranes, which are derived from intracellular membranes by a process resembling autophagy (Bienz et al., 1987; Schlegel et al., 1996). The poliovirus RNA replication complex is enclosed in a rosette-like shell of virus-induced smooth membrane vesicles, which contain a tightly packed second system of membranes (Bienz et al., 1992).

At low ionic strength and low temperature, the rosettes reversibly dissociate into individual tubulated vesicles, which carry a set of viral structural and nonstructural proteins as well as replicative intermediate RNA. The membranous tubules found associated with the vesicles had a diameter of about 40 nm and length of 200 to 500 nm (Egger et al., 1996). Biochemical analysis of poliovirus Nsp 2C-containing membranes has revealed that several host organelles including lysosomes, trans-Golgi, TGN and ER have contributed to the virus-induced membranous structures (Schlegel et al., 1996). Poliovirus infection results in dilation, vacuolarization and disorganization of the cellular secretory pathway (Bienz et al., 1987; 1992, Doedens and Kirkegaard, 1995; Doedens et al., 1997). Poliovirus is a non-enveloped picornavirus and thus does not require a functional secretory pathway for assembly.

This is in contrast to enveloped viruses, which have developed less drastic strategies for RNA replication to preserve a functional secretory pathway necessary for envelope glycoprotein processing. The RNA synthesis of the family arterivirus of the order *Nilovirales*, has been shown to occur on modified intracellular membranes, which are derived from the endoplasmic reticulum or the ER-Golgi intermediate compartment (IC) (Pedersen et al., 1999; van der Meer et al., 1998). Vacuoles with double membranes have been postulated to be formed from ER membranes either through protrusion-and-detachment or double-budding models (Pedersen et al., 1999). In contrast, the other family of the *Nilovirales* order, the coronaviruses, such as mouse hepatitis virus (MHV), replicate on late endosomal membranes and multivesicular bodies (van der Meer, 1999). Replication of the flavivirus Kunjin virus is associated with membrane structures which appear as intracellular packages of vesicles. In addition, Kunjin virus-induced convoluted membranes and paracrystalline arrays containing the components of the virus-

specific protease have been reported (Westaway et al., 1997). Trans-Golgi membranes and the IC were identified as the cellular origin of the flavivirus-modified membranes involved in Kunjin virus replication (Mackenzie et al., 1999).

Several plant viruses replicate at membranes, which originate from the ER (Mas et al., 1999; Restrepo-Hartwig and Ahlquist, 1996; Schaad et al., 1997). Tobacco mosaic virus (TMV) replication takes place in large ER-derived membrane structures, which contain the ER luminal binding protein (BiP) and involve association with microfilaments, microtubules and virus encoded, heavily phosphorylated, moving protein (MP). Early in infection ER-associated TMV replication complexes are transported via microtubules to perinuclear positions, where large ER-derived membrane structures containing MP, replicase and viral RNA are formed. Later in infection viral RNA-MP – complexes move along microtubules towards the cell periphery to initiate cell-to-cell spread, which is achieved by hair-like protrusions of ER membranes that contain viral RNA-MP – complexes and penetrate through the plasma membrane of tobacco protoplasts (Mas et al., 1999). Brome mosaic virus RNA replication complexes identified by incorporation of BrUTP and by the presence of helicase-like 1a and polymerase-like 2a proteins, were colocalized with the ER markers BiP and calreticulin, but not with the markers of medial Golgi or later compartments of the cellular secretory pathway (Restrepo-Hartwig and Ahlquist, 1996).

Immunochemical studies by Froshauer et al. (1988) showed that alphavirus CPVs are modified endosomes and lysosomes and the virus RNA replication occurs on the surface of these organelles. In general terms the endocytic pathway appears to consist of at least four distinct sets of organelles through which endocytic tracers pass sequentially: the early endosome (EE), the endocytic carrier vesicle (multivesicular

body), late endosome (LE; prelysosomal compartment) and the lysosome. The latter two sets of organelles are distinct, although they are both highly enriched in lysosomal enzymes (Griffiths et al., 1989; Griffiths 1996).

The endocytic apparatus of BHK cells has been shown to be efficient and thus it has capacity to effectively distribute and target virus proteins. Fluid phase markers such as horse radish peroxidase (HRP) reach the early endosomal compartment in 2 minutes and label the acidic phosphatase (LAP) positive prelysosomal and lysosomal compartments after a 20 minute chase at 37°C (Griffiths et al., 1989). Although the absolute volume of the early endosomal compartment is only one fifth of the prelysosomal compartment, it has a membrane surface almost equal to the latter compartment (Griffiths et al., 1989). It has been estimated that a single BHK cell internalizes 0.5 μm^3 of fluid per minute, which it delivers to early endosomes. The EEs in BHK cells consist of small peripheral vesicles and tubules, which recycle material rapidly between the plasma membrane and the late endosomal compartment (Griffiths et al., 1989). The delivery of membranes is tightly regulated, so that cellular markers of each compartment do not normally fuse with each other. According to the “kiss and run” hypothesis of Desjardins (1996), the endocytic process is likely to occur in complex patterns of association and disassociation of molecules with and from EE to the biochemically more stable LE compartment described as

Late endosomes in BHK cells are morphologically complex organelles composed of a large vacuolar component with internal membranes and on the average six randomly oriented tubular structures associated with the central vacuole body (Marsh et al., 1986). Most of the membrane surface area is in the tubular structures, while the bulk of the LE volume is in the large vacuolar components. Vesicles

derived from the tubular extensions may mediate the selective recycling of internalized membrane and receptors back to the plasma membrane. In contrast to the LE, lysosomes appear as nearly spherical bodies with few or without internal membranes. Lysosomes often appear in multivesicular clusters, with few tubular extensions (Marsh et al., 1986). In sucrose gradients LE have lighter density than lysosomes. Lamp-1, lamp-2 and lysosomal acid phosphatase (LAP) are common markers for both LE and the lysosomal compartment. LE have often additional markers such as Rab7, Rab9 and CI-MPR, which are missing from purified lysosomes (reviewed by Griffiths, 1996).

Morphological differentiation between the LE and lysosomes is complicated, and there is no clear consensus of how it should be done. In fact, due to the plasticity of the endocytic system in different cell lines, no clear formal separation even between the EE, LE and lysosomes can be made (Kleijmeer et al., 1997). However, Advani et al. (1999) used morphological criteria, based on papers of Griffiths et al. (1989), Klumperman et al. (1993) and Kleijmeer et al. (1997), to distinguish different members of the endosomal apparatus in EM cryosections. They defined EEs as elongated, sometimes curved, electron-lucent vacuoles with few internal membranes. LEs were defined as globular shaped compartments with numerous internal vesicles, which were connected or accompanied with many tubulo-vesicular membrane profiles indicated as endosome-associated vesicles. Electron-dense compartments without or with degraded internal membranes were categorized as lysosomes (Advani et al., 1999).

According to these criteria CPVs can morphologically be defined either as modified LEs or a novel hybrid compartment of EE, LE and lysosomes, rather than typical dense lysosomes. CPVs appeared to be spherical or flattened electron-lucent vacuoles often with internal

membranes. They appeared often as clusters either at the perinuclear region or near the plasma membrane. Further characterization revealed several LE markers in the CPV membranes. CPVs were mostly Rab7 positive, predominately lamp-1 and lamp-2 positive and costained often with LBPA, another LE marker. LBPA is a highly hydrophobic, acidic phospholipid proposed to regulate cellular cholesterol transport. It accounts for 1.5% of the total phospholipids and more than 15% of LE phospholipids in BHK cells (Kobayashi et al., 1998). Taken together the morphological and qualitative information of membrane components, it may be concluded that CPVs most likely represent novel hybrid vacuoles, with some morphological features of EEs and lysosomes, but mainly with hallmarks of an LE (prelysosomal) compartment. Similar hybrid organelles between LE and lysosomes have been reported to form also in normal cellular conditions (Mullock et al., 1998; Gu and Gruenberg, 1999).

GTPases of the Rab family are crucial regulators of membrane trafficking on the endocytotic and secretory pathways. These small GTP-binding proteins are recruited specifically to the cytoplasmic face of distinct organelles and control both spatial and temporal partnering of transport vesicles with their target membranes. Rab5 and Rab7 sequentially regulate transport in the endocytic pathway (Bucci et al., 1992; Meresse et al., 1995; Vitelli et al., 1997). Rab5 has been localized to the EE, to clathrin coated-vesicles (CCV) and to the plasma membrane. This protein regulates the rate of docking/fusion of CCV with EE as well as homotypic fusion of EE with themselves.

The endogenous Rab7 localizes to vesicular compartments mainly confined to the perinuclear region. Rab7 plays a fundamental role in controlling LE membrane fusion (Vitelli et al., 1997).

Overexpression of activated Rab7 mutant in BHK cells led to the appearance of atypically large endocytic structures, while dominant negative mutants led to very fine punctate staining. Rab7 does not function in the early endocytic pathway and does not influence the internalization or recycling of physiological ligands such as transferrin or low density lipoprotein (LDL). In control cells CI-MPR was localized to the EE, LE and TGN, but the bulk of the protein was in the LE compartment and its distribution remained the same in the presence of Rab7 activated mutant (Vitelli et al., 1997). In SFV-infected cells Rab7 seemed to localize mainly in CI-MPR negative LE compartment and only partial colocalization with CI-MPR was observed. The presence of Rab7 in CPVs suggests that it may have a regulatory role in fusion events resulting in the formation of large CPVs in the perinuclear region during late SFV infection. These structures (diameter up to 2 μ m) were larger than any normal cellular endosomal structures.

Interestingly, the distribution of Nsp1 resembles that reported for the lysosomal acid phosphatase (LAP) (Braun et al., 1989; Hille et al., 1992). CPVs were earlier shown to be LAP-positive by immunocytochemistry (Grimley et al., 1972; Peränen and Kääriäinen, 1991). Mature LAP is a soluble lysosomal enzyme, but the preform of LAP can be considered as a lysosomal membrane protein since during biosynthetic transport it is integrally associated with membranes (Waheed et al., 1988). Indirect transport via the cell surface and endocytosis has been postulated for LAP. Individual LAP molecules rapidly cycle multiple times between the plasma membrane and endosomes, since transport to the lysosomes requires 5-6 hours and the recycling can occur as fast as in six minutes (Braun et al., 1989).

3. CPV BIOGENESIS

CPV biogenesis seems to be a virus induced process, which modifies a proper cellular compartment for use in virus RNA replication. The modification involves a progressive enrichment of Nsps into the LE compartment. CPVs acquire some LE/lysosomal markers, such as lamp-1, lamp-2 and LAP, but are essentially devoid of purely lysosomal markers, whose transport to lysosomes is mediated by mannose-6-phosphate signals. One such protein is β -hexoaminidase that is absent from CPVs (Froshauer et al., 1988). Thus, the biogenesis of CPVs is not likely to involve major MPR-mediated membrane recycling between TGN and late endosomal/lysosomal compartments. The maturation of CPVs is likely to be mediated by multiple transient interactions with late endocytotic vesicles according to the “kiss and run” model (Desjardins, 1996) as suggested by the accumulation of lamp and EEA1-positive vacuoles around CPV. A further indication of multiple transient interactions can be seen in EM micrographs of BSA-gold labeled CPV structures with internal vesicular membranes with or without spherules (Fig. 8). Late in infection CPVs with internal vesicles containing TfR were observed, suggesting autophagy type membrane intake into CPVs. Since the internal vesicles are thought to originate from inward budding of the limiting membrane, the differential distribution of membrane proteins in the limiting and internal membranes suggests active protein sorting (Escola et al., 1998). Thus, the maturation of CPVs could involve a complex series of bi-directional exchanges of membranous and luminal content and the fusion events are likely to be regulated by Rab7, which is abundantly present in the CPVs.

The internalization profiles seen on the plasma membrane strongly suggest that some CPVs may recycle between the plasma membrane and the cytosol.

Internalization of spherule containing batches of plasma membrane into intracellular vacuoles could be one putative mechanism of CPV biogenesis. The close connection between CPVs and PM was further verified by BSA-gold labeling experiments, where CPVs could be labeled with extracellular tracer within 10 minutes (Fig 17). In the same experiments some of the BSA-gold labelled CPVs were evidently secreted to the medium in a process that resembles the regulated secretion of exosomes by hemopoietic cells, such as B-lymphocytes (Stinchcombe et al., 1999). Exosomes are a heterogeneous set of endocytic vacuoles with internal membrane vesicles and sheets in antigen presenting cells (Kleijmeer et al., 1997; Escola et al., 1998). Major histocompatibility complex (MCH) class II molecules (MIIC) are present peptide determinants of foreign antigens to T-cells. Multivesicular MIIC containing vacuoles (e.g. exosomes) can fuse with the PM directly, releasing the internal vesicles into the culture medium. Exosomes secreted by B-cell lines are enriched in the tetraspan superfamily of lysosomal membrane proteins (CD37, CD53, CD63; CD81 and CD82), but not in other LE/lysosomal markers, such as lamp-1 and lamp-2 (Escola et al., 1998). Phenomena similar to those observed in SFV-infected cells have been reported for coronavirus infected cells (van der Meer et al., 1999), and they occur also late in RUB-infection (unpublished observations). This might be a mechanism to discharge foreign material and represent a cellular response to viral insult, but it could also be a viral-induced mechanism to promote the transfer of RNA replicase components from cell to cell.

4. A MODEL FOR CPV BIOGENESIS AND SPHERULE CIRCULATION

According to observations obtained in this study combined with earlier published

results of alphavirus infection a hypothetical model of the early events in SFV infection is presented below:

SFV enters the cell by receptor-mediated endocytosis and acid-induced fusion of the viral membrane with the endosomes occurs as earlier described (Kielian and Helenius, 1986). The fusion can be inhibited by increasing the intravesicular pH with lysosomotropic drugs, such as chloroquine. The pH threshold for fusion has been shown to be 6.2, which corresponds to the pH present in the lumen of EEs. Therefore it can be assumed that the membranes of EEs are the initial site for the translation of the Nsps. As the endosomes recycle rapidly between the cytoplasm and the cell surface, the Nsps, translated at the cytosolic surface of endosomal membranes, become scattered to the cytoplasm. The nonstructural component translated first, Nsp1, has a strong affinity for the plasma membrane, and thus guides the nonstructural polyprotein to the inner surface of the PM. The primary assembly of the RNA replication complex takes place at the plasma membrane with the assistance of Nsp1. We have recently identified an amino acid sequence in Nsp1 which binds to anionic phospholipids such as phosphatidylserine (Ahola et al., 1999), which is greatly enriched in the cytoplasmic leaflet of the plasma membrane (Allen, 1996). At the plasma membrane only a small proportion of the RNA replication complexes assemble correctly, followed by rapid internalization via the endosomal pathway to the biochemically more stable late endosomal compartment. Nsps which fail to assemble to a complex are dissociated from each other and distribute to the cytoplasm or nucleus achieving their characteristic localization revealed by indirect immunofluorescence. Interestingly, it has been reported that SIN virus production in mutant COS cells decreased immediately upon phosphatidylserine deprivation, whereas cell growth, viability and cellular macromolecular biosynthesis remained

normal (Kuge et al., 1989). Further, viral RNA synthesis was greatly reduced in phosphatidylserine and phosphatidylethanolamine biosynthesis defective cells, suggesting that nucleocapsids of internalized SIN were not normally released into the cytoplasm. The study demonstrated the absolute requirement of the membrane phospholipids phosphatidylserine and phosphatidylethanolamine in CHO cells for SIN infection (Kuge et al., 1989).

We propose further that successfully assembled RNA replication complexes induce the formation of spherules, which most probably are the units responsible for the RNA replication, containing a set of all Nsps and 42S RNA minus-strand template. This spherule unit can assemble at the plasma membrane or inside the cell. It will be endocytosed readily by the coated pit-coated vesicle pathway as can be seen in several electron microscopic images. It can also return to the plasma membrane along with the endosome cycle. As infection progresses, more and more CPVs become enriched in the perinuclear region acquiring lamp-1, lamp-2, and LBPA in addition to Rab7, which is a known regulator of membrane traffic in late endosomal compartment (Meresse et al., 1995; Vitelli et al., 1997; Bucci et al., 2000). Interestingly, CPVs late in infection continuously receive extracellular material, as evidenced by endocytosis of BSA-gold particles. Thus, we cannot exclude the possibility that also late in infection, when the synthesis of Nsps is shut off (Lachmi and Kääriäinen, 1977; Kääriäinen and Söderlund, 1978), recycling of spherules to the plasma membrane may continue. These replication complexes may still be active in RNA synthesis as suggested by EM-autoradiography (Grimley et al., 1968), although the cell might try to discharge them by an exosome-type mechanism.

The Nsps are concentrated to the limiting membrane of the CPVs, at the same site where the spherules are present.

According to cryo-EM and Nanogold – studies the RNA replicase is located at the limiting membrane, most likely near the mouth of the spherules. The putative double-stranded intermediate RNA is located inside the spherule and it probably circles through the membrane anchored polymerase complex.

5. FUTURE ASPECTS

Further information of togavirus RNA replication and CPV biogenesis will be obtained with transfection studies of SFV nonstructural polyprotein and its proteolytically deficient derivatives. These studies should reveal, which Nsps are required for spherule formation. It is even now evident that Nsp1 alone is not sufficient to form these unique structures. The main goal should be the viral RNA synthesis *in vitro* conditions with purified protein components, where the contribution of essential host factors could be determined. Gentle isolation of spherules from PM of infected or transfected cells could provide functional RNA replication complexes for *in vitro* RNA synthesis studies.

The poorly understood events in RUB RNA replication should be examined with a potent antisera against P90, the proposed

RNA polymerase subunit of RUB RNA replication complex. So far antibodies, which would allow intracellular localization and biochemical characterization of P90 do not exist.

The only RNA-dependent polymerase crystal structures, which have been solved so far are those of two retroviral polymerases [(the unliganded form of reverse transcriptase (RT) of HIV 1 and a fragment of the RT of Moloney leukemia virus)], a fragment of the poliovirus polymerase 3D^{pol} and the catalytic domain (531 aa) of hepatitis C virus nonstructural protein 5B (Hansen et al., 1997; Bressanelli et al., 1999; Jäger and Pata, 1999). These all have certain common structural features and are organized around a central cleft consisting of an RNA binding groove and an NTP tunnel. The structural arrangement is reminiscent of a right hand with subdomains named palm, fingers and thumb (reviewed in Jäger and Pata, 1999). The hepatitis C virus (a member of the flavivirus genus) polymerase is a heart-shaped molecule with dimensions 70x60x40 Å and has a deep cleft in the middle of the palm (Bressanelli et al., 1999). Future structural studies will reveal if togavirus RNA polymerases turn out to belong to the same family together with those of picorna-, flavi- and retroviruses.

ACKNOWLEDGEMENTS

This work was carried out in the Animal virus laboratorio at the Institute of Biotechnology under supervision of Professor Leevi Kääriäinen. I owe my deepest gratitude to Leevi for his support, encouragement and enthusiasm during these years. The Head of the Institute Prof. Mart Saarma is acknowledged for providing excellent working facilities and showing interest in my work. Prof. Carl G. Gahmberg, the Head of the Division of Biochemistry, is thanked for his positive and flexible attitude towards my Ph.D studies. Prof. Marja Makarow, the Head of the Viikki Graduate School in Biosciences is acknowledged for organizing excellent courses and for valuable advice in many practical things. I am grateful to Prof. Carl-Henrik von Bonsdorff and Docent Vesa Olkkonen, who formed the follow up group of my thesis work and revised carefully the text at a very short notice. Heli Ruoho is acknowledged for designing the cover and Donald Smart for revising the language of this thesis.

The present and former members of SFV-group: Johan Peränen, Marja Mikkola (Rikkonen), Pirjo Laakkonen, Tero Ahola, Tarja Välimäki, Helena Vihinen, Petri Auvinen, Titta Blom (Anttinen), Neda Ehsani, Reetta Kettunen, Airi Sinkko, Anne Ikäheimonen, Julia Magden, Anja Lampio, Kimmo Karhi, Andres Merits, Lidia Vasiljeva and Hannu Väänänen are all warmly thanked for help, advice, support and the relaxed atmosphere in the laboratory. Especially Petri, Tero, Helena and Anne have had a significant contribution in my work. The enthusiasm and encouragement of Petri has had a great impact for not giving up this project on moments when everything seemed to fail. Without the aid and patience of Helena "the confocal queen" many images of this thesis would never have been existed. Helena made also the layout of this thesis.

The staff of the Electron microscopy unit is gratefully acknowledged. Especially Arja Strandell for tireless sectioning of my Epon samples, Mervi Lindman and Jyrki Juhanoja for technical support with the microscopes and Dr. Eeva-Liisa Eskelinen (Punnonen) for helpful discussions and for providing new procedures for immunolabeling are greatly appreciated. Dr. John Lucocq, University of Dundee, is acknowledged for introducing me the cryo-EM technique. The visit to Scotland changed my life in many ways.

Coffee group, Kaija Kettunen, Ritva Rajala, Liisa Teräsvuori, Jaana Suopanki, Helena Miettinen, Alpo Vuorio, Ritva Niemelä, Pirjo, Marja and Tarja, is warmly thanked for bringing lively social events and culinary pleasures that pleasantly broke the daily routines of a researcher. BI Knockouts, the official floorball team of the Institute, is acknowledged for providing the spirit needed in and outside the playground.

Thanks are due also to all my friends outside the Institute. Tarja is thanked for the years we shared together. The former student fellows "Pöpöjussit" Pekka Varmanen, Vesa Mäntynen and Markku Keskimäki are acknowledged for many unmemorable occasions and just for being there. Traditional "Kalaporukka" has annually gathered some good old friends together to the beautiful archipelago of Ahvenanmaa, where everything connected to the laboratory could easily be forgotten for a couple of days.

My mother and late father are thanked for their care and support throughout my life.

This study was financially supported by Sigfried Juselius Foundation, Academy of Finland, Foundation of Virus research and Agronomiliitto.

Helsinki, 27th May, 2000

REFERENCACES

- Acheson, N.H. and Tamm, I.** (1967). Replication of Semliki Forest virus: An electron microscopic study. *Virology* 32, 128-143.
- Advani, R.J., Yang, B., Prekeris, R., Lee, K.C., Klumperman, J., and Scheller, R.S.** (1999). VAMP-7 mediates vesicular transport from endosomes to lysosomes. *J.Cell Biol.* 146, 765-775.
- Ahola, T. and Kääriäinen, L.** (1995). Reaction in alphavirus mRNA capping: Formation of a covalent complex of nonstructural protein nsP1 with 7-methyl-GMP. *Proc. Natl. Acad. Sci.USA* 92, 507-511.
- Ahola, T., Laakkonen, P., Vihinen, H., and Kääriäinen, L.** (1997). Critical residues of Semliki Forest virus RNA capping enzyme involved in methyltransferase and guanylyltransferase-like activities. *J.Virol.* 71, 392-397.
- Ahola, T., Lampio, A., Auvinen, P., and Kääriäinen, L.** (1999). Semliki Forest virus mRNA capping enzyme requires association with anionic membrane phospholipids for activity. *EMBO J.* 11, 3164-3172.
- Allen, D.** (1996). Mapping the lipid distribution in the membranes of BHK cells. *Mol. Membr. Biol.* 13, 81-84.
- Argos, P.** (1988). A sequence motif in many polymerases. *Nucleic Acids Res.* 16, 9909-9916.
- Atkins, G.J., Sheahan, B.J., and Mooney, D.A.** (1990). Pathogenicity of Semliki Forest virus for the rat central nervous system and primary rat neural cell cultures - possible implications for the pathogenicity of multiple sclerosis. *Neuropath. Appl. Neurobiol.* 16, 57-68.
- Atkins, G.J., Sheahan, B.J., and Liljeström, P.** (1996). Manipulation of the Semliki Forest virus genome and its potential for vaccine construction. *Mol. Biotech.* 5, 33-38.
- Atkins, G.J., Sheahan, B.J., and Liljeström, P.** (1999). The molecular pathogenesis of Semliki Forest virus: a model virus made useful? *J.Gen.Virol.* 80, 2287-2297.
- Baron, M.D. and Forsell, K.** (1991). Oligomerization of the structural proteins of rubella virus. *Virology* 185, 811-819.
- Barton, D.J., Sawicki, S.G., and Sawicki, D.L.** (1991). Solubilization and immunoprecipitation of alphavirus replication complexes. *J.Virol.* 65, 1496-1506.
- Bienz, K., Egger, D., and Pasamontes, L.** (1987). Association of poliovirus proteins of the P2 genomic region with the viral replication complex and virus-induced membrane synthesis as visualized by electron microscopic immunocytochemistry and autoradiography. *Virology* 160, 220-226.
- Bienz, K., Egger, D., Pfister, T., and Troxler, M.** (1992). Structural and functional characterization of the poliovirus replication complex. *J.Virol.* 66, 2740-2747.
- Bohn, W., Rutter, H., Hohenberg, K., Mannweiler, K., and Nobis, P.** (1986). Involvement of actin microfilaments in the budding of measles virus: studies on cytoskeletons of infected cells. *Virology* 149, 91-106.
- Bonatti, S., Migliaccio, G., and Simons, K.** (1989). Palmitoylation of viral membrane glycoproteins takes place after exit from the endoplasmic reticulum. *J. Biol. Chem.* 264, 12590-12595.
- Bowden, D.S. and Westaway, E.G.** (1989). Rubella virus products and their distribution in infected cells. *Subcell. Biochem.* 15, 203-231.
- Bowden, D.S., Pedersen, J.S., Toh, B.H., and Westaway, E.G.** (1987). Distribution of immunofluorescence of viral products and actin-containing cytoskeletal filaments in

References

- rubella virus-infected cells. *Arch.Virol.* 92, 211-219.
- Bradish, C.J., Allner, K., and Maber, H.B.** (1971). The virulence of original and derived strains of Semliki Forest virus for mice, guinea-pigs and rabbits. *J. Gen. Virol.* 12, 141-160.
- Braun, M, Waheed, A., and von Figura, K.** (1989). Lysosomal acid phosphatase is transported to lysosomes via the cell surface. *EMBO J.* 8, 3633-3640.
- Bressanelli, B., Tomei, L., Roussel, A., Incitti, I., Vitale, R.L., Mathieu, M., De Francesco, R., and Rey, F.A.** (1999). Crystal structure of the RNA-dependent RNA polymerase of hepatitis C virus. *Proc. Natl. Acad. Sci. USA* 96, 13034-13039.
- Bucci, C., Parton, R.G., Mather, I.H., Stunnenberg, H.G., Simons, K., Hoflack, B., and Zerial, M.** (1992). The small GTPase rab5 functions as a regulatory factor in the early endocytic pathway. *Cell* 70, 715-728.
- Bucci, C., Thompsen, P., Nicoziani, P., McCarthy, J., and van Deurs, B.** (2000). Rab7: A key to lysosome biogenesis. *Mol. Biol. Cell* 11, 467-480.
- Burridge, K., Chrzanowska-Wodnicka, M., and Zhong, C.** (1997). Focal adhesion assembly. *Trends Cell Biol.* 7, 342-347.
- Cervera, M., Dreyfuss, G., and Penman, S.** (1981). Messenger RNA is translated when associated with the cytoskeletal framework in normal and VSV-infected HeLa cells. *Cell* 23, 113-120.
- Chamberlain, R.W.** (1980). Epidemiology of arthropod-borne togaviruses: The role of arthropods as hosts and vectors and of vertebrate hosts in natural transmission cycles. In *The Togaviruses: Biology, structure, replication*. R.W. Schlesinger, ed. (Orlando: Academic), pp. 175-227.
- Chen, J.-P., Strauss, J.H., Strauss, E.G., and Frey, T.K.** (1996). Characterization of the rubella virus nonstructural protease domain and its cleavage site. *J.Virol.* 70, 4707-4713.
- Cheng, E.H.Y., Levine, B., Boise, L.H., Thompson, C.B., and Hardwick, J.M.** (1996). Bax-independent inhibition of apoptosis by Bcl-XL. *Nature* 379, 554-556.
- Cheng, R.H., Kuhn, R.J., Olson, N.H., Rossmann, M.G., Choi, H.-K., Smith, T.J., and Baker, T.S.** (1995). Nucleocapsid and glycoprotein organization in an enveloped virus. *Cell* 80, 621-630.
- Choi, H.-K., Tong, L., Minor, W., Dumas, P., Boege, U., Rossmann, M.G., and Wengler, G.** (1991). Structure of Sindbis virus core protein reveals a chymotrypsin-like serine proteinase and the organization of the virion. *Nature* 354, 37-43.
- Clague, M.J.** (1998). Molecular aspects of the endocytic pathway. *Biochem. J.* 336, 271-282.
- Clarke, D.M., Loo, T.W., McDonald, H., and Gillam, S.** (1988). Expression of rubella virus cDNA coding for the structural proteins. *Gene* 65, 23-30.
- Craig, S.W. and Johnson, R.P.** (1996). Assembly of focal adhesions: progress, paradigms, and portents. *Curr. Opin. Cell Biol.* 8, 74-85.
- Cudmore, S., Cossart, P., Griffiths, G., and Way, M.** (1995). Actin-based motility of vaccinia virus. *Nature* 378, 636-638.
- Cudmore, S., Reckmann, I., Griffiths, G., and Way, M.** (1996). Vaccinia virus: a model system for actin-membrane interactions. *J. Cell Sci.* 109, 1739-1747.
- Cudmore, S., Reckmann, I., and Way, M.** (1997). Viral manipulations of the actin cytoskeleton. *Trends Microbiol.* 5, 142-148.
- Damsky, C.H., Sheffield, J.B., Tuszyński, G.P., and Warren, L.** (1977). Is there a role for actin in virus budding? *J. Cell Biol.* 75, 593.
- Davidkin, I. and Valle, M.** (1998). Vaccine-induced measles virus antibodies after two doses of combined measles, mumps and

- rubella vaccine: a 12-year follow-up in two cohorts. *Vaccine* 20, 2052-2057.
- De, B.P., Lesoon, A., and Banerjee, A.K.** (1991). Human parainfluenza virus type 3 transcription in vitro: role of cellular actin in mRNA synthesis. *J.Virol.* 65, 3268-3275.
- Dé, I., Sawicki, S.G., and Sawicki, D.L.** (1996). Sindbis virus RNA-negative mutants that fail to convert from minus-strand to plus-strand synthesis: Role of the nsP2 protein. *J.Virol.* 70, 2706-2719.
- deGroot, R.J., Hardy, W.R., Shirako, Y., and Strauss, J.H.** (1990). Cleavage-site preferences of Sindbis virus polyproteins containing the non-structural proteinase. Evidence for temporal regulation of polyprotein processing *in vivo*. *EMBO J.* 9, 2631-2638.
- deGroot, R.J., Rüménapf, T., Kuhn, R.J., Strauss, E.G., and Strauss, J.H.** (1991). Sindbis virus RNA polymerase is degraded by the N-end rule pathway. *Proc. Natl. Acad. Sci. USA* 88, 8967-8971.
- Desjardins, M., Huber, L.A., Parton, R.G., and Griffiths, G.** (1994). Biogenesis of phagolysosomes proceeds through a sequential series of interactions with the endolytic apparatus. *J. Cell Biol.* 124, 677-688.
- Ding, M. and Schlesinger, M.J.** (1989). Evidence that Sindbis virus nsP2 is an autoprotease which processes the virus nonstructural polyprotein. *Virology* 171, 280-284.
- Doedens, J.R. and Kirkegaard, K.** (1995). Inhibition of cellular protein secretion by poliovirus proteins 2B and 3A. *EMBO J.* 14, 894-907.
- Doedens, J.R., Giddings, T.H., and Kirkegaard, K.** (1997). Inhibition of endoplasmic reticulum-to-Golgi traffic by poliovirus protein 3A: genetic and ultrastructural analysis. *J.Virol.* 71, 9054-9064.
- Dominguez, G., Wang, C.-Y., and Frey, T.K.** (1990). Sequence of the genome RNA of rubella virus: Evidence for genetic rearrangement during Togavirus evolution. *Virology* 177, 225-238.
- Duncan, R., Muller, J., Lee, N., Esmaili, A., and Nakhasi, H.L.** (1999). Rubella virus-induced apoptosis varies among cell lines and is modulated by bcl-x1 and caspase inhibitors. *Virology* 255, 117-128.
- Egger, D., Pasamontes, L., Bolten, R., Boyko, V., and Bienz, K.** (1996). Reversible dissociation of the poliovirus replication complex: Functions and interactions of its components in viral RNA synthesis. *J.Virol.* 70, 8675-8683.
- Escola, J.-M., Kleijmeer, M.J., Stoorvogel, W., Griffith, J.M., Yoshie, O., and Geuze, H.J.** (1998). Selective enrichment of tetraspan proteins on the internal vesicles of multivesicular endosomes and on exosomes secreted by human B-lymphocytes. *J. Biol. Chem.* 273, 20121-10127.
- Favre, D., Studer, E., and Michel, M.R.** (1996). Semliki Forest virus capsid protein inhibits the initiation of translation by up-regulating the double-stranded RNA-activated protein kinase (PKR). *Biosci. Rep.* 16, 485-511.
- Fornig, R.-Y. and Frey, T.K.** (1995). Identification of the rubella virus nonstructural proteins. *Virology* 206, 843-853.
- Forsell, K., Griffiths, G., and Garoff, H.** (1996). Preformed cytoplasmic nucleocapsids are not necessary for alphavirus budding. *EMBO J.* 15, 6495-6505.
- Francy, D.B., Jaenson, T.G., Lundstrom, J.O., Schildt, E.B., Espmark, A., Henriksson, B., and Niklasson, B.** (1989). Ecologic studies of mosquitoes and birds as hosts of Ockelbo virus in Sweden and isolation of Inkoo and Batai viruses from mosquitoes. *Am. J. Trop. Med. Hyg.* 41, 355-363.
- Frey, T.K.** (1994). Molecular biology of rubella virus. *Adv. Virus Res.* 44, 69-161.

References

- Frey, T.K. and Marr, L.D.** (1988). Sequence of the region coding for virion proteins C and E2 and carboxy terminus of the nonstructural proteins of rubella virus: comparison with alphaviruses. *Gene* 62, 85-99.
- Frey, T.K., Marr, L.D., Hemphill, M.L., and Dominiguez, G.** (1986). Molecular cloning and sequencing of the region of the rubella virus genome coding for glycoprotein E1. *Virology* 154, 228-232.
- Frey, T.K., Marr, L.D., Sanchez, A., and Simmons, R.B.** (1989). Identification of the 5' end of the rubella virus subgenomic RNA. *Virology* 168, 191-194.
- Friedman, R.M. and Berezsky, I.K.** (1967). Cytoplasmic fractions associated with Semliki Forest virus ribonucleic acid replication. *J. Virol.* 1, 374-383.
- Friedman, R.M., Levin, J.G., Grimley, P.M., and Berezsky, I.K.** (1972). Membrane-associated replication complex in arbovirus infection. *J. Virol.* 10, 504-515.
- Frolov, I., and Schlesinger, S.** (1994). Comparison of the effects on host cell protein synthesis of Sindbis virus and Sindbis virus replicons on the host cell protein synthesis and cytopathogenicity in BHK cells. *J. Virol.* 68, 1721-1727.
- Froshauer, S., Kartenbeck, J., and Helenius, A.** (1988). Alphavirus RNA replicase is located on the cytoplasmic surface of endosomes and lysosomes. *J. Cell Biol.* 107, 2075-2086.
- Fuerst, T.R., Niles, E.G., Studier, F.W., and Moss, B.** (1986). Eukaryotic transient expression system based on recombinant vaccinia virus that synthesizes bacteriophage T7 RNA polymerase. *Proc. Natl. Acad. Sci. USA* 83, 8122-8126.
- Fuller, S.D.** (1987). The T=4 envelope of Sindbis virus is organized by interactions with a complementary T=3 capsid. *Cell* 48, 923-934.
- Fuller, S.D., Berriman, J.A., Butcher, S.J., and Gowen, B.E.** (1995). Low pH induces swiveling of the glycoprotein heterodimers in the Semliki Forest virus spike complex. *Cell* 81, 715-725.
- Garoff, H., Simons, K., and Renkonen, O.** (1974). Isolation and characterization of the membrane proteins of Semliki Forest virus. *Proc. Natl. Acad. Sci. USA* 71, 3988-3992.
- Garoff, H., Simons, K., and Dobberstein, B.** (1978). Assembly of the Semliki Forest virus membrane glycoproteins in the membrane of the endoplasmic reticulum in vitro. *J. Mol. Biol.* 124, 587-600.
- Garoff, H., Frischauf, A.-M., Simons, K., Lehrach, H., and Delius, H.** (1980a). Nucleotide sequence of cDNA coding for Semliki Forest virus membrane glycoproteins. *Nature* 288, 236-241.
- Garoff, H., Frischauf, A.-M., Simons, K., Lehrach, H., and Delius, H.** (1980b). The capsid protein of Semliki Forest virus has clusters of basic amino acids and prolines in its amino terminal region. *Proc. Natl. Acad. Sci. USA* 77, 6376-6380.
- Garoff, H., Huylebroeck, D., Robinson, A., Tillman, U., and Liljeström, P.** (1990). The signal sequence of the p62 protein of Semliki Forest virus is involved in initiation but not in completing chain translocation. *J. Cell Biol.* 111, 867-876.
- Garoff, H., Hewson, R., and Opstelten, D.J.E.** (1998). Virus maturation by budding. *Microbiol. Mol. Biol. Rev.* 62, 1171-1190.
- Glasgow, G.M., Sheahan, B.J., Atkins, G.J., Wahlberg, J.M., Salminen, A., and Liljeström, P.** (1991). Two mutations in the envelope glycoprotein E2 of Semliki Forest virus affecting the maturation and entry patterns of the virus alter pathogenicity for mice. *Virology* 75, 663-668.
- Glasgow, G.M., McGee, M.M., Mooney, D.A., Sheahan, B.J., and Atkins, G.J.** (1997). Death mechanisms in cultured cells infected by Semliki Forest virus. *J. Gen. Virol.* 78, 1559-1563.

- Glasgow, G.M., McGee, M.M., Tarbatt, C.J., Mooney, D.A., Sheahan, B.J., and Atkins, G.J.** (1998). The Semliki Forest virus vector induces p53-independent apoptosis. *J. Gen. Virol.* 79, 2405-2410.
- Gomatos, P.J., Kääriäinen, L., Keränen, S., Ranki, M., and Sawicki, D.L.** (1980). Semliki Forest virus replication complex capable of synthesizing 42S and 26S nascent RNA chains. *J. Gen. Virol.* 49, 61-69.
- Gomez De Cedron, M., Ehsani, N., Mikkola, M.L., García, J.A., and Kääriäinen, L.** (1999). RNA helicase activity of Semliki Forest virus replicase protein Nsp2. *FEBS Lett.* 448(1),19-22.
- Goode, B.L., Drubin, D.G., and Barnes, G.** (2000). Functional cooperation between the microtubule and actin cytoskeletons. *Curr. Opin. Cell Biol.* 12, 63-71.
- Gorbalenya, A.E. and Koonin, E.V.** (1989). Viral proteins containing the purine NTP-binding sequence pattern. *Nucleic Acids Res.* 17, 8413-8440.
- Gorbalenya, A.E. and Koonin, E.V.** (1993). Helicases: amino acid sequence comparisons and structure-function relationships. *Curr. Opin. Cell Biol.* 3, 419-429.
- Gorbalenya, A.E., Koonin, E.V., and Lai, M.-C.** (1991). Putative papain-related thiol proteases of positive-strand RNA viruses. Identification of rubi- and aphthovirus proteases and delineation of a novel conserved domain associated with proteases of rubi-, alpha- and coronaviruses. *FEBS Lett.* 288, 201-205.
- Grandgigard, D., Studer, E., Monney, L., Belser, T., Fellay, I., Borner, C., and Michel, M.R.** (1998). Alphaviruses induce apoptosis in blc-2-overexpressing cells: evidence for a caspase-mediated, proteolytic activation of blc-2. *EMBO J.* 17, 1268-1278.
- Green, J., Griffiths, G., Louvard, D., Quinn, P., and Warren, G.** (1981). Passage of viral membrane proteins through the Golgi complex. *J. Mol. Biol.* 152, 663-698.
- Griffin, J.A., and Compans, R.W.** (1979). Effect of cytochalasin B on maturation of enveloped viruses. *J. Exp. Med.* 150, 379-391.
- Griffiths, G.** (1996). On vesicles and membrane compartments. *Protoplasma* 195, 37-58.
- Griffiths, G., Quinn, P., and Warren, G.** (1983). Dissection of the Golgi complex. I. Monensin inhibits the transport of viral membrane proteins from medial to trans Golgi cisternae in baby hamster kidney cells infected with Semliki Forest virus. *J. Cell Biol.* 96, 835-850.
- Griffiths, G., McDowell, A., Back, R., and Dubochet, J.** (1984). On the preparation of cryosections for immunochemistry. *J. Ultrastruct.* 89, 65-78.
- Griffiths, G., Back, R., and Marsh, M.** (1989). A quantitative analysis of the endocytic pathway in baby hamster kidney cells. *J. Cell Biol.* 109, 2703-2720.
- Grimley, P.M., Berezsky, I.K., and Friedman, R.M.** (1968). Cytoplasmic structures associated with an arbovirus infection: loci of viral ribonucleic acid synthesis. *J. Virol.* 2, 1326-1338.
- Grimley, P.M., Levin, J.G., Berezsky, I.K., and Friedman, R.M.** (1972). Specific membranous structures associated with the replication of group A arboviruses. *J. Virol.* 10, 492-503.
- Gros, C. and Wengler, G.** (1996). Identification of an RNA-stimulated NTPase in the predicted helicase sequence of the rubella virus nonstructural polyprotein. *Virology* 217, 367-372.
- Gruenberg, J. and Maxfield, F.R.** (1995). Membrane transport in the endocytic pathway. *Curr. Opin. Cell Biol.* 7, 552-563.
- Gu, F., and Gruenberg, J.** (1999). Biogenesis of transport intermediates in the endocytotic pathway. *FEBS Lett.* 452, 61-66.

References

- Hahn, Y.S., Strauss, E.G., and Strauss, J.H.** (1989a). Mapping of RNA⁻ temperature-sensitive mutants of Sindbis virus: Assignment of complementation groups A, B, and G to nonstructural proteins. *J. Virol.* 63, 3142-3150.
- Hahn, Y.S., Grakoui, A., Rice, C.M., Strauss, E.G., and Strauss, J.H.** (1989b). Mapping of RNA⁻ temperature-sensitive mutants of Sindbis virus: Complementation group F mutants have lesions in Nsp4. *J. Virol.* 63, 1194-1202.
- Hall, A.** (1998). Rho GTPases and the actin cytoskeleton. *Science* 279, 509-514.
- Hamaguchi, M., Nishikawa, K., Toyoda, T., Yoshida, T., Hanaichi, T., and Nagai, Y.** (1985). Transcriptional complex of Newcastle disease virus: structural and functional assembly with the cytoskeletal framework. *Virology* 147, 295-308.
- Hansen, J.L., Long, A.M., and Schultz, S.C.** (1997). Structure of the RNA-dependent RNA polymerase of poliovirus. *Structure* 5, 1109-1122.
- Hardy, W.R. and Strauss, J.H.** (1989). Processing the nonstructural polyproteins of Sindbis virus: Nonstructural proteinase is in the C-terminal half of nsP2 and functions both in *cis* and in *trans*. *J. Virol.* 63, 4653-4664.
- Hardy, W.R., Hahn, Y.S., de Groot, R.J., Strauss, E.G., and Strauss, J.H.** (1990). Synthesis and processing of the nonstructural polyproteins of several temperature-sensitive mutants of Sindbis virus. *Virology* 177, 199-208.
- Harlow, E. and Lane, D.** (1988). *Antibodies: A Laboratory Manual*. (New York: Cold Spring Harbor Laboratory).
- Helenius, A., Kartenbeck, J., Simons, K., and Fries, E.** (1980). On the entry of Semliki Forest virus in BHK-21 cells. *J. Cell Biol.* 84, 404-420.
- Hemphill, M.L., Forng, R.-Y., Abernathy, E.S., and Frey, T.K.** (1988). Time course of virus-specific macromolecular synthesis during rubella virus infection in Vero cells. *Virology* 162, 65-75.
- Hille, A., Klumperman, J., Geuze, H.J., Peters, C., Brodsky, F.M., and Figura, K.** (1992). Lysosomal acid phosphatase is internalized via clathrin-coated pits. *Eur. J. Cell Biol* 59, 106-115.
- Hirokawa, N.** (2000). Kinesin and dynein superfamily proteins and the mechanism of organelle transport. *Science* 279, 519-526.
- Hobman, T.C., Lundström, M.L., and Gillam, S.** (1990). Processing and intracellular transport of rubella virus structural proteins in COS cells. *Virology* 178, 122-133.
- Hofmann, J., Pletz, M.W.R., and Liebert, U.G.** (1999). Rubella virus-induced cytopathic effect in vitro is caused by apoptosis. *J. Gen. Virol.* 80, 1657-1664.
- Huang, Y.T., Romito, R.R., De, B.P., and Banerjee, A.K.** (1993). Characterization of the in vitro system for the synthesis of mRNA from human respiratory syncytial virus. *Virology* 193, 862-867.
- Hunziker, W. and Geuze, H.J.** (1995). Intracellular trafficking of lysosomal membrane proteins. *BioEssays* 18, 379-389.
- Jackson, P., and Bellett, A.J.D.** (1989). Relationship between organization of the actin cytoskeleton and the cell cycle in normal and adenovirus-infected rat cells. *J. Virol.* 63, 311-318.
- Joe, A.K., Foo, H.H., Kleman, L., and Levine, B.** (1998). The transmembrane domains of Sindbis virus envelope glycoproteins induce cell death. *J. Virol.* 72, 3935-3943.
- Johnston, R.E. and Peters, C.J.** (1996). Alphaviruses. In *Fields Virology*. B.N. Fields, D.M. Knipe, and P.M. Howley, eds. (Philadelphia: Lippincott-Raven Publishers), pp. 843-898.
- Jockusch, B.M., and Rüdiger, M.** (1996). Crosstalk between cell adhesion molecules:

- vinculin as a paradigm for regulation by conformation. *Trends Cell Biol.* 6, 311-315.
- Jäger, J., and Pata, J.D.** (1999). Getting a grip: polymerases and their substrate complexes. *Curr. Opin. Struct. Biol.* 9, 21-28.
- Kamer, G. and Argos, P.** (1984). Primary structural comparison of RNA-dependent polymerases from plant, animal and bacterial viruses. *Nucleic Acids Res.* 12, 7269-7282.
- Karlsson, K. and Carlsson, S.R.** (1998). Sorting of lysosomal membrane glycoproteins lamp-1 and lamp-2 into vesicles distinct from mannose 6-phosphate receptor/g-Adaptin vesicles at the trans-Golgi network. *J. Biol. Chem.* 273, 18966-18973.
- Keränen, S. and Kääriäinen, L.** (1974). Isolation and basic characterization of temperature-sensitive mutants from Semliki Forest virus. *Acta Path. Microbiol. Scand. Sect. B* 82, 810-820.
- Keränen, S. and Ruohonen, L.** (1983). Nonstructural proteins of Semliki Forest virus: Synthesis, processing, and stability in infected cells. *J. Virol.* 47, 505-551.
- Kielian, M. and Helenius, A.** (1984). Role of cholesterol in fusion of Semliki Forest virus with membranes. *J. Virol.* 52, 281-283.
- Kielian, M. and Helenius, A.** (1986). Entry of alphaviruses. In *The Togaviridae and Flaviviridae*. S. Schlesinger and M.J. Schlesinger, eds. (New York): pp. 91-119.
- Kleijmeer, M.J., Morkowski, S., Griffith, J.M., Rudensky, A.Y., and Geuze, H.J.** (1997). Major histocompatibility complex class II compartments in human and mouse B lymphoblasts represent conventional endocytic compartments. *J. Cell Biol.* 139, 639-649.
- Klumperman, J., Hille, A., Veenendaal, T., Oorschot, V., Stoorvogel, W., von Figura, K., and Geuze, H.J.** (1993). Differences in the endosomal distributions of the two mannose 6-phosphate receptors. *J. Cell Biol.* 121, 997-1010.
- Knipe, D.M.** (1996). Virus-host cell interactions. In *Fields Virology*. B.N. Fields, D.M. Knipe, P.M. Howley, and et al, eds. (Philadelphia: Lippincott-Raven), pp. 273-299.
- Kobayashi, T., Gu, F., and Gruenberg, J.** (1998). Lipids, lipid domains and lipid-protein interactions in endocytic membrane traffic. *Cell Develop. Biol.* 9, 517-526.
- Kobayashi, T., Beuchat, M.H., Lindsay, M., Frias, S., Palmiter, R.D., Sakuraba, H., Parton, R.G., and Gruenberg, J.** (1999). Late endosomal membranes rich in lysobisphosphatidic acid regulate cholesterol transport. *Nature Cell Biol.* 1, 113-118.
- Koonin, E.V.** (1991). The phylogeny of RNA-dependent RNA polymerases of positive-strand RNA viruses. *J. Gen. Virol.* 72, 2197-2206.
- Koonin, E.V. and Dolja, V.V.** (1993). Evolution and taxonomy of positive-strand RNA viruses: Implications of comparative analysis of amino acid sequences. *Crit. Rev. Biochem. Mol. Biol.* 28, 375-430.
- Kroemer, G.** (1997). The proto-oncogene Bcl-2 and its role in regulating apoptosis. *Nature Med.* 3, 614-620.
- Kuge, O., Akamatsu, Y., and Nishijima, M.** (1989). Abortive infection with Sindbis virus of a chinese hamster ovary cell mutant defective in phosphatidylserine and phosphatidylethanolamine biosynthesis. *Biochim. Biophys. Acta* 986, 61-69.
- Kääriäinen, L. and Söderlund, H.** (1978). Structure and replication of alphaviruses. *Curr. Top. Microbiol. Immunol.* 82, 15-69.
- Kääriäinen, L., Takkinen, K., Keränen, S., and Söderlund, H.** (1987). Replication of the genome of alphaviruses. *J. Cell Sci. Suppl.* 7, 231-250.
- Laakkonen, P., Hyvönen, M., Peränen, J., and Kääriäinen, L.** (1994). Expression of Semliki Forest virus nsP1-specific methyltransferase in

References

- insect cells and in *Escherichia coli*. *J. Virol.* 68, 7418-7425.
- Laakkonen, P., Ahola, T., and Kääriäinen, L.** (1996). The effects of palmitoylation on membrane association of Semliki Forest virus RNA capping enzyme. *J. Biol. Chem.* 271, 28567-28571.
- Lachmi, B.-E. and Kääriäinen, L.** (1977). Control of protein synthesis in Semliki Forest virus infected cells. *J. Virol.* 22, 142-149.
- LaStarza, M.W., Lemm, J.A., and Rice, C.M.** (1994). Genetic analysis of the nsP3 region of Sindbis virus: Evidence for roles in minus-strand and subgenomic RNA synthesis. *J. Virol.* 68, 5781-5791.
- Lee, J.-Y., Marshall, J.A., and Bowden, D.S.** (1992). Replication complexes associated with the morphogenesis of rubella virus. *Arch Virol.* 122, 95-106.
- Lee, J.-Y., Marshall, J.A., and Bowden, D.S.** (1994). Characterization of rubella virus replication complexes using antibodies to double-stranded RNA. *Virology* 200, 307-312.
- Lemm, J.A., Durbin, R.K., Stollar, V., and Rice, C.M.** (1990). Mutations which alter the level or structure of Nsp4 can affect the efficiency of Sindbis virus replication in a host-dependent manner. *J. Virol.* 64, 3001-3011.
- Lemm, J.A., Rumenapf, T., Strauss, E.G., Strauss, J.H., and Rice, C.M.** (1994). Polypeptide requirements for assembly of functional Sindbis virus replication complexes: a model for the temporal regulation of minus- and plus-strand RNA synthesis. *EMBO J.* 13, 2925-2934.
- Levine, B., Hardwick, J.M., Trapp, B.D., Clawford, T.O., Bollinger, R.C., and Griffin, D.E.** (1991). Antibody-mediated clearance of alphavirus infection from neurons. *Science* 254, 856-860.
- Levine, B., Huang, Q., Isaacs, J.T., Reed, J.C., Griffin, D.E., and Hardwick, J.M.** (1993). Conversion of lytic to persistent alphavirus infection by the *bcl-2* cellular oncogene. *Nature* 361, 739-742.
- Levine, B., Goldman, J.E., Jiang, H.H., Griffin, D.E., and Hardwick, J.M.** (1996). Bcl-2 protects mice against fatal alphavirus encephalitis. *Proc. Natl. Acad. Sci. USA* 93, 4810-4815.
- Lewis, J., Wesselingh, S.L., Griffin, D.E., and Hardwick, J.M.** (1996). Alphavirus-induced apoptosis in mouse brains correlates with neurovirulence. *J. Virol.* 70, 1828-1835.
- Li, G., LaStarza, M.W., Hardy, W.R., Strauss, J.H., and Rice, C.M.** (1990). Phosphorylation of Sindbis virus nsP3 *in vivo* and *in vitro*. *Virology* 179, 416-427.
- Liao, G., Nagasaki, T., and Gundersen, G.G.** (1995). Low concentrations of nocodazole interfere with fibroblast locomotion without significantly affecting microtubule level: implications for the role of dynamic microtubules in cell locomotion. *J. Cell Sci.* 108, 3473-3483.
- Liljeström, P. and Garoff, H.** (1991). A new generation of animal cell expression vectors based on the Semliki Forest virus replicon. *Bio/Technology* 9, 1356-1361.
- Liljeström, P., Lusa, S., Huylebroeck, D., and Garoff, H.** (1991). In vitro mutagenesis of a full-length cDNA clone of Semliki Forest virus: The small 6,000-molecular-weight membrane protein modulates virus release. *J. Virol.* 65, 4107-4113.
- Lin, K.-I., Lee, S.-H., Narayanan, R., Baraban, J.M., Hardwick, J.H., and Ratan, R.R.** (1995). Thiol agents and bcl-2 identify an alphavirus-induced apoptotic pathway that requires activation of the transcription factor NFκB. *J. Cell Biol.* 131, 1149-1161.
- Liposits, Z. Görcs, T., Gallyas, F., Kosaras, B. and Setalo, G.** (1982). Improvement of the electron microscopic detection of peroxidase activity by means of the silver intensification of the diaminobenzidine reaction in the rat nervous system. *Neurosci. Lett.* 31, 7-11.

- Liou, W., Geuze, H.J., and Slot, J.W.** (1996). Improving structural integrity of cryosections for immunogold labeling. *J. Histochem. Cytochem.* 106, 41-58.
- Liu, X., Ropp, S.L., Jackson, R.J., and Frey, T.K.** (1998). The rubella virus nonstructural protease requires divalent cations for activity and functions in trans. *J. Virol.* 72, 4463-4466.
- Lundstom, K.** (1999). Alphaviruses as tools in neurobiology and gene therapy. *J. Recept. Signal Transduct. Res.* 19, 673-686.
- Lundstom, K., Vargas, A., and Allet, B.** (1995). Functional activity of a biotinylated human neurokinin 1 receptor fusion expressed in the Semliki Forest virus system. *Biochem. Biophys. Res. Commun.* 208, 260-266.
- Lusa, S., Garoff, H., and Liljeström, P.** (1991). Fate of the 6K membrane protein of Semliki Forest virus during virus assembly. *Virology* 185, 843-846.
- Machesky, L.M. and Hall, A.** (1996). Rho: a connection between membrane receptor signalling and the cytoskeleton. *Trends Cell Biol.* 6, 304-310.
- Mackenzie, J.M., Jones, M.K., and Westaway, E.G.** (1999). Markers for trans-Golgi membranes and the intermediate compartment localize to induced membranes with distinct replication functions in Flavivirus-infected cells. *J. Virol.* 73, 9555-9567.
- Magliano, D., Marshall, J.A., Bowden, D.S., Vardaxis, N., Meanger, J., and Lee, J.-Y.** (1998). Rubella virus replication complexes are virus-modified lysosomes. *Virology* 240, 57-63.
- Maldarelli, F., King, N.W., and Yagi, M.J.** (1987). Effects of cytoskeletal disrupting agents on mouse mammary tumor virus replication. *Virus Research* 7, 281-295.
- Marr, L.D., Wang, C.-Y., and Frey, T.K.** (1994). Expression of the rubella virus nonstructural protein ORF and demonstration of proteolytic processing. *Virology* 198, 586-592.
- Marsh, M. and Helenius, A.** (1980). Adsorptive endocytosis of Semliki Forest virus. *J. Mol. Biol.* 142, 439-454.
- Marsh, M., Bolzau, E., and Helenius, A.** (1983). Penetration of Semliki Forest virus from acidic prelysosomal vacuoles. *Cell* 32, 931-940.
- Marsh, M., Griffiths, G., Dean, G.E., Mellman, I., and Helenius, A.** (1986). Three-dimensional structure of endosomes in BHK-21 cells. *Proc. Natl. Acad. Sci. USA* 83, 2899-2903.
- Mas, P. and Beachy, R.N.** (1999). Replication of tobacco mosaic virus on endoplasmic reticulum and role of the cytoskeleton and virus movement protein in intracellular distribution of viral RNA. *J. Cell Biol.* 147, 945-958.
- Mathiot, C.C., Grimaud, G., Garry, P., Bouquety, J.C., Mada, A., Daguisy, A.M., and Georges, A.J.** (1990). An outbreak of human Semliki Forest virus infection in Central African Republic. *Am. J. Trop. Med. Hyg.* 42, 386-393.
- McIntosh, B.M., Brookworth, C., and Kokernot, R.H.** (1961). Isolation of Semliki Forest virus from *Aedes (Aedimorphus) argenteopunctatus (Theobald)* collected in Portuguese East Africa. *Transact. Royal Soc. Trop. Med. Hyg.* 55, 192-198.
- Megyeri, K., Berencsi, K., Halazonetis, T.D., Prendergast, G.C., Gri, G., Plotkin, S.A., Rovera, G., and Gönczöl, E.** (1999). Involvement of a p53-dependent pathway in rubella virus-induced apoptosis. *Virology* 259, 74-84.
- Meresse, S., Gorvel, J.-P., and Chavrier, P.** (1995). The rab7 GTPase resides on a vesicular compartment connected to lysosomes. *J. Cell Sci.* 108, 3349-3358.
- Michel, M.R., Elgizoli, M., Dai, Y., Jakob, R., Koblet, H., and Arrigo, A.P.** (1990).

References

- Karyophilic properties of Semliki Forest virus nucleocapsid protein. *J. Virol.* 64, 5123-5131.
- Mitchison, T.J., and Cramer, L.P.** (1996). Actin-based cell motility and cell locomotion. *Cell* 84, 371-379.
- Mortara, R.A., and Koch, G.L.E.** (1986). Analysis of pseudopodial structure and assembly with viral projections. *J. Cell Sci. Suppl.* 5, 129-144.
- Mortara, R.A., and Koch, G.L.E.** (1989). An association between actin and nucleocapsid polypeptides in isolated murin retroviral particles. *J. Submicrosc. Cytol. Pathol.* 21, 295-306.
- Moyer, S.A., Baker, S.C., and Horikami, S.M.** (1990). Host cell proteins required for measles virus reproduction. *J. Gen. Virol.* 71, 775-783.
- Moyer, S.A., Baker, S.C., and Lessard, J.L.** (1986). Tubulin: a factor necessary for the synthesis of both Sendai virus and vesicular stomatitis virus RNAs. *Proc. Natl. Acad. Sci. USA* 83, 5405-5409.
- Mullock, B.M., Bright, N.A., Fearon, C.W., Gray, S.R., and Luzio, J.P.** (1998). Fusion of lysosomes with late endosomes produces a hybrid organelle of intermediate density and is NSF dependent. *J. Cell Biol.* 140, 591-601.
- Nagata, K., and Hall, A.** (1996). The Rho GTPase regulates protein kinase activity. *BioEssays* 18, 29-531.
- Nicola, A.V., Chen, W., and Helenius, A.** (1999). Co-translational folding of an alphavirus capsid protein in the cytosol of living cells. *Nature Cell Biol.* 1, 341-345.
- Nobes, C.D. and Hall, A.** (1995). Rho, Rac, and Cdc42 GTPases regulate the assembly of multimolecular focal complexes associated with actin fibers, lamellipodia, and filopodia. *Cell* 81, 53-62.
- O'Brien, V.** (1998). Viruses and apoptosis. *J. Gen. Virol.* 79, 1833-1845.
- Oker-Blom, C.** (1984). The gene order for rubella virus structural proteins is NH₂-C-E₂-E₁-COOH. *J. Virol.* 51, 354-358.
- Oker-Blom, C., Kalkkinen, N., Kääriäinen, L., and Pettersson, R.F.** (1983). Rubella virus contains one capsid protein and three envelope proteins, E1, E2a, and E2b. *J. Virol.* 46, 964-973.
- Oker-Blom, C., Ulmanen, I., Kääriäinen, L., and Pettersson, R.F.** (1984). Rubella virus 40S genome RNA specifies a 24S subgenomic mRNA that codes for a precursor to structural proteins. *J. Virol.* 49, 403-408.
- Pearce-Pratt, R., Malamud, D., and Phillips, D.M.** (1994). Role of the cytoskeleton in cell-to-cell transmission of human immunodeficiency virus. *J. Virol.* 68, 2898-2905.
- Pedersen, K.W., van der Meer, Y., Roos, N., and Snijder, E.J.** (1999). Open reading frame 1a-encoded subunits of the Arterivirus replicase induce endoplasmic reticulum-derived double-membrane vesicles which carry the viral replication complex. *J. Virol.* 73, 2016-2026.
- Pehrson, J.R. and Fuji, R.N.** (1998). Evolutionary conservation of histone macroH2A subtypes and domains. *Nucleic Acids Res.* 26, 2837-2842.
- Peränen, J.** (1990). Characterization of Semliki Forest virus nonstructural proteins. PhD. thesis, Helsinki, Yliopistopaino.
- Peränen, J.** (1991). Localization and phosphorylation of Semliki Forest virus nonstructural protein nsP3 expressed in COS cells from a cloned cDNA. *J. Gen. Virol.* 72, 195-199.
- Peränen, J. and Kääriäinen, L.** (1991). Biogenesis of type I cytopathic vacuoles in Semliki Forest virus-infected BHK cells. *J. Virol.* 65, 1623-1627.
- Peränen, J., Takkinen, K., Kalkkinen, N., and Kääriäinen, L.** (1988). Semliki Forest virus-specific non-structural protein nsP3 is a phosphoprotein. *J. Gen. Virol.* 69, 2165-2178.

- Peränen, J., Rikkonen, M., Liljeström, P., and Kääriäinen, L.** (1990). Nuclear localization of Semliki Forest virus-specific nonstructural protein nsP2. *J. Virol.* 64, 1888-1896.
- Peränen, J., Laakkonen, P., Hyvönen, M., and Kääriäinen, L.** (1995). The alphavirus replicase protein nsP1 is membrane-associated and has affinity to endocytic organelles. *Virology* 208, 610-620.
- Peränen, J., Rikkonen, M., Hyvönen, M., and Kääriäinen, L.** (1996). T7 vectors with a modified T7lac promoter for expression of proteins in *Escherichia coli*. *Anal. Biochem.* 236, 371-373.
- Pesonen, M. and Kääriäinen, L.** (1982). Incomplete complex oligosaccharides in Semliki Forest virus envelope proteins arrested within the cell in the presence of monensin. *J. Mol. Biol.* 158, 213-230.
- Petruzzello, R., Orsi, N., Macchia, S., Rieti, S., Frey, T.K., and Mastromarino, P.** (1996). Pathway of rubella virus infectious entry into Vero cells. *J. Gen. Virol.* 77, 303-308.
- Plotkin, S.A., and Vaheri, A.** (1967). Human fibroblasts infected with rubella virus produce a growth inhibitor. *Science* 156, 659-661.
- Pollard, T.D., and Cooper, J.A.** (1986). Actin and actin binding proteins. A critical evaluation of mechanisms and functions. *Annu. Rev. Biochem.* 55, 987-1035.
- Pugachev, K.V. and Frey, T.K.** (1998a). Effects of defined mutations in the 5' nontranslated region of rubella virus genomic RNA on virus viability and macromolecule synthesis. *J. Virol.* 72, 641-650.
- Pugachev, K.V. and Frey, T.K.** (1998b). Rubella virus induces apoptosis in culture cells. *Virology* 250, 359-370.
- Pugachev, K.V., Abernathy, E.S., and Frey, T.K.** (1997). Improvement of the specific infectivity of the rubella virus (RUB) infectious clone: Determinants of cytopathogenicity induced by RUB map to the nonstructural proteins. *J. Virol.* 71, 562-568.
- Punnonen, E.-L., Fages, C., Wartiovaara, J., and Rauvala, H.** (1999). Ultrastructural localization of β -actin and amphotericin mRNA in cultured cells: application of tyramide signal amplification and comparison of detection methods. *J. Histochem. Cytochem.* 47, 99-112.
- Quinn, P., Griffiths, G., and Warren, G.** (1984). Density of newly synthesized membrane proteins in intracellular membranes. II. Biochemical studies. *J. Cell Biol.* 98, 2142-2147.
- Ranki, M. and Kääriäinen, L.** (1979). Solubilized RNA replication complex from Semliki Forest virus-infected cells. *Virology* 98, 298-307.
- Ranki, M., Ulmanen, I., and Kääriäinen, L.** (1979). Semliki Forest virus-specific nonstructural protein is associated with ribosomes. *FEBS Lett.* 108, 299-302.
- Rennels, M.B.** (1984). Arthropod-borne virus infections of the central nervous system. *Neurol. Clin.* 2, 241-254.
- Restrepo-Hartwig, M.A. and Ahlquist, P.** (1996). Brome mosaic virus helicase- and polymerase-like proteins colocalize on the endoplasmic reticulum at sites of viral RNA synthesis. *J. Virol.* 70, 8908-8916.
- Ridley, A.J.** (1996). Rho: theme and variations. *Current Biology* 6, 1256-1264.
- Ridley, A.J. and Hall, A.** (1992). The small GTP-binding protein rho regulates the assembly of focal adhesions and actin stress fibers in response to growth factors. *Cell* 70, 389-399.
- Ridley, A.J. and Hall, A.** (1994). Signal transduction pathways regulating Rho-mediated stress fibre formation: requirement for a tyrosine kinase. *EMBO J.* 13, 2600-2610.
- Ridley, A.J., Paterson, H.F., Johnston, C.L., Diekmann, D., and Hall, A.** (1992). The small

References

- GTP-binding protein rac regulates growth factor-induced membrane ruffling. *Cell* 70, 401-410.
- Rikkonen, M.** (1996). Functional significance of the nuclear-targeting and NTP-binding motifs of Semliki Forest virus nonstructural protein nsP2. *Virology* 218, 352-361.
- Rikkonen, M., Peränen, J., and Kääriäinen, L.** (1992). Nuclear and nucleolar targeting signals of Semliki Forest virus nonstructural protein nsP2. *Virology* 189, 462-473.
- Rikkonen, M., Peränen, J., and Kääriäinen, L.** (1994). ATPase and GTPase activities associated with Semliki Forest virus nonstructural protein nsP2. *J. Virol.* 68, 5804-5810.
- Sambrook, J., Fritsch, E.F., and Maniatis, T.** (1989). *Molecular cloning: a laboratory manual*. (Cold Spring Harbor: Cold Spring Harbor Laboratory).
- Sanderson, C.H., Way, M., and Smith, G.F.** (1998). Virus-induced cell motility. *J. Virol.* 72, 1235-1243.
- Saraste, J. and Kuismanen, E.** (1984). Pre- and post-Golgi vacuoles operate in the transport of Semliki Forest virus membrane glycoproteins to the cell surface. *Cell* 38, 535-543.
- Sariola, M., Saraste, J., and Kuismanen, E.** (1995). Communication of post-Golgi elements with early endocytic pathway: regulation of endoproteolytic cleavage of Semliki Forest virus p62 precursor. *J. Cell Sci.* 108, 2465-2475.
- Sasaki, H., Nakamura, M., Ohiro, T., Matsuda, Y., Yuda, Y., and Nokomura, Y.** (1995). Myosin-actin interaction plays an important role in HIV-1 release from host cells. *Proc. Natl. Acad. Sci. USA* 92, 2026-2030.
- Sawicki, D.L. and Sawicki, S.G.** (1980). Short-lived minus-strand polymerase for Semliki Forest virus. *J. Virol.* 34, 108-118.
- Sawicki, D.L. and Sawicki, S.G.** (1985). Functional analysis of the A complementation group mutants of Sindbis HR virus. *Virology* 144, 20-34.
- Sawicki, S.G. and Sawicki, D.L.** (1986a). The effect of loss regulation of minus-strand RNA synthesis on Sindbis virus replication. *Virology* 151, 339-349.
- Sawicki, S.G. and Sawicki, D.L.** (1986b). The effect of overproduction of nonstructural proteins on alphavirus plus-strand and minus-strand RNA synthesis. *Virology* 152, 507-512.
- Sawicki, D.L., Sawicki, S.G., Keränen, S., and Kääriäinen, L.** (1981). Specific Sindbis virus-coded function for minus-strand RNA synthesis. *J. Virol.* 39, 348-358.
- Scallan, M.F., Allsopp, T.E., and Fazakerley, J.K.** (1997). b1c-2 acts early to restrict Semliki Forest virus replication and delays virus-induced programmed cell death. *J. Virol.* 71, 1583-1590.
- Schaad, M.C., Jensen, P.E., and Carrington, J.C.** (1997). Formation of plant RNA virus replication complexes on membranes: role of an endoplasmic reticulum-targeted viral protein. *EMBO J.* 16, 4049-4059.
- Schafer, D.A. and Cooper, J.A.** (1995). Control of actin assembly at filament ends. *Annu. Rev. Cell Dev. Biol.* 11, 497-518.
- Schlegel, A., Giddings, J.T.H., Ladinsky, M.S., and Kirkegaard, K.** (1996). Cellular origin and ultrastructure of membranes induced during poliovirus infection. *J. Virol.* 70, 6576-6588.
- Schlesinger, S.** (1993). Alphaviruses - vectors for the expression of heterologous genes. *Trends Biotechnol.* 11, 18-22.
- Schlesinger, S. and Schlesinger, M.J.** (1996). Togaviridae: The viruses and their replication. In *Fields Virology*. B.N. Fields, D.M. Knipe, and P.M. Howley, eds. (Philadelphia: Lipicott-Raven Publishers), pp. 825-841.

- Simon, K.O., Whitaker-Dowling, P.A., Youngner, J.S., and Widnell, C.C.** (1990). Sequential disassembly of the cytoskeleton in BHK21 cells infected with vesicular stomatitis virus. *Virology* 177, 289-297.
- Simons, K. and Warren, G.** (1983). Semliki Forest virus: a probe for membrane traffic in the animal cell. *Adv. Protein Chem.* 36, 79-132.
- Singer, R.H., Langevin, G.L., and Lawrence, J.B.** (1989). Ultrastructural visualization of cytoskeletal mRNAs and their associated proteins using double-label in situ hybridization. *J. Cell Biol.* 108, 2343-2353.
- Singh, I. and Helenius, A.** (1992). Role of ribosomes in Semliki Forest virus nucleocapsid uncoating. *J. Virol.* 66, 7049-7058.
- Sinijärvi, R., Järvekylg, L., Andreeva, E., and Saarma, M.** (1988). Detection of potato virus X by one incubation europium time-resolved fluoroimmuno-assay and ELISA. *J. Gen. Virol.* 69, 991-998.
- Slot, J.W. and Geuze, H.J.** (1985). A new method of preparing gold probes for multiple-labeling cytochemistry. *Eur. J. Cell Biol* 38, 87-93.
- Smithburn, K.C. and Haddow, A.J.** (1944). Semliki Forest virus. I. Isolation and pathogenic properties. *J. Immunol.* 49, 141-157.
- Soldati, T., Rancano, C., Geissler, H., and Pfeffer, S.R.** (1995). Rab7 and Rab9 are recruited onto late endosomes by biochemically distinguishable processes. *J. Biol. Chem.* 270, 25541-25548.
- Sormunen, R.** (1997). α -Spectrin in detergent-extracted whole-mount cytoskeletons of chicken embryo heart fibroblasts. *Histochem. J.* 25, 678-686.
- Sreevalsan, T.** (1970). Association of viral ribonucleic acid with cellular membranes in chick embryo cells infected with Sindbis virus. *J. Virol.* 6, 438-444.
- Stinchcombe, J.C., and Griffiths, G.M.** (1999). Regulated secretion from hemopoietic cells. *J. Cell Biol.* 147, 1-5.
- Strauss, J.H. and Strauss, E.G.** (1994). The alphaviruses: gene expression, replication, and evolution. *Microbiol. Rev.* 58, 491-562.
- Strauss, E.G., Rice, C.M., and Strauss, J.H.** (1983). Sequence coding for the alphavirus nonstructural proteins is interrupted by an opal termination codon. *Proc. Natl. Acad. Sci. USA* 80, 5271-5275.
- Strauss, E.G., Rice, C.M., and Strauss, J.H.** (1984). Complete nucleotide sequence of the genomic RNA of Sindbis virus. *Virology* 133, 92-110.
- Sundell, C.L., and Singer, R.H.** (1991). Requirement of microfilament in sorting of actin messenger RNA. *Science* 253, 1275-1277.
- Suomalainen, M., Garoff, H., and Baron, M.D.** (1990). The E2 signal sequence of rubella virus remains part of the capsid protein and confers membrane association in vitro. *J. Virol.* 64, 5500-5509.
- Suomalainen, M., Liljeström, P., and Garoff, H.** (1992). Spike protein-nucleocapsid interactions drive the budding of alphaviruses. *J. Virol.* 66, 4737-4747.
- Suopanki, J., Sawicki, D.L., Sawicki, S.G., and Kääriäinen, L.** (1998). Regulation of alphavirus 26S mRNA transcription by replicase component nsP2. *J. Gen. Virol.* 79, 309-319.
- Söderlund, H.** (1973). Kinetics of formation of the Semliki Forest virus nucleocapsid. *Intervirology* 1, 354-361.
- Söderlund, H. and Kääriäinen, L.** (1974). Association of capsid protein with Semliki Forest virus messenger RNAs. *Acta Path. Microbiol. Scand. Sect. B* 82, 33-40.
- Söderlund, H. and Umanen, I.** (1977). Transient association of Semliki Forest virus capsid protein with ribosomes. *J. Virol.* 24, 907-909.

References

- Takkinen, K.** (1986). Complete nucleotide sequence of the nonstructural protein genes of Semliki Forest virus. *Nucleic Acids Res.* 14, 5667-5682.
- Takkinen, K., Vidgren, G., Ekstrand, J., Hellman, U., Kalkkinen, N., Wernstedt, C., and Pettersson, R.F.** (1988). Nucleotide sequence of the rubella virus capsid protein gene reveals an unusually high G/C content. *J. Gen. Virol.* 69, 603-612.
- Takkinen, K., Peränen, J., Keränen, S., Söderlund, H., and Kääriäinen, L.** (1990). The Semliki-Forest-virus-specific nonstructural protein nsP4 is an autoprotease. *Eur. J. Biochem.* 189, 33-38.
- Takkinen, K., Peränen, J., and Kääriäinen, L.** (1991). Proteolytic processing of Semliki Forest virus-specific non-structural polyprotein. *J. Gen. Virol.* 72, 1627-1633.
- ten Dam, E., Flint, M., and Ryan, M.D.** (1999). Virus-coded proteinases of the *Togaviridae*. *J. Gen. Virol.* 80, 1879-1888.
- Tjelle, T.E., Brech, A., Juvet, L.K., Griffiths, G., and Berg, T.** (1996). Isolation and characterization of early endosomes, late endosomes and terminal lysosomes: their role in protein degradation. *J. Cell Sci.* 109, 2905-2914.
- Tokuyasu, K.T.** (1973). A technique for ultracryotomy of cell suspensions and tissues. *J. Cell Biol.* 57, 551-565.
- Tokuyasu, K.T.** (1989). Use of polyvinylpyrrolidone and polyvinyl alcohol for cryoultratomy. *J. Histochem. Cytochem.* 21, 163-171.
- Trembleau, A., Morales, M., and Bloom, F.E.** (1996). Aggregation of vasopressin mRNA in a subset of axonal swellings of the median eminence and posterior pituitary: light and electron microscopic evidence. *J. Neurosci.* 14, 39-53.
- Tubulekas, I., Berglund, P., Fleeton, M., and Liljeström, P.** (1997). Alphavirus expression vectors and their use as recombinant vaccines - a minireview. *Gene* 190, 191-195.
- Tuomi, K., Kääriäinen, L., and Söderlund, H.** (1975). Quantitation of Semliki Forest virus RNAs in infected cells using ³²P equilibrium labelling. *Nucleic Acids Res.* 2, 555-565.
- Turunen, M., Kuusisto, P., Uggeldahl, P.E., and Toivanen, A.** (1998). Pogosta disease: clinical observations during an outbreak in the province of North Karelia, Finland. *Br. J. Rheumatol.* 37, 1177-1180.
- Ulmanen, I., Söderlund, H., and Kääriäinen, L.** (1976). Semliki Forest virus capsid protein associates with the 60 S ribosomal subunit in infected cells. *J. Virol.* 20, 203-210.
- Ulmanen, I., Peränen, J., Tenhunen, J., Tilgman, C., Karhunen, T., Panula, P., Bernasconi, L., Aubry, J.P., and Lundstrom, K.** (1997). Expression and intracellular localization of catechol O-methyltransferase in transfected mammalian cells. *Eur. J. Biochem.* 243, 452-459.
- Vaheri, A., Sedwick, W.D., Plotkin, S.A., and Maes, R.** (1965). Cytopathic effect of rubella virus in RHK21 cells and growth to high titers in suspension culture. *Virology* 27, 239-241.
- van der Meer, Y., van Tol, H., Krijnse Locker, J., and Snijder, E.J.** (1998). ORF1a-encoded replicase subunits are involved in the membrane association of the arterivirus replication complex. *J. Virol.* 72, 6689-6698.
- van der Meer, Y., Snijder, E.J., Dobbe, J.C., Schleich, S., Denison, M.R., Spaan, W.J.M., and Krijnse Locker, J.** (1999). Localization of mouse hepatitis virus nonstructural proteins and RNA synthesis indicates a role for late endosomes in viral replication. *J. Virol.* 73, 7641-7657.
- Vasiljjeva, L., Merits, A., Auvinen, P., and Kääriäinen, L.** (2000). Identification of a novel function of the alphavirus capping apparatus - RNA 5' triphosphatase activity of Nsp2. *J. Biol. Chem.* (in press).

- Vidgren, G., Takkinen, K., Kalkkinen, N., Kääriäinen, L., and Pettersson, R.F.** (1987). Nucleotide sequence of the genes coding for the membrane glycoproteins E1 and E2 of rubella virus. *J. Gen. Virol.* 68, 2347-2357.
- Vihinen, H. and Saarinen, J.** (2000). Phosphorylation site analysis of Semliki Forest virus nonstructural protein 3. *J. Biol. Chem.* (in press).
- Vihinen, H., Ahola, T., Merits, A., Tuittila, M., and Kääriäinen, L.** (2000). Identification and elimination of the phosphorylation sites of Semliki Forest virus replicase protein Nsp3. (submitted).
- Vitelli, R., Santillo, M., Lattero, D., Chiariello, M., Bifulco, M., Bruni, C.B., and Bucci, C.** (1997). Role of the small GTPase rab7 in the late endocytic pathway. *J. Biol. Chem.* 272, 4391-4397.
- Vogel, R., Provencher, S., von Bonsdorff, C.-M., Adrian, M., and Dubochet, J.** (1986). Envelope structure of Semliki Forest virus reconstructed from cryo-electron micrographs. *Nature* 320, 533-535.
- von Bonsdorff, C.-H. and Vaheri, A.** (1969). Growth of rubella virus in BHK21 cells: Electronmicroscopy of morphogenesis. *J. Gen. Virol.* 5, 47-51.
- Väänänen, P.** (1982). The use of red cells with fused Semliki Forest virus envelope proteins in antibody determinations by hemolysis in gel. *J. Virol. Methods* 4, 117-126.
- Väänänen, P. and Kääriäinen, L.** (1980). Fusion and haemolysis of erythrocytes caused by three togaviruses: Semliki Forest, Sindbis and rubella. *J. Gen. Virol.* 46, 467-475.
- Waheed, A., Gottschalk, S., Hille, A., Krentler, C., Pohlmann, R., Bräulke, T., Hauser, H., Geuze, H., and von Figura, K.** (1988). Human lysosomal acid phosphatase is transported as a transmembrane protein to lysosomes in transfected baby hamster kidney cells. *EMBO J.* 7, 2351-2358.
- Wahlberg, J.W. and Garoff, H.** (1992). Membrane fusion process of Semliki Forest virus. I: Low pH-induced rearrangement in spike protein quaternary structure precedes virus penetration into cells. *J. Cell Biol.* 116, 339-348.
- Wahlberg, J.M., Boere, W.A.M., and Garoff, H.** (1989). The heterodimeric association between the membrane proteins of Semliki Forest virus changes its sensitivity to low pH during virus maturation. *J. Virol.* 63, 4991-4997.
- Wahlberg, J.W., Bron, R., Wilschut, J., and Garoff, H.** (1992). Alphavirus membrane fusion involves homotrimers of the fusion protein. *J. Virol.* 66, 7309-7318.
- Wang, K.-S., Kuhn, R.J., Strauss, E.G., Ou, S., and Strauss, J.H.** (1992). High-affinity laminin receptor is a receptor for Sindbis virus in mammalian cells. *J. Virol.* 66, 4992-5001.
- Wang, Y.-F., Sawicki, S.G., and Sawicki, D.L.** (1991). Sindbis virus nsP1 functions in negative-strand RNA synthesis. *J. Virol.* 65, 985-988.
- Wang, Y.-F., Sawicki, S.G., and Sawicki, D.L.** (1994). Alphavirus nsP3 functions to form replication complexes transcribing negative-strand RNA. *J. Virol.* 68, 6466-6475.
- Weiss, B., Nitscko, H., Ghattas, I., Wright, R., and Schlesinger, S.** (1989). Evidence for specificity in the encapsidation of Sindbis virus RNAs. *J. Virol.* 63, 5310-5318.
- Wengler, G., Wengler, G., and Gross, H.J.** (1982). Terminal sequences of Sindbis virus-specific nucleic acids: Identity in molecules synthesized in vertebrate and insect cells and characteristic properties of the replicative form RNA. *Virology* 123, 273-283.
- Wengler, G., Wurkner, D. and Wengler, G.** (1992). Identification of a sequence element in the alphavirus core protein which mediates interaction of cores with ribosomes and the disassembly of cores. *Virology* 191, 880-888.

References

- Westaway, E.G., Mackenzie, J.M., Kenney, M.T., Jones, M.K., and Khromykh, A.A.** (1997). Ultrastructure of Kunjin virus-infected cells: colocalization of NS1 and NS3 with double-stranded RNA, and NS2B with NS3, in virus-induced membrane structures. *J. Virol.* 71, 6650-6661.
- Winkler, W.G. and Blenden, D.C.** (1995). Transmission and control of viral zoonoses in the laboratory. In *Laboratory Safety: Principles and Practise*. D.O. Fleming, J.H. Richardson, J.L. Tulis, and D. Vesley, eds. Washington, American Society for Microbiology.
- Wolinsky, J.S.** (1996). Rubella. In *Fields Virology* (B.N. Fields, D.M. Knipe, et al., Chapter 29, 899-921.
- Wolinsky, J.S., McCarthy, M., Allen-Cannady, O., Moore, W.T., Jin, R., Cao, S.-N., Lovett, A., and Simmons, D.** (1991). Monoclonal antibody-defined epitope map of expressed rubella virus protein domains. *J. Virol.* 65, 3986-3994.
- Wyatt, L.S., Moss, B., and Rozenblatt, S.** (1995). Replication-deficient vaccinia virus encoding bacteriophage T7 RNA polymerase for transient gene expression in mammalian cells. *Virology* 210, 202-205.
- Zhao, H. and Garoff, H.** (1992). Role of cell surface spikes in alphavirus budding. *J. Virol.* 66, 7089-7095.
- Zhao, H., Lindquist, B., Garoff, H., von Bonsdorff, C.-H., and Liljeström, P.** (1994). A tyrosine-based motif in the cytoplasmic domain of the alphavirus envelope protein is essential for budding. *EMBO J.* 13, 4204-4211.
- Zhou, X.P., Berglund, G., Rhodes, G., Parker, S.E., Jondal, M., and Liljeström, P.** (1994). Self-replicating Semliki Forest RNA as recombinant vaccine. *Vaccine* 12, 1510-1514.
- Zigmond, S.H.** (1996). Signal transduction and actin filament organization. *Curr. Opin. Cell Biol.* 8, 66-73.